Intracellular and extracellular promoters of metastasis to different organs

By

Jess Dale Hebert

B.S., Biology
Georgetown University, 2012

SUBMITTED TO THE DEPARTMENT OF BIOLOGY IN PARTIAL FULFILLMENT OF THE REQUIREMENTS FOR THE DEGREE OF

DOCTOR OF PHILOSOPHY

AT THE

MASSACHUSETTS INSTITUTE OF TECHNOLOGY

JUNE 2019

Signature of Author:……

Department of Biology

May 21, 2019

Certified By:…….

Richard O. Hynes

Daniel K. Ludwig Professor for Cancer Research

Thesis Supervisor

Accepted By:…….

Amy E. Keating

Professor of Biology

Co-Director, Biology Graduate Committee

Intracellular and extracellular promoters of metastasis to different organs

By

Jess Dale Hebert

Submitted to the department on May 21, 2019, in partial fulfillment of the requirements for the degree of Doctor of Philosophy in Biology

Abstract

Metastasis is the cause of the vast majority of cancer-related deaths, yet much remains unknown about this complex process, from how tumor cells complete the many steps of the metastatic cascade to how they can adapt to survive in multiple, vastly different secondary sites. I have therefore conducted two studies into different aspects of metastasis. First, I investigated the scaffold protein IQGAP1, which promotes primary tumor growth and invasiveness in several cancers. However, the role of IQGAP1 in metastasis has been unclear. We used IQGAP1 knockdown and knockout to investigate its role in the metastatic cascade in melanoma and breast cancer. I found that reduction of IQGAP1 expression inhibited the formation of metastases, without limiting primary or metastatic tumor growth. Furthermore, IQGAP1 knockout significantly decreased extravasation of tumor cells from circulation. These data demonstrate that IQGAP1 promotes metastasis *in vivo* through regulation of extravasation and suggest that it may represent a valid therapeutic target for inhibiting metastasis. Second, I examined how cells from the same primary tumor can adapt to several different secondary environments. A critical component of every metastatic niche is the extracellular matrix (ECM), which provides structural support, migration control, and growth and survival signals. However, a comprehensive comparison of the ECM components of metastatic niches at various secondary sites had not yet been conducted. I isolated metastases from the brain, lungs, liver and bone marrow, which were all derived from parental MDA-MB-231 human breast cancer cells. We then enriched these tumor samples for ECM proteins and used quantitative mass spectrometry to analyze their ECM composition. Strikingly, the niches created at each site were distinct. Using these data, I compared protein abundance across all metastatic sites to determine which ECM proteins were most significantly elevated in each particular tissue relative to the others. Following this analysis, I knocked down tumor cell expression of SERPINB1, a protein characteristically elevated in brain metastases, and observed reduced metastasis to the brain. Together, these studies offer insight into the fundamental biology of metastasis and metastatic niches, as well as provide potential targets of metastatic breast cancer for imaging and therapy.

Thesis Supervisor: Richard O. Hynes

Title: Daniel K. Ludwig Professor for Cancer Research, Professor of Biology

Acknowledgments

There is an old saying, often attributed to Leonardo da Vinci, that “Art is never finished, only abandoned.” Much the same could be said about a PhD, which never comes to any perfect and complete conclusion. However, it might be more accurate (and positive) to say that a PhD is over when you realize it’s time for it to end. The following are some of the many people responsible both for guiding me to that finishing line, and for helping me appreciate when I had already left it behind.

First is my advisor, Richard Hynes, who has been a better mentor than I ever could have hoped for when I was a wide-eyed first-year student with very little idea of what he was doing. I know that my infinite pragmatism (Richard would say pessimism) was a constant challenge for him, and I spent a significant amount of time trying to learn from him how to be more self-promoting (Richard would say how to be less self-effacing). Richard also ingrained in me the fundamentals of careful science, thorough scholarship and independent judgment that I will carry with me for the rest of my life.

I would like to thank the members of my thesis committee, Frank Gertler and Tyler Jacks, for guiding my progress through my thesis, always offering considered experimental advice, and believing in my ability to succeed amidst the many ups and downs of graduate school. I would also very much like to thank Joan Brugge for serving as the external member for my thesis defense.

The Hynes lab has been an incredible learning environment, and I hope I have absorbed some fraction of the scientific expertise and wisdom that has been present during my time there. I want to thank my first mentors in the lab, Alexandra Naba and John Lamar. Alexandra taught me so much about meticulous experimental design and painstaking organization, as well as the endless process of acquiring new skills. I am indebted to John for passing on his commitment to re-thinking every experiment, considering more controls than remotely feasible before paring the number down, and constant willingness to argue about sports. I also want to thank Hynes lab postdocs Pat Murphy, Noor Jailkhani, Steffen Rickelt, Chenxi Tian and Genevieve Abbruzzese for their unending advice, no matter how many times I bothered them when they clearly had other work to do. Furthermore, I would like to thank Bigyan Bista for his tremendous mentorship during my early years in the lab, and for always being up for a good debate. I want to thank Thao Nguyen for her support, both scientific and musical, and for occasionally singing in the lab when she didn’t realize I was still there. Moreover, I need to thank David Benjamin for being a constant source of encouragement, commiseration, insight and bad puns. Finally, I want to thank Sam Myers, my collaborator from the Broad Institute, for his expertise in mass spectrometry and for being a constant force of motivation.

Music has been a constant presence throughout my time at MIT. While I joined the MIT Wind Ensemble in my first year thinking I would just keep up with my saxophone playing, I ended up becoming more and more deeply involved as the years went on. I have found the guarantee of improvement from practicing music a satisfying companion to the convoluted process of making progress in science. Much of this I owe to Fred Harris, whose unending curiosity, sense of

musical emotion, and commitment to bringing out the best in all of us has been an amazing inspiration to me. I am also deeply indebted to Philipp Stäudlin for caring so much about, and continuing to believe in, surely the least talented of his students. I would like to thank the members of the MIT Wind Ensemble for enriching my life, especially my past and present compatriots in Course Sax. You have all given me so much more than I deserved. In particular, I would like to thank Tina Kambil, who has been there since I started at MIT, for always encouraging me to improve while adamantly disagreeing with me about pretty much everything; and Rachel Morgan for her constant positivity and optimism throughout my winding graduate career.

There are also a number of friends whose support has gone tremendous lengths to making this PhD possible. I would like to thank Jack Quindlen for pushing me to make bad decisions, and Andrew Owens for pushing me to make good ones. They were both the right choices at various times. I would also like to thank AJ Amor, whose spontaneous suggestions have ended up being some of the most fun I've had at MIT.

Ashdown House has been my home at MIT for my entire time as a graduate student, and I would like to acknowledge the Ashdown community for making me feel welcome. I want to thank Adam Berinsky, Deirdre Logan, Katie Roman and Yuriy Roman for their continued friendship, trust and encouragement, which did so much to make me feel welcome. I would also like to thank the many students who worked with me as part of the Ashdown government, especially Jordan Romvary and Orpheus Chatzivasileiou. I learned a lot of lessons about management and leadership from working with all of you through good times and bad.

Finally, I would like to thank my family. Don, Mary and George did so much to make Boston feel like home when it was still an unfamiliar city to me. I would like to thank Kipp and Leyna for believing in my work even when I didn't, and my parents for their infinite support, even when it wasn't clear when this whole grad school thing would end. We all did this together.

Table of Contents

Chapter 1.

Introduction

This chapter was written by Jess Hebert with editing by Richard Hynes.

Metastasis is the spread of a cancer from its site of origin to other sites within the body, and it represents the final and most fatal stage in the progression of this disease within a patient. Indeed, the vast majority of patients who die from cancer do so only once metastasis has occurred (Lambert et al., 2017). Once a cancer has become metastatic, its treatment becomes considerably more difficult, as the disseminated metastases, which can be only a few cells in size, are extremely challenging to detect and can be numerous, making radiation treatment or surgical removal of all tumors not feasible (Pantel et al., 2009). In addition, metastases are frequently resistant to broadly acting chemotherapies, meaning that frontline systemic treatments are insufficient for eliminating them (Chaffer and Weinberg, 2011). Consequently, given the deadliness of metastatic cancer and the current deficiency of effective treatments, there is a dramatic need for improved options for both detecting metastases as well as destroying them.

However, despite this pressing need, the development of new therapies is inhibited by the current markedly incomplete understanding of the biology of metastasis. Although metastasis is as ancient as cancer itself, with archaeological evidence of bone metastases in a skeleton found in modern-day Sudan dating back to 1200 B.C. (Binder et al., 2014), concerted research into metastasis is relatively recent. One of the first observations about metastasis per se was that metastases tended to form in certain organs depending on the site of the primary tumor, which led to the formulation of the seed and soil hypothesis that tumor “seeds” tend to grow in the particular “soil” that is most suitable for them (Paget, 1889). Nevertheless, further research into this observation in particular, and metastasis in general, was sparse for much of the following century.

A series of experiments, many by Isaiah Fidler and colleagues, significantly increased knowledge of the fundamentals of metastasis. Quantitative observation of metastasizing cells

became possible with the advent of techniques for radiolabeling cells, which revealed how only a small number of cells was necessary to cause a metastatic outgrowth (Fidler, 1970; Fisher and Fisher, 1967). *In vivo* selection experiments were also developed, in which cancer cells were injected into a mouse, the resulting metastases removed and cultured as cells *in vitro*, then re-injected. Such experiments, performed with B16 melanoma cells put through several rounds of selection, demonstrated that cells could be selected to become more metastatic and organotropic, indicating the presence of stable, cell-intrinsic metastatic qualities (Fidler, 1973). Furthermore, injection of B16 cells into mice bearing subcutaneous grafts of kidney, lung or ovary tissue revealed that the tumor cells would frequently metastasize to the lung and ovary tissue (around 70% of mice), while they only metastasized infrequently to the ovary (14% of mice) (Hart and Fidler, 1980). Thus, after nearly a century, the medical observation that certain tumors tended to metastasize to certain organs was finally shown experimentally.

The rise of molecular biology and techniques for both measuring and altering gene expression in cells led to another series of breakthroughs in understanding how cells metastasize. One of the key changes often found to occur in cells that metastasize is the induction of the epithelial-mesenchymal transition (EMT), a developmental program by which tumor cells lose epithelial characteristics and become more mesenchymal, which also makes them more migratory, invasive and resistant to chemotherapy (Thiery, 2002; Thiery et al., 2009). This program is regulated by several transcription factors, including Slug, Snail, Twist and Zeb1, as well as miRNAs and epigenetic controls (Lamouille et al., 2014; Nieto et al., 2016), and it can be induced by growth factors like TGFβ, which is secreted by platelets (Labelle et al., 2011; Thiery et al., 2009). This transition is not a binary process, and there exist a number of intermediate cell states between fully epithelial and mesenchymal (Nieto et al., 2016). While an EMT is not

absolutely necessary for the acquisition of invasive behavior, many cells acquire at least some mesenchymal characteristics when leaving the primary tumor (Chaffer et al., 2016; Ye et al., 2017). This process can also be reversed by a mesenchymal-epithelial transition (MET), which may promote the outgrowth of metastatic cells once they have arrived at a new site (Jolly et al., 2017; Ocaña et al., 2012; Tsai et al., 2012).

The study of gene expression also led to the first analyses into the underpinnings of metastatic tropism, as cell populations with different metastatic abilities could be compared on a global level. Highly metastatic, *in vivo*-selected cells could be compared to their less metastatic parental cells, revealing some of the changes that increase metastatic ability (Clark et al., 2000). Cells that were selected for their ability to metastasize to different organs could also be analyzed, yielding early glimpses at factors that could mediate metastasis to particular tissues (Bos et al., 2009; Kang et al., 2003; Minn et al., 2005). More detailed surveys of the elements contributing to metastatic tropism will be reviewed in their own section later. However, more detailed exploration of the factors driving metastatic cells, as well as the causes behind their tendencies to metastasize to particular organs, requires a better understanding of the individual stages of metastasis from start to finish, a process often known as the metastatic cascade.

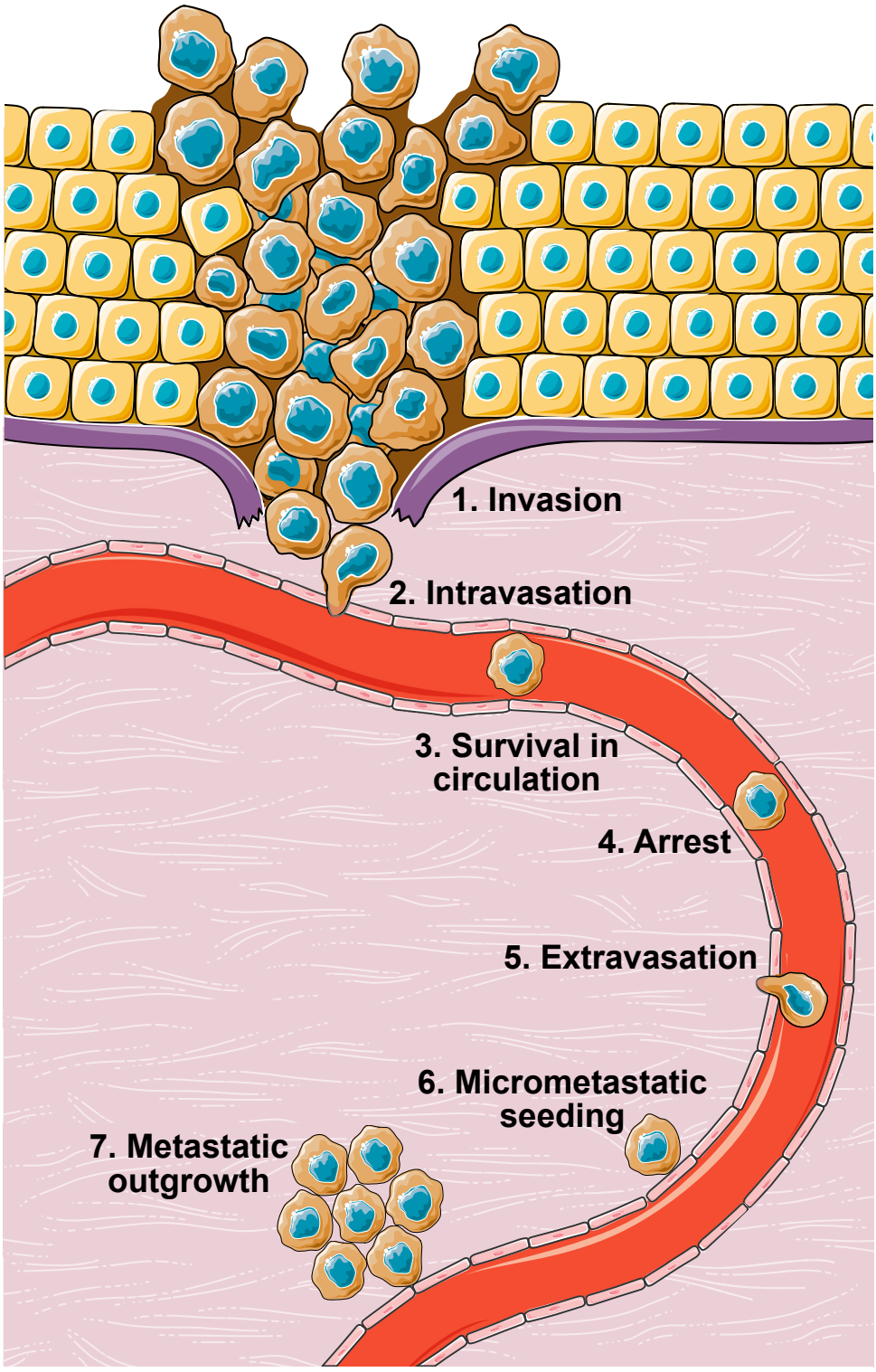

Figure 1. Steps of the metastatic cascade. To progress from a primary tumor to a metastatic tumor, tumor cells must complete several steps: 1. Invasion, 2. Intravasation, 3. Survival in circulation, 4. Arrest, 5. Extravasation, 6. Micrometastatic seeding, 7. Metastatic outgrowth. Images shown are modified from the Servier Medical Art database under a Creative Commons Attribution 3.0 license (https://smart.servier.com/).

The metastatic cascade

The process by which cancer cells leave the primary tumor and eventually establish secondary metastatic tumors is composed of several distinct stages (Figure 1). Tumor cells must invade away from their primary site toward a nearby blood vessel, intravasate into that vessel, survive transit through circulation, arrest at a different site, extravasate out of the vessel at the new site, seed a micrometastasis, and grow into an overt metastatic tumor (Klein, 2008; Mina and Sledge Jr, 2011). Proteins that act at any or all of these steps can promote or hinder metastasis. Crucially, the cellular behaviors and properties necessary to complete the steps of the metastatic cascade are not the same as those necessary to form a primary tumor, which consist more generally of promoting growth and evading the normal physiological checks in place to prevent such rampant proliferation (Hanahan and Weinberg, 2011). Thus, the metastatic cascade and the proteins that promote it represent both a distinct therapeutic challenge as well as a separate set of potential targets.

The first step of this process is invasion, in which would-be metastatic cells leave the primary tumor. As previously noted, this is generally accompanied by the acquisition of more mesenchymal characteristics in an EMT, since that transition makes the tumor cells more invasive (Kalluri and Weinberg, 2009; Thiery, 2002). Depending on the exact location of the primary tumor and its degree of vascularization, tumor cells must invade through varying amounts of the extracellular matrix (ECM), including the basement membrane, in order to reach a nearby blood vessel. Indeed, the ability to degrade the type IV collagen present in basement membranes was long ago found to correlate with metastatic ability (Liotta et al., 1980). The ability to invade through the ECM is dependent on the activity of matrix metalloproteinases (MMPs), a family of secreted or membrane-bound endopeptidases (Deryugina and Quigley,

2006). One such MMP of particular relevance is MT1-MMP (also called MMP14), a membrane-bound protein that is the active protease present in invadopodia, actin-rich protrusions first noted in transformed cells for their punctate degradation of fibronectin substrates *in vitro* (Chen, 1989; Chen and Chen, 1987; Chen et al., 1984, 1985). *In vivo*, invadopodia are used by invading tumor cells to punch their way through the ECM (Beaty and Condeelis, 2014; Castro-Castro et al., 2016; Itoh and Seiki, 2006; Nakahara et al., 1997; Sabeh et al., 2004).

Upon reaching a blood vessel, tumor cells must next enter into circulation by passing through the tight junctions between endothelial cells. Much like invasion through the ECM, intravasation requires the activity of cellular proteases and invadopodia (Gligorijevic et al., 2012). This process can also be aided by the presence of macrophages, which secrete epidermal growth factor (EGF) (Wyckoff et al., 2007). Moreover, the co-localization of a tumor cell expressing the ENA/VASP protein MENA, a macrophage and an endothelial cell has been called a tumor microenvironment of metastasis (TMEM) (Robinson et al., 2009). Such TMEMs are associated with a transient increase in vascular permeability, promoting tumor cell intravasation (Harney et al., 2015). Tumor cells may similarly invade lymphatic vessels and metastasize to lymph nodes, although metastatic spread through blood circulation appears to be the primary mode of transit for tumor cells that colonize distant organs (Naxerova et al., 2017).

Following entry into a blood vessel, tumor cells must survive their trip through the circulatory system, which is complicated by several factors. Circulating tumor cells must become immune to anoikis, a form of apoptosis that typically occurs when cells dependent on anchorage to the ECM become completely detached, which may occur through mutations in the caspase activation pathway or the Bcl-2 anti-apoptotic proteins, as well as the activation of oncogenes like Src (Simpson et al., 2008; Wei et al., 2004). Circulating tumor cells (CTCs) are also

susceptible to destructive shear stress caused by blood circulation itself, and to elimination by circulating natural killer (NK) cells, both of which may be evaded by aggregating with platelets to form a protective shell around the CTC (Joyce and Pollard, 2009; Wirtz et al., 2011).

Having survived transit through the circulatory system, tumor cells then arrest at a distant site. Much of this arrest is not specific to either the CTC or the site of its arrest, as tumor cells become physically lodged in vessels too small for them to pass (Benjamin and Hynes, 2017; MacDonald et al., 1992; Massagué and Obenauf, 2016; Morris et al., 1997), or they arrest at sites of lower, more permissive blood flow (Follain et al., 2018). Furthermore, tumor cells may circulate in aggregation with platelets and as tumor cell clusters, making their arrest due to size restrictions even more likely (Follain et al., 2018; Gasic et al., 1968; Gay and Felding-Habermann, 2011; Kim et al., 1999; Labelle et al., 2014; Lorger and Felding-Habermann, 2010). Arrest can also be aided by neutrophil extracellular traps (NETs), webs of DNA secreted by neutrophils that can snare circulating tumor cells and collect platelets (Cools-Lartigue et al., 2013; Demers and Wagner, 2013). There may also be tissue-specific factors that predispose tumor cells to arrest in certain organs, which will be reviewed later as part of the section on metastatic tropism.

Once arrested at a new site, a metastasizing tumor cell next exits the vessel. This can be accomplished by proliferating to the point of vessel rupture (Al-Mehdi et al., 2000). Otherwise, the tumor cell must actively invade out of the vessel through extravasation, generally passing between two endothelial cells (paracellular transit) (Strilic and Offermanns, 2017). Much like the reverse process of intravasation, extravasation is dependent on the degradative ability of invadopodia, as well as the proteases MMP1 and MMP2, along with the activity of platelets, neutrophils and macrophages (Gupta et al., 2007; Labelle and Hynes, 2012; Leong et al., 2014;

Qian et al., 2009). However, extravasation is not identical to intravasation, as the absence of a nearby primary tumor means that the arresting vessel is more stable and less leaky in comparison to the tumor cell's point of entry into circulation. Thus, tumor cells can secrete a number of proteins to promote vascular permeability at the site of extravasation, including CCL2, ANGPTL4, SPARC, COX2 and EREG (Gupta et al., 2007; Padua et al., 2008; Tichet et al., 2015; Wolf et al., 2012). Furthermore, recruited platelets (also involved in survival and arrest as described above) can secrete TGFβ, promoting a more invasive phenotype in tumor cells through activation of the TGFβ/Smad and NF-κB pathways and recruitment of neutrophils (Labelle et al., 2011).

After exiting a blood vessel at a distant site, a disseminated tumor cell must then seed a micrometastasis. The metastatic environment represents a dramatic shift compared to the metastatic cell's tissue of origin, and it presents a challenge to continued survival commensurate with the magnitude of that shift. Disseminated tumor cells can take advantage of a number of mechanisms to survive the shock of their new environment and seed a micrometastasis. Increased Src activation can provide resistance to death signals from TNF-related apoptosis-inducing ligand (TRAIL) (Zhang et al., 2009). TNFα from macrophages can promote cell-cell adhesion and protect against NK cells (Hafner et al., 1996; Stoelcker et al., 1995), while upregulation of L1CAM mediates pericyte-like spreading along vessels, activating YAP and MRTF (Er et al., 2018), with YAP itself being a potent promoter of metastasis and cell survival (Lamar et al., 2012, 2019).

Nevertheless, even if disseminated tumor cells manage to survive their new location, they are still confronted with the separate task of growing into a full metastatic tumor. Adjusting to grow at the metastatic site is daunting enough that these tumor cells can enter a state of

dormancy, which may last years (Mina and Sledge Jr, 2011). This dormancy can occur to single disseminated tumor cells that become quiescent, or to small clusters of cells that can grow no larger due to insufficient vascularization or frequent immune targeting (Aguirre Ghiso et al., 1999; Massagué and Obenauf, 2016; Sosa et al., 2014; Wikman et al., 2008). BMP7 and TGF-β2 secreted by the stroma can also enforce this dormant state (Bragado et al., 2013; Kobayashi et al., 2011). Much remains unknown about the specific factors that allow tumor cells eventually to escape these counterbalancing factors on their growth, but the relative length of the dormancy period, along with the threat posed by recurrent growth from dormant micrometastases, makes targeting dormant cells an important prospect for therapy (Ghajar, 2015).

The steps of the metastatic cascade are challenging to complete for even the most aggressive tumor cells, as fewer than .01% of the cells that leave a primary tumor manage to form metastases (Fidler, 1970; Luzzi et al., 1998). Furthermore, metastases can take decades to form, even though primary tumors can begin disseminating tumor cells at very early stages (Harper et al., 2016; Hosseini et al., 2016). However, many cancers are not detected until metastases have already formed, so even if the earlier stages of the metastatic cascade could be therapeutically targeted to prevent metastasis, strategies must be developed to eliminate established metastases, as well. The creation of such approaches depends on a complete understanding of all the factors present in a metastasis, known as the tumor microenvironment.

The tumor microenvironment

Tumor cells themselves only constitute part of the bulk of a metastasis, and understanding how to treat metastatic tumors effectively requires a more complete picture. Tumor cells recruit and influence other stromal cells to help their own growth, modify and

enhance the local vasculature to provide additional nutrients, and remodel the ECM to create a more permissive environment. Collectively, the assemblage of tumor cells, stromal cells, vasculature, metabolites and ECM is known as the tumor microenvironment, and each part of it contributes to metastatic growth.

One of the most important modifications that a tumor makes to its environment is the reshaping of the vasculature. Just as with normal cells, tumor cells require the delivery of oxygen and nutrients from blood circulation, and they produce waste that must be removed. Consequently, as a tumor grows, its abnormal presence requires a corresponding expansion of the local vasculature beyond its typical organization and limits. Angiogenesis, the formation of new blood vessels from existing ones, has therefore long been a focus of study in cancer biology (Folkman, 2002). Much of this research has focused on the primary tumor, the large size and random location of which can place extreme demands on the vasculature. Metastases, on the other hand, typically begin adjacent to the blood vessels from which they extravasated, placing them already in a supportive, perivascular niche (Kienast et al., 2010). Nevertheless, much like a primary tumor, their continued growth will eventually necessitate angiogenic expansion of this initial vasculature. This angiogenesis is dependent on signaling from vascular endothelial growth factor A (VEGF-A), which can be produced by nearly every cell type in the tumor microenvironment (Hanahan and Coussens, 2012). Its importance is such that inhibiting VEGF-A in metastases can send them into a state of dormancy or enhance their aggressiveness (Kienast et al., 2010).

The distribution of the vasculature is critical due to its control over the delivery and removal of various metabolites. The most obvious of these is oxygen, and oxygen levels can vary heavily from one tissue to another. For instance, the lung obviously has very high levels of

oxygen, while the liver is more oxygen-poor (Schild et al., 2018). The amount of oxygen can affect how metastatic cells metabolize, as tumor cells in hypoxic areas will tend toward more glycolytic activity, on top of the fact that tumor cells already have a predilection toward more glucose fermentation (known as the Warburg effect) (Vander Heiden et al., 2009). The availability of glucose is thus another crucial and variable feature of tumor microenvironments in different tissues, with glucose levels differing widely among metastatic tissues according to their normal energy requirements (Schild et al., 2018). Furthermore, limited glucose levels can result in competition between tumor and immune stromal cells for scarce resources, reducing the effectiveness of immune clearance by glucose-starved immune cells (Chang et al., 2015). Some tissue environments have more exotic nutrients. In particular, the brain is able to fuel itself with acetate or ketone bodies when glucose levels are low (Ebert et al., 2003), and tumor cells in the brain have also been found to take advantage of acetate as an alternative energy source (Mashimo et al., 2014). The nutrients present in a tumor microenvironment therefore vary considerably from tissue to tissue, and they accordingly place different strains on tumor cells growing there.

There are several different stromal cell populations in the tumor microenvironment, including a number of immune cell types, which can become affected or even co-opted by the tumor cells. The tumor can evade cytotoxic T leukocytes, responsible for immune clearance of tumor cells, by preventing their extravasation, limiting proliferation, inducing apoptosis, or physically excluding them through excessive ECM production (Joyce and Fearon, 2015). Neutrophils are recruited to tumors by numerous tumor-cell-secreted ligands for the neutrophil chemokine receptors CXCR1 and CXCR2, as well as more general tissue damage signals like damage-associated molecular patterns (Powell and Huttenlocher, 2016). Once present,

neutrophils can inhibit T cell function through secretion of arginase 1, modulate the ECM by secreting proteases, promote angiogenesis by producing Oncostatin M, and support tumor proliferation by secreting growth factors like hepatocyte growth factor (Dumitru et al., 2013; Queen et al., 2005; Rotondo et al., 2009; Wislez et al., 2003). Additionally, neutrophils can secrete NETs, which can enhance tumor cell migration and invasion, as well as awaken tumor cells from dormancy (Albrengues et al., 2018; Park et al., 2016). However, neutrophils can alternatively have anti-tumor effects depending on the amount of TGFβ present (Fridlender et al., 2009). Macrophages at metastatic sites can promote tumor cell growth through physical interaction, binding to tumor cell VCAM-1 and activating Akt (Chen et al., 2011; Qian et al., 2009). They can also protect tumor cells from chemotherapy via the production of cathepsins B and S, which induces myeloid-derived suppressor cells to secrete anti-immune IL-1β (Bruchard et al., 2013; Shree et al., 2011). Macrophages promote angiogenesis by making VEGF-A, and they can both secrete ECM proteins like SPARC as well as modify the ECM through secretion of various proteases (Hanahan and Coussens, 2012; Lin et al., 2007; Tichet et al., 2015).

Nevertheless, when it comes to ECM production, the most proficient stromal cells are fibroblasts, which have been particularly recognized for their corruption by tumor cells, as so-called cancer-associated fibroblasts (CAFs). The exact definition of a CAF remains unsettled, though there are at least two distinct types: myofibroblastic CAFs (myCAFs), which are positive for αSMA and produce large amounts of ECM proteins; and inflammatory CAFs (iCAFs), which are positive for IL-6 and CXCL12, and which secrete many cytokines (Öhlund et al., 2017). CAFs, and fibroblasts in general, are major sources of ECM in a tumor, in addition to producing several growth factors and pro-angiogenic proteins (Hanahan and Coussens, 2012). Moreover, CAFs can suppress immune clearance by secreting TGFβ, and they can increase resistance to

chemotherapy by inducing the multidrug resistance transporter ABCG2 (Stover et al., 2007; Su et al., 2018). Much like the other stromal components of the tumor microenvironment, fibroblasts can be used by tumor cells to further their progression in a complex variety of ways.

The extracellular matrix and the matrisome

The final part of the tumor microenvironment is the ECM. The collection of extracellular matrix proteins and their associated factors is also known as the matrisome, which was defined bioinformatically by searching the proteome for known ECM domains and negatively selecting against predicted transmembrane, kinase and phosphatase domains (Naba et al., 2012a). This resulted in just over one thousand predicted matrisome proteins in humans, of which around three hundred are "core matrisome" proteins and the remainder are "matrisome-associated" proteins (Naba et al., 2012b). Core matrisome proteins are those traditionally thought of as ECM, in the sense that they are often large proteins that assemble into mostly insoluble structures like interstitial matrices, basement membranes and cartilage, frequently through the activity of crosslinking enzymes (Hynes, 2012). However, the core matrisome has an enormous diversity of other proteins that bind to it, with an equally diverse set of additional functions. Understanding the full variety of proteins in the matrisome is key to understanding their vast potential for modulating metastatic growth. Full lists of all proteins in each category have been previously published (Naba et al., 2012a) and can also be found online (http://matrisomeproject.mit.edu/).

By far the most abundant of the core matrisome proteins are collagens, which constitute around 30% of the total protein mass in humans (Ricard-Blum, 2011). The unifying feature of the 28 members of the collagen superfamily is a triple helix that can take up nearly the entire length of the protein (as with collagen I), composed primarily of Gly-X-Y repeats, where X and

Y are typically proline and 4-hydroxyproline, respectively. Each triple helix is made up of three α chains, which can be either identical (homotrimers) or different (heterotrimers). Collagens can be broadly categorized as either fibril-forming collagens, fibril-associated collagens with interrupted triple-helices (FACIT) or network-forming basement membrane collagens (such as collagen IV) (Ricard-Blum, 2011; Yurchenco, 2011). Collagens are frequently covalently cross-linked by lysyl hydroxylases in a tissue-specific manner, thereby forming the intricately interwoven structures that support all of human physiology (Eyre and Wu, 2005).

The next set of core matrisome proteins are ECM glycoproteins, which, as their name suggests, are a broad category of extracellular proteins that have covalently attached oligosaccharide chains. This includes laminins, core components of basement membranes, and fibronectin, which can regulate adhesion, migration and differentiation (Schwarzbauer and DeSimone, 2011; Yurchenco, 2011). The ECM glycoproteins also encompass the so-called "matricellular proteins," which are expressed during development but only dynamically produced in adult tissue, typically in response to inflammation or wound repair. These include tenascins, osteopontin, periostin and SPARC (Insua-Rodríguez and Oskarsson, 2016). As a category united by their assembly into the insoluble matrix, the ECM glycoproteins span a wide range of different roles.

The final core matrisome proteins are the proteoglycans, a subset of glycoproteins that have attached glycosaminoglycan (GAG) chains composed of repeating disaccharides. These GAGs can be one of several types: chondroitin sulfate, dermatan sulfate, keratan sulfate and heparan sulfate (Theocharis and Karamanos, 2019). The large carbohydrate content of proteoglycans makes them unusually anionic, and they can sequester both water and cations, acting as porous gels (Hynes and Naba, 2012; Insua-Rodríguez and Oskarsson, 2016). Some

proteoglycans, like perlecan (HSPG2) and agrin, are present in basement membranes, while others can bind growth factors and cytokines, serving as a reservoir for future release by proteolysis (Sarrazin et al., 2011). The proteoglycan decorin is particularly notable for its tumor suppressive properties, as it can inhibit epidermal growth factor receptor (EGFR) signaling (Santra et al., 2000; Sofeu Feugaing et al., 2013).

The first group of "matrisome-associated" proteins are ECM regulators. This category includes crosslinking enzymes like the lysyl oxidase and hydroxylase family, which can crosslink collagens (Robins, 2007). Another major set of ECM regulators are proteases, which, in addition to being necessary for the proper processing of proteins like collagens into their final forms, can also dramatically remodel the ECM by cleaving it, releasing any sequestered growth factors and remodeling the matrix structure and stiffness (Yuzhalin et al., 2018). There are several families of extracellular proteases, such as MMPs, cathepsins and ADAMs. The last collection of ECM regulators are protease inhibitors, including the SERPIN family of serine protease suicide inhibitors (Law et al., 2006).

Next are the ECM-affiliated proteins, a miscellaneous collection of proteins that are either known to associate with the core matrisome despite not generally being considered as conventional fibril-associated proteins themselves, or that are often experimentally observed in ECM-enriched tissue samples (Naba et al., 2012b). Many of these proteins share structural similarities with core ECM proteins, though they have sometimes been considered secreted factors. The ECM-affiliated proteins include the heavily glycosylated mucins, collagen-binding complement component 1q (C1q) complex, carbohydrate-binding lectins, semaphorins and their receptors the plexins. It also encompasses the annexin and galectin protein families, which share

domains with classical ECM proteins and have an immensely varied array of intracellular and extracellular functions (Gerke and Moss, 2002; Liu and Rabinovich, 2005).

The final matrisome proteins are the secreted factors. Most obviously, this category contains growth factors such as EGF, the fibroblast growth factor (FGF) family, platelet-derived growth factor (PDGF) family, transforming growth factor (TGF) family, vascular endothelial growth factor (VEGF) family, and bone morphogenetic protein (BMP) family, all of which are known to bind specifically to ECM glycoproteins such as fibronectin and proteoglycans (Hynes, 2009). The secreted factor category also includes cytokines and chemokines, which can be bound and sequestered by the ECM much like growth factors; and the S100 family of proteins, which have a wide-ranging set of intracellular and extracellular signaling roles (Bresnick et al., 2015). The list of secreted factors is deliberately inclusive; that is, it includes secreted proteins that might bind to the ECM, even if they have not previously been shown to do so (Naba et al., 2012b).

The extracellular matrix in metastasis

Given the diversity of matrisome proteins just described, a metastatic tumor can employ the matrisome to its own ends in numerous ways. First, as mentioned previously, many ECM proteins can sequester growth factors, which can be released through the activity of secreted proteases to promote tumor cell proliferation (Hynes, 2009). As a result, secreted proteases, including MMPs and cathepsins, are frequently upregulated in metastases (Yuzhalin et al., 2018). Some growth factors, like FGF, TGFβ and other BMP family members, can actually bind to cell-surface receptors while still bound to an ECM co-factor, in this case the proteoglycan heparan sulfate, without the need for proteolytic degradation (Hynes, 2009; Mohammadi et al., 2005; Shi

and Massagué, 2003). Moreover, binding of TGFβ to latent transforming growth factor-β binding proteins (LTBPs) in the ECM is necessary for TGFβ to reach its active form (Rifkin, 2005). The ECM therefore regulates many aspects of growth factor signaling.

The biomechanical properties of the ECM can also regulate cell behavior and represent a relevant consideration in therapy (Chin et al., 2016). The prevailing view has long been that a stiffer matrix is associated with more aggressive tumors and worse patient survival (Najafi et al., 2019; Seewaldt, 2014). Indeed, a stiffer substrate can lead to activation of the metastasis promoter YAP, which boosts tumor cell survival and proliferation (Dupont et al., 2011; Lamar et al., 2012; Yuan et al., 2015). Moreover, a fibrotic, collagen-rich ECM has been shown to be able to wake breast cancer metastases from dormancy (Barkan et al., 2010). Excessive ECM deposition can even act as a barrier to drug delivery, and in some cases, depleting this ECM can increase drug perfusion and efficacy in metastases (Rahbari et al., 2016). However, non-specific reduction of the ECM can lead to more aggressive tumors in some situations like pancreatic ductal adenocarcinoma (PDAC), suggesting the need for a more nuanced view toward therapeutic modulation of the ECM (Amakye et al., 2013).

Several specific ECM proteins have also been identified with roles in certain metastatic niches. Fibronectin has long been noted for its association with metastatic cancer and upregulation in many tumors, and peptides from fibronectin's cell-adhesive region can inhibit metastasis of melanoma to the lungs (Akiyama et al., 1995; Humphries et al., 1986). Indeed, fibronectin was one of a few genes shown to be upregulated in highly metastatic, *in vivo*-selected melanoma cells (Clark et al., 2000). More recently, increased fibronectin production has been revealed to enhance metastasis of ovarian cancer, head and neck squamous cell carcinoma, colorectal cancer, Lewis lung carcinoma and melanoma, suggesting a broad role for fibronectin

in metastasis (Barbazán et al., 2017; Hsu et al., 2017; Kenny et al., 2014; Malik et al., 2010). Tenascin C was identified in breast cancer metastases to the lungs, where it enhances stem cell signaling as well as tumor cell migration and proliferation, and knocking down tenascin C in tumor cells reduces their metastasis to the lungs (Midwood and Orend, 2009; Minn et al., 2005; Oskarsson et al., 2011). Moreover, tenascin C can promote tumor progression and dissemination of lung adenocarcinoma (Gocheva et al., 2017). However, tenascin C has additionally been found to suppress T cell activation in the prostate and activate Notch signaling in the brain, so it may be relevant in tissues aside from the lungs (Jachetti et al., 2015; Sarkar et al., 2017). Similarly, osteopontin, originally detected as being secreted by several transformed cell lines (Senger et al., 1979, 1980), has been shown to be important in metastasis to multiple tissues, including the lungs and bone (Allan et al., 2006; Kang et al., 2003; Weber, 2001). Periostin expression has been demonstrated to be critical for breast cancer metastasis to the lungs in some experimental models, and it can promote Wnt signaling, induce angiogenesis, and bind tenascin C to incorporate it into the ECM (Kii et al., 2010; Malanchi et al., 2011; Shao et al., 2004; Wang et al., 2013). Expression of SPARC, which is regulated by integrin β4 signaling, was likewise shown to be crucial for breast cancer lung metastasis (Gerson et al., 2012; Minn et al., 2005). Modulating even individual ECM proteins can thus have critical effects on metastasis in particular contexts.

Metastatic tropism

As described above, metastasis is a complicated process, consisting of multiple steps and involving numerous metastatic niche components of the tumor microenvironment. When a cancer cell leaves its primary tumor, what then determines where that cell will end up and grow?

All cancers are able to metastasize to multiple distant sites, yet each cancer also has certain organs to which it most commonly metastasizes (Figure 2). Although there are some discernable patterns, like the frequency of metastases to the lungs, liver and bone from many cancers, the overall landscape of metastatic tropism is complex (Budczies et al., 2014). Nevertheless, there are several types of factors that are known to contribute to the organotropism of a particular cancer.

The first and most direct factor controlling metastatic tropism is the available route of dissemination. Tumor cells will often arrest physically in the first vessel that is too small for them to pass through, so the first tissue that they reach after leaving the primary site will accrue many disseminated tumor cells (Massagué and Obenauf, 2016). This is especially notable in colorectal tumors. Blood from the colon and proximal rectum is drained by hepatic circulation to the liver, while blood from the distal rectum goes to the lung; accordingly, colorectal tumors metastasize primarily to the liver and secondarily to the lung (Riihimäki et al., 2016). Similarly, some tumors are able to bypass hematogenous spread and much of the metastatic cascade, with visible effects on their tropism. Gastrointestinal and ovarian tumor cells can spread through ascitic fluid to other organs in the peritoneal cavity, as well as to the peritoneum itself (Mikuła-Pietrasik et al., 2018). For other primary tumors with less direct routes of dissemination, metastatic tropism is affected by other factors.

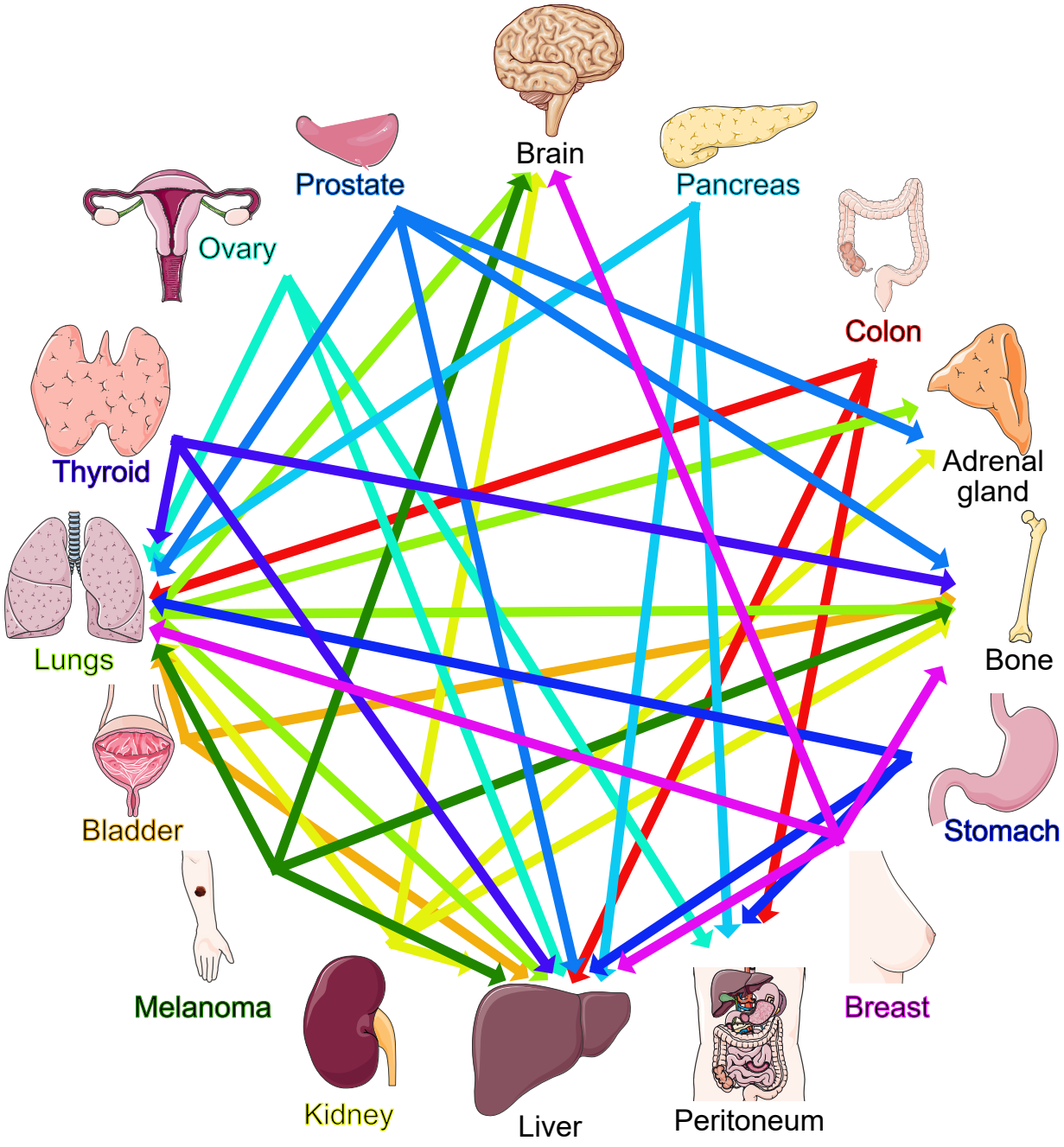

Figure 2. The complicated network of metastatic organotropism. Summary of some common cancers and their main sites of metastasis. Colors indicate tissue of origin, and arrows indicate direction of metastasis. Adapted from information available at https://www.cancer.gov/types/metastatic-cancer. Images shown are modified from the Servier Medical Art database under a Creative Commons Attribution 3.0 license (https://smart.servier.com/).

Another such determining step in tropism is arrest. While many tumor cells arrest simply due to the restrictive size of vessels, some circulating cells arrest due to specific adhesive interactions. For instance, prostate cancer cells, among other carcinomas, tend to upregulate the E-Selectin ligand Sialyl-Lewis X, thereby enhancing their arrest in the constitutively E-Selectin-expressing bone endothelium (Barthel et al., 2009; Borsig et al., 2002; Schweitzer et al., 1996). As another specific example, metastasizing breast cancer cells can express metadherin, enhancing their arrest in the lungs; indeed, a single metadherin domain on its own has been shown to be sufficient to bind to the lung vasculature (Brown and Ruoslahti, 2004; Hu et al., 2009), although metadherin has more recently been identified as a general promoter of tumor progression (Wan et al., 2014a, 2014b). More generally, phage-display peptide libraries screened *in vivo* have shown the potential to home to multiple different organs (Pasqualini and Ruoslahti, 1996). This has led to the hypothesis of vascular "zip codes" that can direct adhesion in each tissue. While research into this hypothesis has not revealed specific receptors mediating tumor cell homing aside from attraction to chemokines like CXCL12 in the lungs and bone marrow (Müller et al., 2001), these results at least raise the possibility for additional, specific adhesive interactions relevant to metastatic tropism (Ruoslahti, 2004; Teesalu et al., 2012).

Following arrest, tropism can also be affected by the process of extravasation in each secondary tissue. First, the endothelium that tumor cells must cross in order to extravasate varies in organization from tissue to tissue. The liver endothelium, for example, is fenestrated, loosely organized with many openings, and it lacks a sub-endothelial basement membrane (Obenauf and Massagué, 2015). As a consequence, the liver endothelium is more permissive to extravasation. On the other hand, the brain is protected by the tight endothelial formation of the blood-brain barrier. To cross it, tumor cells must express certain specific extravasation mediators or take an

alternate route. For instance, breast cancer cells that express high levels of the protease cathepsin S are more adept at metastasizing to the brain (Sevenich et al., 2014), while leukemia cells can bypass the blood-brain barrier by entering the brain through the meningeal bone marrow (Yao et al., 2018). The lung, while not as tightly sealed as the brain, still has an organized endothelial barrier and basement membrane, making it more difficult for tumor cells to enter compared to the liver (Nguyen et al., 2009). Furthermore, some of the factors that tumor cells secrete to increase vascular permeability and ease their passage through the endothelium act in a tissue-specific manner. ANGPTL4 secreted by breast cancer cells can enhance their extravasation to the lungs but has no effect on bone metastasis (Padua et al., 2008). Thus, the relative extravasation ability of circulating tumor cells, including their expression of proteases and factors targeting the endothelium, can determine the tissues to which tumor cells can effectively metastasize.

The metabolic environment of different organs is another contributing element to tropism, as the survival and proliferation of tumor cells after arriving at a secondary site requires adaptation to its metabolic characteristics (Schild et al., 2018). As previously noted, the brain is able to use a variety of energy sources when glucose is low, including acetate (Ebert et al., 2003). Similarly, brain metastases from several different primary tumors have been found to be able to convert acetate to acetyl-CoA in order to fuel the tricarboxylic acid (TCA) cycle, a unique adaptation to the brain's available nutrients (Mashimo et al., 2014). On the other hand, the lungs have high levels of oxygen and toxic compounds, making them a very pro-oxidant environment (Valavanidis et al., 2013). Consequently, tumor cells metastasizing to the lungs have been shown to upregulate PGC-1α, PRDX2 and NRF2, stimulating anti-oxidant production to deal with reactive oxygen species toxicity (Basnet et al., 2019; LeBleu et al., 2014; Stresing et al., 2013). The liver microenvironment, meanwhile, is much more hypoxic and conducive to

anerobic energy production through glycolysis, and primary hepatocellular carcinomas preferentially use glycolytic metabolism (Jiao et al., 2018; Lin et al., 2018). Accordingly, breast cancer metastases to the liver have been demonstrated to reduce their TCA cycle metabolism by upregulating pyruvate dehydrogenase kinase 1. Metastases to the bone can increase *de novo* L-serine synthesis and lactate secretion to promote osteoclast differentiation and proliferation, thereby freeing nutrients and niche space through osteolysis (Lemma et al., 2017; Pollari et al., 2011). Tropism can therefore be affected by the suitability of disseminated tumor cells to adapt to their new metabolic environment and take advantage of any unique nutrients.

The immunological milieu of a secondary tissue can also determine how well tumor cells can metastasize there. Liver tissue has an abundance of innate immune cells, complicating tumor cell attempts at metastatic survival and outgrowth (Obenauf and Massagué, 2015). Liver-resident NK cells have been shown to constitutively express the apoptosis-inducing TRAIL, and neutralizing TRAIL with a blocking antibody can increase liver metastasis (Takeda et al., 2001). Conversely, the brain is an immunologically privileged site, so immune surveillance is routinely handled by microglia, brain-resident macrophages that have low antigen-presenting ability (Bowman et al., 2016; Nimmerjahn et al., 2005). However, disruption of the blood-brain barrier by metastases can radically change this immune environment by allowing the entry of myeloid and lymphoid cells that are typically excluded (Sevenich, 2019). The availability of a supply of developing hematopoietic cells in the bone marrow provides tumor cells with opportunities to modulate their own immune microenvironment (D'Amico and Roato, 2015). For instance, tumor cells can induce plasmacytoid dendritic cells in the bone marrow to recruit myeloid-derived suppressor cells (MDSCs) and inhibit anti-tumor immune responses, as well as induce those MDSCs to differentiate into osteoclasts to increase osteolytic activity (Das et al., 2011; Sawant et

al., 2012; Zhuang et al., 2012). In the lung, resident populations of conventional dendritic cells and so-called "patrolling" monocytes have been demonstrated to mediate early immune responses against disseminated tumor cells, and inhibiting either immune cell type significantly increases lung metastasis (Hanna et al., 2015; Headley et al., 2016). Depending on the tissue, tumor cells are presented with a different set of both immune challenges and chances to co-opt the immune system.

Finally, ECM proteins can also affect the tissues in which disseminated tumor cell seeds will take root. Some such ECM proteins were mentioned in the previous section. Knocking down tenascin C or periostin, for example, inhibits breast cancer metastasis to the lungs (Malanchi et al., 2011; Oskarsson et al., 2011). Other ECM or ECM-associated proteins have been identified in analyses of *in vivo*-selected cell lines. SPARC was found to be upregulated in lung-tropic breast cancer cells, and ADAMTS1 was over-expressed in bone tropic cells (Kang et al., 2003; Minn et al., 2005). However, these studies have several limitations. They do not distinguish between proteins that actually promote a specific organotropism and those that simply promote metastasis in general. They also focus on only one or a subset of metastatic tissues at a time, making it difficult to ascertain whether a given protein that promotes metastasis to a certain organ is specific and truly organotropic. Indeed, MMP1 was identified as a promoter of both lung and bone metastasis in the above studies, and osteopontin, despite being initially recognized for promoting bone metastasis, has since been shown to promote lung metastasis, as well (Allan et al., 2006; Kang et al., 2003; Minn et al., 2005). Moreover, studies on organotropic genes have traditionally focused on RNA expression data, but RNA levels do not always correlate well with protein levels, particularly for ECM proteins with long half-lives (Edfors et al., 2016; Mertins et al., 2016; Payne, 2015; Vogel and Marcotte, 2012). Accordingly, further research is required that

both makes use of proteomic methods and compares the protein levels of the ECM among multiple metastatic tissues.

This thesis seeks to provide new insight into how metastasis is promoted on both a general and tissue-specific level, through an exploration of one particular metastasis promoter and a broad, proteomic survey of metastases to different organs.

- In Chapter 2, I will discuss the intracellular scaffold protein IQGAP1 and demonstrate that it can promote metastasis in both melanoma and breast cancer models. I will also show that its expression is particularly important for the extravasation of circulating tumor cells.
- In Chapter 3, I will describe a quantitative proteomic analysis of brain, lung, liver and bone metastases derived from the same parental breast cancer cell line. I will then explore what these data reveal about how the tumor and stroma create different metastatic niches, and I will demonstrate that knocking down a particular ECM protein, SERPINB1, can alter the metastatic tropism of the parental cells.
- In Chapter 4, I will summarize the work detailed in this thesis, propose potential further studies, and discuss significant unanswered issues as well as overall implications.

References

Aguirre Ghiso, J.A., Kovalski, K., and Ossowski, L. (1999). Tumor dormancy induced by downregulation of urokinase receptor in human carcinoma involves integrin and MAPK signaling. J. Cell Biol. *147*, 89–104.

Akiyama, S.K., Olden, K., and Yamada, K.M. (1995). Fibronectin and integrins in invasion and metastasis. Cancer Metastasis Rev. *14*, 173–189.

Albrengues, J., Shields, M.A., Ng, D., Park, C.G., Ambrico, A., Poindexter, M.E., Upadhyay, P., Uyeminami, D.L., Pommier, A., Küttner, V., et al. (2018). Neutrophil extracellular traps produced during inflammation awaken dormant cancer cells in mice. Science *361*, eaao4227.

Allan, A.L., George, R., Vantyghem, S.A., Lee, M.W., Hodgson, N.C., Engel, C.J., Holliday, R.L., Girvan, D.P., Scott, L.A., Postenka, C.O., et al. (2006). Role of the Integrin-Binding Protein Osteopontin in Lymphatic Metastasis of Breast Cancer. Am. J. Pathol. *169*, 233–246.

Al-Mehdi, A.B., Tozawa, K., Fisher, A.B., Shientag, L., Lee, A., and Muschel, R.J. (2000). Intravascular origin of metastasis from the proliferation of endothelium-attached tumor cells: a new model for metastasis. Nat. Med. *6*, 100–102.

Amakye, D., Jagani, Z., and Dorsch, M. (2013). Unraveling the therapeutic potential of the Hedgehog pathway in cancer. Nat. Med. *19*, 1410–1422.

Barbazán, J., Alonso-Alconada, L., Elkhatib, N., Geraldo, S., Gurchenkov, V., Glentis, A., Niel, G. van, Palmulli, R., Fernández, B., Viaño, P., et al. (2017). Liver Metastasis Is Facilitated by the Adherence of Circulating Tumor Cells to Vascular Fibronectin Deposits. Cancer Res. *77*, 3431–3441.

Barkan, D., Touny, L.H.E., Michalowski, A.M., Smith, J.A., Chu, I., Davis, A.S., Webster, J.D., Hoover, S., Simpson, R.M., Gauldie, J., et al. (2010). Metastatic Growth from Dormant Cells Induced by a Col-I–Enriched Fibrotic Environment. Cancer Res. *70*, 5706–5716.

Barthel, S.R., Wiese, G.K., Cho, J., Opperman, M.J., Hays, D.L., Siddiqui, J., Pienta, K.J., Furie, B., and Dimitroff, C.J. (2009). Alpha 1,3 fucosyltransferases are master regulators of prostate cancer cell trafficking. Proc. Natl. Acad. Sci. U. S. A. *106*, 19491–19496.

Basnet, H., Tian, L., Ganesh, K., Huang, Y.-H., Macalinao, D.G., Brogi, E., Finley, L.W., and Massagué, J. (2019). Flura-seq identifies organ-specific metabolic adaptations during early metastatic colonization. ELife *8*.

Beaty, B.T., and Condeelis, J. (2014). Digging a little deeper: The stages of invadopodium formation and maturation. Eur. J. Cell Biol.

Benjamin, D.C., and Hynes, R.O. (2017). Intravital imaging of metastasis in adult Zebrafish. BMC Cancer *17*, 660.

Binder, M., Roberts, C., Spencer, N., Antoine, D., and Cartwright, C. (2014). On the Antiquity of Cancer: Evidence for Metastatic Carcinoma in a Young Man from Ancient Nubia (c. 1200BC). PLOS ONE *9*, e90924.

Borsig, L., Wong, R., Hynes, R.O., Varki, N.M., and Varki, A. (2002). Synergistic effects of L- and P-selectin in facilitating tumor metastasis can involve non-mucin ligands and implicate leukocytes as enhancers of metastasis. Proc. Natl. Acad. Sci. U. S. A. *99*, 2193–2198.

Bos, P.D., Zhang, X.H.-F., Nadal, C., Shu, W., Gomis, R.R., Nguyen, D.X., Minn, A.J., van de Vijver, M.J., Gerald, W.L., Foekens, J.A., et al. (2009). Genes that mediate breast cancer metastasis to the brain. Nature *459*, 1005–1009.

Bowman, R.L., Klemm, F., Akkari, L., Pyonteck, S.M., Sevenich, L., Quail, D.F., Dhara, S., Simpson, K., Gardner, E.E., Iacobuzio-Donahue, C.A., et al. (2016). Macrophage Ontogeny Underlies Differences in Tumor-Specific Education in Brain Malignancies. Cell Rep. *17*, 2445–2459.

Bragado, P., Estrada, Y., Parikh, F., Krause, S., Capobianco, C., Farina, H.G., Schewe, D.M., and Aguirre-Ghiso, J.A. (2013). TGF-β2 dictates disseminated tumour cell fate in target organs through TGF-β-RIII and p38α/β signalling. Nat. Cell Biol. *15*, 1351–1361.

Bresnick, A.R., Weber, D.J., and Zimmer, D.B. (2015). S100 proteins in cancer. Nat. Rev. Cancer *15*, 96–109.

Brown, D.M., and Ruoslahti, E. (2004). Metadherin, a cell surface protein in breast tumors that mediates lung metastasis. Cancer Cell *5*, 365–374.

Bruchard, M., Mignot, G., Derangère, V., Chalmin, F., Chevriaux, A., Végran, F., Boireau, W., Simon, B., Ryffel, B., Connat, J.L., et al. (2013). Chemotherapy-triggered cathepsin B release in myeloid-derived suppressor cells activates the Nlrp3 inflammasome and promotes tumor growth. Nat. Med. *19*, 57–64.

Budczies, J., von Winterfeld, M., Klauschen, F., Bockmayr, M., Lennerz, J.K., Denkert, C., Wolf, T., Warth, A., Dietel, M., Anagnostopoulos, I., et al. (2014). The landscape of metastatic progression patterns across major human cancers. Oncotarget *6*, 570–583.

Castro-Castro, A., Marchesin, V., Monteiro, P., Lodillinsky, C., Rossé, C., and Chavrier, P. (2016). Cellular and Molecular Mechanisms of MT1-MMP-Dependent Cancer Cell Invasion. Annu. Rev. Cell Dev. Biol. *32*, 555–576.

Chaffer, C.L., and Weinberg, R.A. (2011). A Perspective on Cancer Cell Metastasis. Science *331*, 1559–1564.

Chaffer, C.L., San Juan, B.P., Lim, E., and Weinberg, R.A. (2016). EMT, cell plasticity and metastasis. Cancer Metastasis Rev. *35*, 645–654.

Chang, C.-H., Qiu, J., O'Sullivan, D., Buck, M.D., Noguchi, T., Curtis, J.D., Chen, Q., Gindin, M., Gubin, M.M., van der Windt, G.J.W., et al. (2015). Metabolic Competition in the Tumor Microenvironment Is a Driver of Cancer Progression. Cell *162*, 1229–1241.

Chen, W.T. (1989). Proteolytic activity of specialized surface protrusions formed at rosette contact sites of transformed cells. J. Exp. Zool. *251*, 167–185.

Chen, J.M., and Chen, W.T. (1987). Fibronectin-degrading proteases from the membranes of transformed cells. Cell *48*, 193–203.

Chen, Q., Zhang, X.H.-F., and Massagué, J. (2011). Macrophage Binding to Receptor VCAM-1 Transmits Survival Signals in Breast Cancer Cells that Invade the Lungs. Cancer Cell *20*, 538–549.

Chen, W.T., Olden, K., Bernard, B.A., and Chu, F.F. (1984). Expression of transformation-associated protease(s) that degrade fibronectin at cell contact sites. J. Cell Biol. *98*, 1546–1555.

Chen, W.T., Chen, J.M., Parsons, S.J., and Parsons, J.T. (1985). Local degradation of fibronectin at sites of expression of the transforming gene product pp60src. Nature *316*, 156–158.

Chin, L., Xia, Y., Discher, D.E., and Janmey, P.A. (2016). Mechanotransduction in cancer. Curr. Opin. Chem. Eng. *11*, 77–84.

Clark, E.A., Golub, T.R., Lander, E.S., and Hynes, R.O. (2000). Genomic analysis of metastasis reveals an essential role for RhoC. Nature *406*, 532–535.

Cools-Lartigue, J., Spicer, J., McDonald, B., Gowing, S., Chow, S., Giannias, B., Bourdeau, F., Kubes, P., and Ferri, L. (2013). Neutrophil extracellular traps sequester circulating tumor cells and promote metastasis. J. Clin. Invest.

D'Amico, L., and Roato, I. (2015). The Impact of Immune System in Regulating Bone Metastasis Formation by Osteotropic Tumors. J. Immunol. Res. *2015*, 143526.

Das, S., Samant, R.S., and Shevde, L.A. (2011). Hedgehog Signaling Induced by Breast Cancer Cells Promotes Osteoclastogenesis and Osteolysis. J. Biol. Chem. *286*, 9612–9622.

Demers, M., and Wagner, D.D. (2013). Neutrophil extracellular traps: A new link to cancer-associated thrombosis and potential implications for tumor progression. Oncoimmunology *2*, e22946.

Deryugina, E.I., and Quigley, J.P. (2006). Matrix metalloproteinases and tumor metastasis. Cancer Metastasis Rev. *25*, 9–34.

Dumitru, C.A., Lang, S., and Brandau, S. (2013). Modulation of neutrophil granulocytes in the tumor microenvironment: Mechanisms and consequences for tumor progression. Semin. Cancer Biol. *23*, 141–148.

Dupont, S., Morsut, L., Aragona, M., Enzo, E., Giulitti, S., Cordenonsi, M., Zanconato, F., Le Digabel, J., Forcato, M., Bicciato, S., et al. (2011). Role of YAP/TAZ in mechanotransduction. Nature *474*, 179–183.

Ebert, D., Haller, R.G., and Walton, M.E. (2003). Energy Contribution of Octanoate to Intact Rat Brain Metabolism Measured by 13C Nuclear Magnetic Resonance Spectroscopy. J. Neurosci. *23*, 5928–5935.

Edfors, F., Danielsson, F., Hallström, B.M., Käll, L., Lundberg, E., Pontén, F., Forsström, B., and Uhlén, M. (2016). Gene-specific correlation of RNA and protein levels in human cells and tissues. Mol. Syst. Biol. *12*, 883.

Er, E.E., Valiente, M., Ganesh, K., Zou, Y., Agrawal, S., Hu, J., Griscom, B., Rosenblum, M., Boire, A., Brogi, E., et al. (2018). Pericyte-like spreading by disseminated cancer cells activates YAP and MRTF for metastatic colonization. Nat. Cell Biol. *20*, 966.

Eyre, D.R., and Wu, J.-J. (2005). Collagen Cross-Links. In Collagen: Primer in Structure, Processing and Assembly, J. Brinckmann, H. Notbohm, and P.K. Müller, eds. (Berlin, Heidelberg: Springer Berlin Heidelberg), pp. 207–229.

Fidler, I.J. (1970). Metastasis: quantitative analysis of distribution and fate of tumor emboli labeled with 125 I-5-iodo-2'-deoxyuridine. J. Natl. Cancer Inst. *45*, 773–782.

Fidler, I.J. (1973). Selection of Successive Tumour Lines for Metastasis. Nature. New Biol. *242*, 148–149.

Fisher, B., and Fisher, E.R. (1967). The organ distribution of disseminated 51 Cr-labeled tumor cells. Cancer Res. *27*, 412–420.

Folkman, J. (2002). Role of angiogenesis in tumor growth and metastasis. Semin. Oncol. *29*, 15–18.

Follain, G., Osmani, N., Azevedo, A.S., Allio, G., Mercier, L., Karreman, M.A., Solecki, G., Garcia Leòn, M.J., Lefebvre, O., Fekonja, N., et al. (2018). Hemodynamic Forces Tune the Arrest, Adhesion, and Extravasation of Circulating Tumor Cells. Dev. Cell *45*, 33-52.e12.

Fridlender, Z.G., Sun, J., Kim, S., Kapoor, V., Cheng, G., Ling, L., Worthen, G.S., and Albelda, S.M. (2009). Polarization of Tumor-Associated Neutrophil Phenotype by TGF-β: "N1" versus "N2" TAN. Cancer Cell *16*, 183–194.

Gasic, G.J., Gasic, T.B., and Stewart, C.C. (1968). Antimetastatic effects associated with platelet reduction. Proc. Natl. Acad. Sci. U. S. A. *61*, 46–52.

Gay, L.J., and Felding-Habermann, B. (2011). Contribution of platelets to tumour metastasis. Nat. Rev. Cancer *11*, 123–134.

Gerke, V., and Moss, S.E. (2002). Annexins: From Structure to Function. Physiol. Rev. *82*, 331–371.

Gerson, K.D., Shearstone, J.R., Maddula, V.S.R.K., Seligmann, B.E., and Mercurio, A.M. (2012). Integrin β4 regulates SPARC protein to promote invasion. J. Biol. Chem. *287*, 9835–9844.

Ghajar, C.M. (2015). Metastasis prevention by targeting the dormant niche. Nat. Rev. Cancer *15*, 238–247.

Gligorijevic, B., Wyckoff, J., Yamaguchi, H., Wang, Y., Roussos, E.T., and Condeelis, J. (2012). N-WASP-mediated invadopodium formation is involved in intravasation and lung metastasis of mammary tumors. J. Cell Sci. *125*, 724–734.

Gocheva, V., Naba, A., Bhutkar, A., Guardia, T., Miller, K.M., Li, C.M.-C., Dayton, T.L., Sanchez-Rivera, F.J., Kim-Kiselak, C., Jailkhani, N., et al. (2017). Quantitative proteomics identify Tenascin-C as a promoter of lung cancer progression and contributor to a signature prognostic of patient survival. Proc. Natl. Acad. Sci. U. S. A. *114*, E5625–E5634.

Gupta, G.P., Nguyen, D.X., Chiang, A.C., Bos, P.D., Kim, J.Y., Nadal, C., Gomis, R.R., Manova-Todorova, K., and Massagué, J. (2007). Mediators of vascular remodelling co-opted for sequential steps in lung metastasis. Nature *446*, 765–770.

Hafner, M., Orosz, P., Krüger, A., and Männel, D.N. (1996). TNF promotes metastasis by impairing natural killer cell activity. Int. J. Cancer *66*, 388–392.

Hanahan, D., and Coussens, L.M. (2012). Accessories to the Crime: Functions of Cells Recruited to the Tumor Microenvironment. Cancer Cell *21*, 309–322.

Hanahan, D., and Weinberg, R.A. (2011). Hallmarks of Cancer: The Next Generation. Cell *144*, 646–674.

Hanna, R.N., Cekic, C., Sag, D., Tacke, R., Thomas, G.D., Nowyhed, H., Herrley, E., Rasquinha, N., McArdle, S., Wu, R., et al. (2015). Patrolling monocytes control tumor metastasis to the lung. Science *350*, 985–990.

Harney, A.S., Arwert, E.N., Entenberg, D., Wang, Y., Guo, P., Qian, B.-Z., Oktay, M.H., Pollard, J.W., Jones, J.G., and Condeelis, J.S. (2015). Real-Time Imaging Reveals Local, Transient Vascular Permeability, and Tumor Cell Intravasation Stimulated by TIE2hi Macrophage–Derived VEGFA. Cancer Discov. *5*, 932–943.

Harper, K.L., Sosa, M.S., Entenberg, D., Hosseini, H., Cheung, J.F., Nobre, R., Avivar-Valderas, A., Nagi, C., Girnius, N., Davis, R.J., et al. (2016). Mechanism of early dissemination and metastasis in Her2+ mammary cancer. Nature *540*, 588–592.

Hart, I.R., and Fidler, I.J. (1980). Role of Organ Selectivity in the Determination of Metastatic Patterns of B16 Melanoma. Cancer Res. *40*, 2281–2287.

Headley, M.B., Bins, A., Nip, A., Roberts, E.W., Looney, M.R., Gerard, A., and Krummel, M.F. (2016). Visualization of immediate immune responses to pioneer metastatic cells in the lung. Nature *531*, 513–517.

Hosseini, H., Obradović, M.M.S., Hoffmann, M., Harper, K.L., Sosa, M.S., Werner-Klein, M., Nanduri, L.K., Werno, C., Ehrl, C., Maneck, M., et al. (2016). Early dissemination seeds metastasis in breast cancer. Nature *540*, 552–558.

Hsu, J.-Y., Chang, J.-Y., Chang, K.-Y., Chang, W.-C., and Chen, B.-K. (2017). Epidermal growth factor-induced pyruvate dehydrogenase kinase 1 expression enhances head and neck squamous cell carcinoma metastasis via up-regulation of fibronectin. FASEB J. Off. Publ. Fed. Am. Soc. Exp. Biol. *31*, 4265–4276.

Hu, G., Chong, R.A., Yang, Q., Wei, Y., Blanco, M.A., Li, F., Reiss, M., Au, J.L.-S., Haffty, B.G., and Kang, Y. (2009). MTDH activation by 8q22 genomic gain promotes chemoresistance and metastasis of poor-prognosis breast cancer. Cancer Cell *15*, 9–20.

Humphries, M.J., Olden, K., and Yamada, K.M. (1986). A synthetic peptide from fibronectin inhibits experimental metastasis of murine melanoma cells. Science *233*, 467–470.

Hynes, R.O. (2009). The Extracellular Matrix: Not Just Pretty Fibrils. Science *326*, 1216–1219.

Hynes, R.O. (2012). The evolution of metazoan extracellular matrix. J Cell Biol *196*, 671–679.

Hynes, R.O., and Naba, A. (2012). Overview of the Matrisome—An Inventory of Extracellular Matrix Constituents and Functions. Cold Spring Harb. Perspect. Biol. *4*, a004903.

Insua-Rodríguez, J., and Oskarsson, T. (2016). The extracellular matrix in breast cancer. Adv. Drug Deliv. Rev. *97*, 41–55.

Itoh, Y., and Seiki, M. (2006). MT1-MMP: A potent modifier of pericellular microenvironment. J. Cell. Physiol. *206*, 1–8.

Jachetti, E., Caputo, S., Mazzoleni, S., Brambillasca, C.S., Parigi, S.M., Grioni, M., Piras, I.S., Restuccia, U., Calcinotto, A., Freschi, M., et al. (2015). Tenascin-C Protects Cancer Stem-like Cells from Immune Surveillance by arresting T cell activation. Cancer Res.

Jiao, L., Zhang, H.-L., Li, D.-D., Yang, K.-L., Tang, J., Li, X., Ji, J., Yu, Y., Wu, R.-Y., Ravichandran, S., et al. (2018). Regulation of glycolytic metabolism by autophagy in liver cancer involves selective autophagic degradation of HK2 (hexokinase 2). Autophagy *14*, 671–684.

Jolly, M.K., Ware, K.E., Gilja, S., Somarelli, J.A., and Levine, H. (2017). EMT and MET: necessary or permissive for metastasis? Mol. Oncol. *11*, 755–769.

Joyce, J.A., and Fearon, D.T. (2015). T cell exclusion, immune privilege, and the tumor microenvironment. Science *348*, 74–80.

Joyce, J.A., and Pollard, J.W. (2009). Microenvironmental regulation of metastasis. Nat. Rev. Cancer *9*, 239–252.

Kalluri, R., and Weinberg, R.A. (2009). The basics of epithelial-mesenchymal transition. J. Clin. Invest. *119*, 1420–1428.

Kang, Y., Siegel, P.M., Shu, W., Drobnjak, M., Kakonen, S.M., Cordón-Cardo, C., Guise, T.A., and Massagué, J. (2003). A multigenic program mediating breast cancer metastasis to bone. Cancer Cell *3*, 537–549.

Kenny, H.A., Chiang, C.-Y., White, E.A., Schryver, E.M., Habis, M., Romero, I.L., Ladanyi, A., Penicka, C.V., George, J., Matlin, K., et al. (2014). Mesothelial cells promote early ovarian cancer metastasis through fibronectin secretion. J. Clin. Invest. *124*, 4614–4628.

Kienast, Y., von Baumgarten, L., Fuhrmann, M., Klinkert, W.E.F., Goldbrunner, R., Herms, J., and Winkler, F. (2010). Real-time imaging reveals the single steps of brain metastasis formation. Nat. Med. *16*, 116–122.

Kii, I., Nishiyama, T., Li, M., Matsumoto, K., Saito, M., Amizuka, N., and Kudo, A. (2010). Incorporation of Tenascin-C into the Extracellular Matrix by Periostin Underlies an Extracellular Meshwork Architecture. J. Biol. Chem. *285*, 2028–2039.

Kim, Y.J., Borsig, L., Han, H.L., Varki, N.M., and Varki, A. (1999). Distinct selectin ligands on colon carcinoma mucins can mediate pathological interactions among platelets, leukocytes, and endothelium. Am. J. Pathol. *155*, 461–472.

Klein, C.A. (2008). The Metastasis Cascade. Science *321*, 1785–1787.

Kobayashi, A., Okuda, H., Xing, F., Pandey, P.R., Watabe, M., Hirota, S., Pai, S.K., Liu, W., Fukuda, K., Chambers, C., et al. (2011). Bone morphogenetic protein 7 in dormancy and metastasis of prostate cancer stem-like cells in bone. J. Exp. Med. *208*, 2641–2655.

Labelle, M., and Hynes, R.O. (2012). The Initial Hours of Metastasis: The Importance of Cooperative Host–Tumor Cell Interactions during Hematogenous Dissemination. Cancer Discov. *2*, 1091–1099.

Labelle, M., Begum, S., and Hynes, R.O. (2011). Direct Signaling between Platelets and Cancer Cells Induces an Epithelial-Mesenchymal-Like Transition and Promotes Metastasis. Cancer Cell *20*, 576–590.

Labelle, M., Begum, S., and Hynes, R.O. (2014). Platelets guide the formation of early metastatic niches. Proc. Natl. Acad. Sci. *111*, E3053–E3061.

Lamar, J.M., Stern, P., Liu, H., Schindler, J.W., Jiang, Z.-G., and Hynes, R.O. (2012). The Hippo pathway target, YAP, promotes metastasis through its TEAD-interaction domain. Proc. Natl. Acad. Sci. *109*, E2441–E2450.

Lamar, J.M., Xiao, Y., Norton, E., Jiang, Z.-G., Gerhard, G.M., Kooner, S., Warren, J.S.A., and Hynes, R.O. (2019). SRC tyrosine kinase activates the YAP/TAZ axis and thereby drives tumor growth and metastasis. J. Biol. Chem. *294*, 2302–2317.

Lambert, A.W., Pattabiraman, D.R., and Weinberg, R.A. (2017). Emerging Biological Principles of Metastasis. Cell *168*, 670–691.

Lamouille, S., Xu, J., and Derynck, R. (2014). Molecular mechanisms of epithelial-mesenchymal transition. Nat. Rev. Mol. Cell Biol. *15*, 178–196.

Law, R.H., Zhang, Q., McGowan, S., Buckle, A.M., Silverman, G.A., Wong, W., Rosado, C.J., Langendorf, C.G., Pike, R.N., Bird, P.I., et al. (2006). An overview of the serpin superfamily. Genome Biol. *7*, 216.

LeBleu, V.S., O'Connell, J.T., Gonzalez Herrera, K.N., Wikman, H., Pantel, K., Haigis, M.C., de Carvalho, F.M., Damascena, A., Domingos Chinen, L.T., Rocha, R.M., et al. (2014). PGC-1α mediates mitochondrial biogenesis and oxidative phosphorylation in cancer cells to promote metastasis. Nat. Cell Biol. *16*, 992–1003.

Lemma, S., Di Pompo, G., Porporato, P.E., Sboarina, M., Russell, S., Gillies, R.J., Baldini, N., Sonveaux, P., and Avnet, S. (2017). MDA-MB-231 breast cancer cells fuel osteoclast metabolism and activity: A new rationale for the pathogenesis of osteolytic bone metastases. Biochim. Biophys. Acta BBA - Mol. Basis Dis. *1863*, 3254–3264.

Leong, H.S., Robertson, A.E., Stoletov, K., Leith, S.J., Chin, C.A., Chien, A.E., Hague, M.N., Ablack, A., Carmine-Simmen, K., McPherson, V.A., et al. (2014). Invadopodia Are Required for Cancer Cell Extravasation and Are a Therapeutic Target for Metastasis. Cell Rep. *8*, 1558–1570.

Lin, E.Y., Li, J., Bricard, G., Wang, W., Deng, Y., Sellers, R., Porcelli, S.A., and Pollard, J.W. (2007). Vascular endothelial growth factor restores delayed tumor progression in tumors depleted of macrophages. Mol. Oncol. *1*, 288–302.

Lin, Y.-H., Wu, M.-H., Huang, Y.-H., Yeh, C.-T., Cheng, M.-L., Chi, H.-C., Tsai, C.-Y., Chung, I.-H., Chen, C.-Y., and Lin, K.-H. (2018). Taurine up-regulated gene 1 functions as a master regulator to coordinate glycolysis and metastasis in hepatocellular carcinoma. Hepatol. Baltim. Md *67*, 188–203.

Liotta, L.A., Tryggvason, K., Garbisa, S., Hart, I., Foltz, C.M., and Shafie, S. (1980). Metastatic potential correlates with enzymatic degradation of basement membrane collagen. Nature *284*, 67.

Liu, F.-T., and Rabinovich, G.A. (2005). Galectins as modulators of tumour progression. Nat. Rev. Cancer *5*, 29–41.

Lorger, M., and Felding-Habermann, B. (2010). Capturing changes in the brain microenvironment during initial steps of breast cancer brain metastasis. Am. J. Pathol. *176*, 2958–2971.

Luzzi, K.J., MacDonald, I.C., Schmidt, E.E., Kerkvliet, N., Morris, V.L., Chambers, A.F., and Groom, A.C. (1998). Multistep nature of metastatic inefficiency: dormancy of solitary cells after successful extravasation and limited survival of early micrometastases. Am. J. Pathol. *153*, 865–873.

MacDonald, I.C., Schmidt, E.E., Morris, V.L., Chambers, A.F., and Groom, A.C. (1992). Intravital videomicroscopy of the chorioallantoic microcirculation: a model system for studying metastasis. Microvasc. Res. *44*, 185–199.

Malanchi, I., Santamaria-Martínez, A., Susanto, E., Peng, H., Lehr, H.-A., Delaloye, J.-F., and Huelsken, J. (2011). Interactions between cancer stem cells and their niche govern metastatic colonization. Nature *481*, 85–89.

Malik, G., Knowles, L.M., Dhir, R., Xu, S., Yang, S., Ruoslahti, E., and Pilch, J. (2010). Plasma Fibronectin Promotes Lung Metastasis by Contributions to Fibrin Clots and Tumor Cell Invasion. Cancer Res. *70*, 4327–4334.

Mashimo, T., Pichumani, K., Vemireddy, V., Hatanpaa, K.J., Singh, D.K., Sirasanagandla, S., Nannepaga, S., Piccirillo, S.G., Kovacs, Z., Foong, C., et al. (2014). Acetate Is a Bioenergetic Substrate for Human Glioblastoma and Brain Metastases. Cell *159*, 1603–1614.

Massagué, J., and Obenauf, A.C. (2016). Metastatic colonization by circulating tumour cells. Nature *529*, 298–306.

Mertins, P., Mani, D.R., Ruggles, K.V., Gillette, M.A., Clauser, K.R., Wang, P., Wang, X., Qiao, J.W., Cao, S., Petralia, F., et al. (2016). Proteogenomics connects somatic mutations to signalling in breast cancer. Nature *534*, 55–62.

Midwood, K.S., and Orend, G. (2009). The role of tenascin-C in tissue injury and tumorigenesis. J. Cell Commun. Signal. *3*, 287–310.

Mikuła-Pietrasik, J., Uruski, P., Tykarski, A., and Książek, K. (2018). The peritoneal "soil" for a cancerous "seed": a comprehensive review of the pathogenesis of intraperitoneal cancer metastases. Cell. Mol. Life Sci. CMLS *75*, 509–525.

Mina, L.A., and Sledge Jr, G.W. (2011). Rethinking the metastatic cascade as a therapeutic target. Nat. Rev. Clin. Oncol. *8*, 325–332.

Minn, A.J., Gupta, G.P., Siegel, P.M., Bos, P.D., Shu, W., Giri, D.D., Viale, A., Olshen, A.B., Gerald, W.L., and Massagué, J. (2005). Genes that mediate breast cancer metastasis to lung. Nature *436*, 518–524.

Mohammadi, M., Olsen, S.K., and Goetz, R. (2005). A protein canyon in the FGF-FGF receptor dimer selects from an à la carte menu of heparan sulfate motifs. Curr. Opin. Struct. Biol. *15*, 506–516.

Morris, V.L., Schmidt, E.E., MacDonald, I.C., Groom, A.C., and Chambers, A.F. (1997). Sequential steps in hematogenous metastasis of cancer cells studied by in vivo videomicroscopy. Invasion Metastasis *17*, 281–296.

Müller, A., Homey, B., Soto, H., Ge, N., Catron, D., Buchanan, M.E., McClanahan, T., Murphy, E., Yuan, W., Wagner, S.N., et al. (2001). Involvement of chemokine receptors in breast cancer metastasis. Nature *410*, 50–56.

Naba, A., Clauser, K.R., Hoersch, S., Liu, H., Carr, S.A., and Hynes, R.O. (2012a). The Matrisome: In Silico Definition and In Vivo Characterization by Proteomics of Normal and Tumor Extracellular Matrices. Mol. Cell. Proteomics *11*, M111.014647-M111.014647.

Naba, A., Hoersch, S., and Hynes, R.O. (2012b). Towards definition of an ECM parts list: An advance on GO categories. Matrix Biol. *31*, 371–372.

Najafi, M., Farhood, B., and Mortezaee, K. (2019). Extracellular matrix (ECM) stiffness and degradation as cancer drivers. J. Cell. Biochem. *120*, 2782–2790.

Nakahara, H., Howard, L., Thompson, E.W., Sato, H., Seiki, M., Yeh, Y., and Chen, W.T. (1997). Transmembrane/cytoplasmic domain-mediated membrane type 1-matrix metalloprotease docking to invadopodia is required for cell invasion. Proc. Natl. Acad. Sci. U. S. A. *94*, 7959–7964.

Naxerova, K., Reiter, J.G., Brachtel, E., Lennerz, J.K., Wetering, M. van de, Rowan, A., Cai, T., Clevers, H., Swanton, C., Nowak, M.A., et al. (2017). Origins of lymphatic and distant metastases in human colorectal cancer. Science *357*, 55–60.

Nguyen, D.X., Bos, P.D., and Massagué, J. (2009). Metastasis: from dissemination to organ-specific colonization. Nat. Rev. Cancer *9*, 274–284.

Nieto, M.A., Huang, R.Y.-J., Jackson, R.A., and Thiery, J.P. (2016). EMT: 2016. Cell *166*, 21–45.

Nimmerjahn, A., Kirchhoff, F., and Helmchen, F. (2005). Resting microglial cells are highly dynamic surveillants of brain parenchyma in vivo. Science *308*, 1314–1318.

Obenauf, A.C., and Massagué, J. (2015). Surviving at a Distance: Organ-Specific Metastasis. Trends Cancer *1*, 76–91.

Ocaña, O.H., Córcoles, R., Fabra, Á., Moreno-Bueno, G., Acloque, H., Vega, S., Barrallo-Gimeno, A., Cano, A., and Nieto, M.A. (2012). Metastatic Colonization Requires the Repression of the Epithelial-Mesenchymal Transition Inducer Prrx1. Cancer Cell *22*, 709–724.

Öhlund, D., Handly-Santana, A., Biffi, G., Elyada, E., Almeida, A.S., Ponz-Sarvise, M., Corbo, V., Oni, T.E., Hearn, S.A., Lee, E.J., et al. (2017). Distinct populations of inflammatory fibroblasts and myofibroblasts in pancreatic cancer. J. Exp. Med. *214*, 579–596.

Oskarsson, T., Acharyya, S., Zhang, X.H.-F., Vanharanta, S., Tavazoie, S.F., Morris, P.G., Downey, R.J., Manova-Todorova, K., Brogi, E., and Massagué, J. (2011). Breast cancer cells produce tenascin C as a metastatic niche component to colonize the lungs. Nat. Med. *17*, 867–874.

Padua, D., Zhang, X.H.-F., Wang, Q., Nadal, C., Gerald, W.L., Gomis, R.R., and Massagué, J. (2008). TGFβ Primes Breast Tumors for Lung Metastasis Seeding through Angiopoietin-like 4. Cell *133*, 66–77.

Paget, S. (1889). THE DISTRIBUTION OF SECONDARY GROWTHS IN CANCER OF THE BREAST. The Lancet *133*, 571–573.

Pantel, K., Alix-Panabières, C., and Riethdorf, S. (2009). Cancer micrometastases. Nat. Rev. Clin. Oncol. *6*, 339–351.

Park, J., Wysocki, R.W., Amoozgar, Z., Maiorino, L., Fein, M.R., Jorns, J., Schott, A.F., Kinugasa-Katayama, Y., Lee, Y., Won, N.H., et al. (2016). Cancer cells induce metastasis-supporting neutrophil extracellular DNA traps. Sci. Transl. Med. *8*, 361ra138.

Pasqualini, R., and Ruoslahti, E. (1996). Organ targeting in vivo using phage display peptide libraries. Nature *380*, 364–366.

Payne, S.H. (2015). The utility of protein and mRNA correlation. Trends Biochem. Sci. *40*, 1–3.

Pollari, S., Käkönen, S.-M., Edgren, H., Wolf, M., Kohonen, P., Sara, H., Guise, T., Nees, M., and Kallioniemi, O. (2011). Enhanced serine production by bone metastatic breast cancer cells stimulates osteoclastogenesis. Breast Cancer Res. Treat. *125*, 421–430.

Powell, D.R., and Huttenlocher, A. (2016). Neutrophils in the Tumor Microenvironment. Trends Immunol. *37*, 41–52.

Qian, B., Deng, Y., Im, J.H., Muschel, R.J., Zou, Y., Li, J., Lang, R.A., and Pollard, J.W. (2009). A Distinct Macrophage Population Mediates Metastatic Breast Cancer Cell Extravasation, Establishment and Growth. PLOS ONE *4*, e6562.

Queen, M.M., Ryan, R.E., Holzer, R.G., Keller-Peck, C.R., and Jorcyk, C.L. (2005). Breast Cancer Cells Stimulate Neutrophils to Produce Oncostatin M: Potential Implications for Tumor Progression. Cancer Res. *65*, 8896–8904.

Rahbari, N.N., Kedrin, D., Incio, J., Liu, H., Ho, W.W., Nia, H.T., Edrich, C.M., Jung, K., Daubriac, J., Chen, I., et al. (2016). Anti-VEGF therapy induces ECM remodeling and mechanical barriers to therapy in colorectal cancer liver metastases. Sci. Transl. Med. *8*, 360ra135-360ra135.

Ricard-Blum, S. (2011). The Collagen Family. Cold Spring Harb. Perspect. Biol. *3*, a004978.

Rifkin, D.B. (2005). Latent Transforming Growth Factor-β (TGF-β) Binding Proteins: Orchestrators of TGF-β Availability. J. Biol. Chem. *280*, 7409–7412.

Riihimäki, M., Hemminki, A., Sundquist, J., and Hemminki, K. (2016). Patterns of metastasis in colon and rectal cancer. Sci. Rep. *6*, 29765.

Robins, S.P. (2007). Biochemistry and functional significance of collagen cross-linking. Biochem. Soc. Trans. *35*, 849–852.

Robinson, B.D., Sica, G.L., Liu, Y.-F., Rohan, T.E., Gertler, F.B., Condeelis, J.S., and Jones, J.G. (2009). Tumor microenvironment of metastasis in human breast carcinoma: a potential prognostic marker linked to hematogenous dissemination. Clin. Cancer Res. Off. J. Am. Assoc. Cancer Res. *15*, 2433–2441.

Rotondo, R., Barisione, G., Mastracci, L., Grossi, F., Orengo, A.M., Costa, R., Truini, M., Fabbi, M., Ferrini, S., and Barbieri, O. (2009). IL-8 induces exocytosis of arginase 1 by neutrophil polymorphonuclears in nonsmall cell lung cancer. Int. J. Cancer *125*, 887–893.

Ruoslahti, E. (2004). Vascular zip codes in angiogenesis and metastasis. Biochem. Soc. Trans. *32*, 397–402.

Sabeh, F., Ota, I., Holmbeck, K., Birkedal-Hansen, H., Soloway, P., Balbin, M., Lopez-Otin, C., Shapiro, S., Inada, M., Krane, S., et al. (2004). Tumor cell traffic through the extracellular matrix is controlled by the membrane-anchored collagenase MT1-MMP. J Cell Biol *167*, 769–781.

Santra, M., Eichstetter, I., and Iozzo, R.V. (2000). An anti-oncogenic role for decorin. Down-regulation of ErbB2 leads to growth suppression and cytodifferentiation of mammary carcinoma cells. J. Biol. Chem. *275*, 35153–35161.

Sarkar, S., Mirzaei, R., Zemp, F.J., Wei, W., Senger, D.L., Robbins, S.M., and Yong, V.W. (2017). Activation of NOTCH Signaling by Tenascin-C Promotes Growth of Human Brain Tumor-Initiating Cells. Cancer Res. *77*, 3231–3243.

Sarrazin, S., Lamanna, W.C., and Esko, J.D. (2011). Heparan Sulfate Proteoglycans. Cold Spring Harb. Perspect. Biol. *3*, a004952.

Sawant, A., Hensel, J.A., Chanda, D., Harris, B.A., Siegal, G.P., Maheshwari, A., and Ponnazhagan, S. (2012). Depletion of plasmacytoid dendritic cells inhibits tumor growth and prevents bone metastasis of breast cancer cells. J. Immunol. Baltim. Md 1950 *189*, 4258–4265.

Schild, T., Low, V., Blenis, J., and Gomes, A.P. (2018). Unique Metabolic Adaptations Dictate Distal Organ-Specific Metastatic Colonization. Cancer Cell *33*, 347–354.

Schwarzbauer, J.E., and DeSimone, D.W. (2011). Fibronectins, Their Fibrillogenesis, and In Vivo Functions. Cold Spring Harb. Perspect. Biol. *3*, a005041.

Schweitzer, K.M., Dräger, A.M., van der Valk, P., Thijsen, S.F., Zevenbergen, A., Theijsmeijer, A.P., van der Schoot, C.E., and Langenhuijsen, M.M. (1996). Constitutive expression of E-selectin and vascular cell adhesion molecule-1 on endothelial cells of hematopoietic tissues. Am. J. Pathol. *148*, 165–175.

Seewaldt, V. (2014). ECM stiffness paves the way for tumor cells. Nat. Med. *20*, 332–333.

Senger, D.R., Wirth, D.F., and Hynes, R.O. (1979). Transformed mammalian cells secrete specific proteins and phosphoproteins. Cell *16*, 885–893.

Senger, D.R., Wirth, D.F., and Hynes, R.O. (1980). Transformation-specific secreted phosophoproteins. Nature *286*, 619–621.

Sevenich, L. (2019). Turning “Cold” Into “Hot” Tumors—Opportunities and Challenges for Radio-Immunotherapy Against Primary and Metastatic Brain Cancers. Front. Oncol. *9*.

Sevenich, L., Bowman, R.L., Mason, S.D., Quail, D.F., Rapaport, F., Elie, B.T., Brogi, E., Brastianos, P.K., Hahn, W.C., Holsinger, L.J., et al. (2014). Analysis of tumour- and stroma-supplied proteolytic networks reveals a brain-metastasis-promoting role for cathepsin S. Nat. Cell Biol. *16*, 876–888.

Shao, R., Bao, S., Bai, X., Blanchette, C., Anderson, R.M., Dang, T., Gishizky, M.L., Marks, J.R., and Wang, X.-F. (2004). Acquired Expression of Periostin by Human Breast Cancers Promotes Tumor Angiogenesis through Up-Regulation of Vascular Endothelial Growth Factor Receptor 2 Expression. Mol. Cell. Biol. *24*, 3992–4003.

Shi, Y., and Massagué, J. (2003). Mechanisms of TGF-beta signaling from cell membrane to the nucleus. Cell *113*, 685–700.

Shree, T., Olson, O.C., Elie, B.T., Kester, J.C., Garfall, A.L., Simpson, K., Bell-McGuinn, K.M., Zabor, E.C., Brogi, E., and Joyce, J.A. (2011). Macrophages and cathepsin proteases blunt chemotherapeutic response in breast cancer. Genes Dev. *25*, 2465–2479.

Simpson, C.D., Anyiwe, K., and Schimmer, A.D. (2008). Anoikis resistance and tumor metastasis. Cancer Lett. *272*, 177–185.

Sofeu Feugaing, D.D., Götte, M., and Viola, M. (2013). More than matrix: the multifaceted role of decorin in cancer. Eur. J. Cell Biol. *92*, 1–11.

Sosa, M.S., Bragado, P., and Aguirre-Ghiso, J.A. (2014). Mechanisms of disseminated cancer cell dormancy: an awakening field. Nat. Rev. Cancer *14*, 611–622.

Stoelcker, B., Hafner, M., Orosz, P., Nieswandt, B., and Männel, D.N. (1995). Role of adhesion molecules and platelets in TNF-induced adhesion of tumor cells to endothelial cells: implications for experimental metastasis. J. Inflamm. *46*, 155–167.

Stover, D.G., Bierie, B., and Moses, H.L. (2007). A delicate balance: TGF-beta and the tumor microenvironment. J. Cell. Biochem. *101*, 851–861.

Stresing, V., Baltziskueta, E., Rubio, N., Blanco, J., Arriba, M., Valls, J., Janier, M., Clézardin, P., Sanz-Pamplona, R., Nieva, C., et al. (2013). Peroxiredoxin 2 specifically regulates the oxidative and metabolic stress response of human metastatic breast cancer cells in lungs. Oncogene *32*, 724–735.

Strilic, B., and Offermanns, S. (2017). Intravascular Survival and Extravasation of Tumor Cells. Cancer Cell *32*, 282–293.

Su, S., Chen, J., Yao, H., Liu, J., Yu, S., Lao, L., Wang, M., Luo, M., Xing, Y., Chen, F., et al. (2018). CD10+GPR77+ Cancer-Associated Fibroblasts Promote Cancer Formation and Chemoresistance by Sustaining Cancer Stemness. Cell *172*, 841-856.e16.

Takeda, K., Hayakawa, Y., Smyth, M.J., Kayagaki, N., Yamaguchi, N., Kakuta, S., Iwakura, Y., Yagita, H., and Okumura, K. (2001). Involvement of tumor necrosis factor-related apoptosis-

inducing ligand in surveillance of tumor metastasis by liver natural killer cells. Nat. Med. *7*, 94–100.

Teesalu, T., Sugahara, K.N., and Ruoslahti, E. (2012). Mapping of vascular ZIP codes by phage display. Methods Enzymol. *503*, 35–56.

Theocharis, A.D., and Karamanos, N.K. (2019). Proteoglycans remodeling in cancer: Underlying molecular mechanisms. Matrix Biol. *75–76*, 220–259.

Thiery, J.P. (2002). Epithelial-mesenchymal transitions in tumour progression. Nat. Rev. Cancer *2*, 442–454.

Thiery, J.P., Acloque, H., Huang, R.Y.J., and Nieto, M.A. (2009). Epithelial-Mesenchymal Transitions in Development and Disease. Cell *139*, 871–890.

Tichet, M., Prod'Homme, V., Fenouille, N., Ambrosetti, D., Mallavialle, A., Cerezo, M., Ohanna, M., Audebert, S., Rocchi, S., Giacchero, D., et al. (2015). Tumour-derived SPARC drives vascular permeability and extravasation through endothelial VCAM1 signalling to promote metastasis. Nat. Commun. *6*, 6993.

Tsai, J.H., Donaher, J.L., Murphy, D.A., Chau, S., and Yang, J. (2012). Spatiotemporal Regulation of Epithelial-Mesenchymal Transition Is Essential for Squamous Cell Carcinoma Metastasis. Cancer Cell *22*, 725–736.

Valavanidis, A., Vlachogianni, T., Fiotakis, K., and Loridas, S. (2013). Pulmonary Oxidative Stress, Inflammation and Cancer: Respirable Particulate Matter, Fibrous Dusts and Ozone as Major Causes of Lung Carcinogenesis through Reactive Oxygen Species Mechanisms. Int. J. Environ. Res. Public. Health *10*, 3886–3907.

Vander Heiden, M.G., Cantley, L.C., and Thompson, C.B. (2009). Understanding the Warburg Effect: The Metabolic Requirements of Cell Proliferation. Science *324*, 1029–1033.

Vogel, C., and Marcotte, E.M. (2012). Insights into the regulation of protein abundance from proteomic and transcriptomic analyses. Nat. Rev. Genet. *13*, 227–232.

Wan, L., Hu, G., Wei, Y., Yuan, M., Bronson, R.T., Yang, Q., Siddiqui, J., Pienta, K.J., and Kang, Y. (2014a). Genetic ablation of metadherin inhibits autochthonous prostate cancer progression and metastasis. Cancer Res. *74*, 5336–5347.

Wan, L., Lu, X., Yuan, S., Wei, Y., Guo, F., Shen, M., Yuan, M., Chakrabarti, R., Hua, Y., Smith, H.A., et al. (2014b). MTDH-SND1 interaction is crucial for expansion and activity of tumor-initiating cells in diverse oncogene- and carcinogen-induced mammary tumors. Cancer Cell *26*, 92–105.

Wang, X., Liu, J., Wang, Z., Huang, Y., Liu, W., Zhu, X., Cai, Y., Fang, X., Lin, S., Yuan, L., et al. (2013). Periostin Contributes to the Acquisition of Multipotent Stem Cell-Like Properties in Human Mammary Epithelial Cells and Breast Cancer Cells. PLOS ONE *8*, e72962.

Weber, G.F. (2001). The metastasis gene osteopontin: a candidate target for cancer therapy. Biochim. Biophys. Acta BBA - Rev. Cancer *1552*, 61–85.

Wei, L., Yang, Y., Zhang, X., and Yu, Q. (2004). Altered regulation of Src upon cell detachment protects human lung adenocarcinoma cells from anoikis. Oncogene *23*, 9052–9061.

Wikman, H., Vessella, R., and Pantel, K. (2008). Cancer micrometastasis and tumour dormancy. APMIS Acta Pathol. Microbiol. Immunol. Scand. *116*, 754–770.

Wirtz, D., Konstantopoulos, K., and Searson, P.C. (2011). The physics of cancer: the role of physical interactions and mechanical forces in metastasis. Nat. Rev. Cancer *11*, 512–522.

Wislez, M., Rabbe, N., Marchal, J., Milleron, B., Crestani, B., Mayaud, C., Antoine, M., Soler, P., and Cadranel, J. (2003). Hepatocyte growth factor production by neutrophils infiltrating bronchioloalveolar subtype pulmonary adenocarcinoma: role in tumor progression and death. Cancer Res. *63*, 1405–1412.

Wolf, M.J., Hoos, A., Bauer, J., Boettcher, S., Knust, M., Weber, A., Simonavicius, N., Schneider, C., Lang, M., Stürzl, M., et al. (2012). Endothelial CCR2 Signaling Induced by Colon Carcinoma Cells Enables Extravasation via the JAK2-Stat5 and p38MAPK Pathway. Cancer Cell *22*, 91–105.

Wyckoff, J.B., Wang, Y., Lin, E.Y., Li, J., Goswami, S., Stanley, E.R., Segall, J.E., Pollard, J.W., and Condeelis, J. (2007). Direct Visualization of Macrophage-Assisted Tumor Cell Intravasation in Mammary Tumors. Cancer Res. *67*, 2649–2656.

Yao, H., Price, T.T., Cantelli, G., Ngo, B., Warner, M.J., Olivere, L., Ridge, S.M., Jablonski, E.M., Therrien, J., Tannheimer, S., et al. (2018). Leukaemia hijacks a neural mechanism to invade the central nervous system. Nature *560*, 55–60.

Ye, X., Brabletz, T., Kang, Y., Longmore, G.D., Nieto, M.A., Stanger, B.Z., Yang, J., and Weinberg, R.A. (2017). Upholding a role for EMT in breast cancer metastasis. Nature *547*, E1–E3.

Yuan, Y., Zhong, W., Ma, G., Zhang, B., and Tian, H. (2015). Yes-associated protein regulates the growth of human non-small cell lung cancer in response to matrix stiffness. Mol. Med. Rep. *11*, 4267–4272.

Yurchenco, P.D. (2011). Basement Membranes: Cell Scaffoldings and Signaling Platforms. Cold Spring Harb. Perspect. Biol. *3*, a004911.

Yuzhalin, A.E., Lim, S.Y., Kutikhin, A.G., and Gordon-Weeks, A.N. (2018). Dynamic matrisome: ECM remodeling factors licensing cancer progression and metastasis. Biochim. Biophys. Acta BBA - Rev. Cancer *1870*, 207–228.

Zhang, X.H.-F., Wang, Q., Gerald, W., Hudis, C.A., Norton, L., Smid, M., Foekens, J.A., and Massagué, J. (2009). Latent Bone Metastasis in Breast Cancer Tied to Src-Dependent Survival Signals. Cancer Cell *16*, 67–78.

Zhuang, J., Zhang, J., Lwin, S.T., Edwards, J.R., Edwards, C.M., Mundy, G.R., and Yang, X. (2012). Osteoclasts in Multiple Myeloma Are Derived from Gr-1+CD11b+Myeloid-Derived Suppressor Cells. PLOS ONE *7*, e48871.

Chapter 2.

The scaffold protein IQGAP1 promotes extravasation and metastasis

This chapter was written by Jess Hebert, with editing by Richard Hynes and John Lamar. All experiments described in this chapter were performed by Jess Hebert, except for extravasation assays performed by Chenxi Tian and immunohistochemistry performed by Steffen Rickelt. This study was designed by Jess Hebert, John Lamar and Richard Hynes. This chapter is adapted from a study that has been submitted for publication as:

Hebert, J.D., Tian, C., Lamar, J.M., Rickelt, S., and Hynes, R.O. (2019). The scaffold protein IQGAP1 promotes extravasation and metastasis. Sci. Rep. [In Revision].

Abstract

IQGAP1 is a scaffold protein involved in a range of cellular activities, including migration, invasion, adhesion and proliferation. It is also oncogenic in a variety of cancers, promoting primary tumor growth and invasiveness. However, the role of IQGAP1 in tumor progression and metastasis remains unclear. In this study, we use IQGAP1 knockdown and knockout to investigate its role in the metastatic cascade in both melanoma and breast cancer *in vivo*. We find that reduction of IQGAP1 expression severely inhibits the formation of both spontaneous and experimental metastases, without limiting primary or metastatic tumor growth. Furthermore, IQGAP1 knockout significantly decreases extravasation of tumor cells from circulation, possibly involving invadopodial function. By expressing mutant forms of IQGAP1 in a knockout context, we also determine that IQGAP1's pro-metastatic functions are dependent on multiple domains and functions. These data demonstrate that IQGAP1 promotes metastasis *in vivo* through regulation of extravasation and suggest that it may represent a valid therapeutic target for inhibiting metastasis.

Introduction

Metastasis, the spread of a cancer from its original site to additional, secondary sites throughout the body, is the cause of the vast majority of cancer-related deaths (Gupta and Massagué, 2006), and patient five-year survival rates drop precipitously once a cancer has metastasized (Siegel et al., 2018). Thus, there is a dramatic, unmet demand for treatments that can either eliminate metastatic cancer or prevent a tumor from spreading in the first place. However, current knowledge of the metastatic process is incomplete, and so previous anti-metastasis therapies have had very limited efficacy (Steeg, 2016). Consequently, there is a need

to understand better the proteins that drive metastatic cancer, both to inform the design of future therapies as well as to identify additional therapeutic targets.

The scaffold protein IQGAP1 has been an active subject of investigation for its oncogenic potential due to its involvement in multiple functions classically associated with cancer, including proliferation, migration, invasion and cell-cell adhesion (White et al., 2009). Indeed, IQGAP1 is elevated at both the mRNA and protein level in a variety of cancers, and its levels correlate with aggressiveness (White et al., 2009). Overexpression of IQGAP1 promotes growth and invasiveness of xenograft tumors of MCF-7 breast cancer cells *in vivo* (Jadeski et al., 2008), while IQGAP1 knockout mice are resistant to Ras-driven tumorigenesis (Jameson et al., 2013). The IQGAP family also contains two other proteins, IQGAP2 and IQGAP3, but IQGAP2 has been shown to have tumor-suppressive properties, while IQGAP3 has not been well studied (White et al., 2009).

Direct evidence for the involvement of IQGAP1 itself in metastasis has been deficient. We previously demonstrated that IQGAP1 is significantly upregulated in *in vivo*-selected, highly metastatic melanoma tumor cells when compared with their parental counterparts (Clark et al., 2000). Aside from this correlative evidence, further investigation of IQGAP1's role in metastasis has largely been limited to *in vitro* studies. Manipulation of IQGAP1 levels has been shown to affect the proliferation, migration and invasion of esophageal squamous cell carcinoma (Wang et al., 2014), hepatocellular carcinoma (Jin et al., 2015), glioma (Diao et al., 2017), and breast cancer cells (Jadeski et al., 2008; Zhao et al., 2017). Moreover, knockdown of IQGAP1 in a xenograft model of esophageal squamous cell carcinoma reduced primary tumor growth, with unclear effects on metastasis (Wang et al., 2014). Accordingly, these data have thus far left

unanswered the question of whether IQGAP1 truly regulates metastasis and, as a consequence, whether it represents a potential therapeutic target for inhibiting metastasis.

Although the involvement of IQGAP1 in several, metastasis-associated pathways make it a promising subject to study, this diverse array of interactions also complicates any investigation into specific mechanisms of action. IQGAP1 has several important functional domains, each of which binds to multiple proteins often implicated in metastasis. The calponin homology (CH) domain of IQGAP1 regulates cell migration by binding N-WASP and actin to promote actin assembly, branching and crosslinking at the leading edge (Bashour et al., 1997; Le Clainche et al., 2007). The WW and IQ domains act as scaffolds for the Erk mitogen-activated protein kinase (MAPK) pathway, binding to B/C-Raf (Ren et al., 2007), Mek 1/2 (Roy et al., 2005), and Erk 1/2 to coordinate cell proliferation (Roy et al., 2004). IQGAP1's RasGAP-related domain (GRD) binds to and stabilizes the active forms of the Rho GTPases Rac1 and Cdc42, which regulate cell migration and invasion (Hart et al., 1996). IQGAP1's RasGAP C-terminal (RGCT) domain associates with the exocyst complex proteins Sec3 and Sec8, and this association is necessary for the formation of mature invadopodia (Sakurai-Yageta et al., 2008), actin-rich protrusions used by tumor cells to degrade and invade through the extracellular matrix (Beaty and Condeelis, 2014). The RGCT also binds to both E-cadherin and beta-catenin, and this association weakens E-cadherin-mediated cell-cell adhesion (Kuroda, 1998). Any or all of these interactions could be necessary for mediating potential pro-metastatic functions of IQGAP1, and the above proteins represent only a small subset of the total number of currently known IQGAP1 binding partners (Hedman et al., 2015). Still, understanding which domain or domains of IQGAP1 are critical for metastasis would be essential for the future design of therapeutics to disrupt these key interactions.

This study therefore seeks to answer directly the question of whether IQGAP1 is pro-metastatic, and if so, which of IQGAP1's domains and functions are actually necessary for such an effect. We investigated the effects of IQGAP1 knockdown and knockout on both experimental and spontaneous metastasis models *in vivo*, and we found that reduction in IQGAP1 levels heavily curtailed the formation of metastases from both melanoma and breast cancer cells. Notably, we found IQGAP1 knockout cells to be severely deficient in extravasation ability. This pro-metastatic phenotype seemed to be dependent on multiple domains of IQGAP1. These results firmly establish IQGAP1 as a metastasis promoter and suggest that it represents a promising candidate for future research, including as a potential therapeutic target.

Results

IQGAP1 knockdown reduces metastasis

To test the importance of IQGAP1 in metastasis *in vivo*, we first created stable IQGAP1 knockdowns in MA2 melanoma cells using miR30-based shRNAs (sh1 and sh6), along with control cells expressing shRNA against firefly luciferase (shFF) (Fig. 1A, B). Consistent with previous reports,(Dong et al., 2016) IQGAP1 knockdown caused cells to adopt a more spread and rounded morphology (Supplementary Fig. S1), along with a concordant reorganization of the actin and tubulin cytoskeletons (Supplementary Fig. S2). Furthermore, as previously reported (Sakurai-Yageta et al., 2008), IQGAP1 knockdown significantly reduced the degradation of gelatin by cells in an *in vitro* assay for invadopodia activity (Fig. 1C).

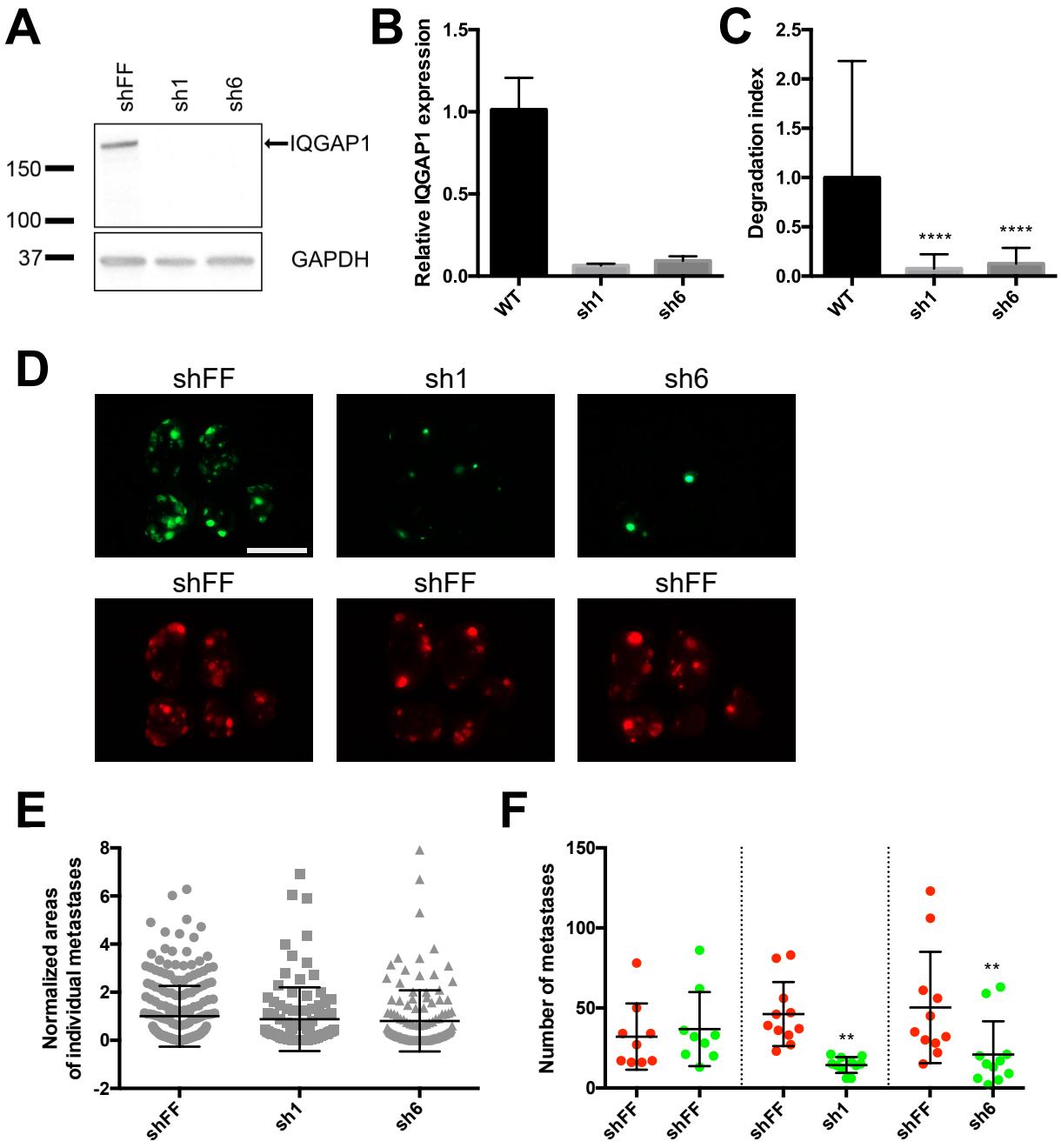
A
shFF
sh1
sh6
IQGAP1
GAPDH
150
100
37
B
Relative IQGAP1 expression
1.5
1.0
0.5
0.0
WT
sh1
sh6
C
Degradation index
2.5
2.0
1.5
1.0
0.5
0.0
****
****
WT
sh1
sh6
D
shFF
sh1
sh6
shFF
shFF
shFF
E
Normalized areas of individual metastases
8
6
4
2
0
-2
shFF
sh1
sh6
F
Number of metastases
150
100
50
0
**
**
shFF
shFF
shFF
sh1
shFF
sh6

Figure 1. IQGAP1 knockdown reduces metastasis of MA2 cells from circulation.
(A) Western blot of IQGAP1 and GAPDH in MA2 melanoma cells expressing shRNA against firefly luciferase (shFF) or IQGAP1 (sh1 and sh6). Molecular weight markers in kilodaltons (kDa) are indicated. Full-length IQGAP1 is shown with an arrow. Blot is cropped for clarity, with full-length blot presented in Supplementary Fig. S7A. (B) qPCR of expression of IQGAP1 relative to GAPDH in knockdown lines, normalized to WT parental MA2 cells. (C) Gelatin degradation assay, with area of gelatin degraded by IQGAP1 knockdown cells normalized to WT. (D-F) Tail-vein injection of a 50/50 mix of red (tdTomato) and green (ZsGreen) MA2 cells. n=9-11 mice per group. (D) Representative images of lungs taken from mice 6 weeks after injection. Each red/green image pair is of the same set of lungs. Scale bar, 10 mm. (E) Size distribution of areas of individual green metastases from each experimental group. Values are normalized to red control tumor sizes from each mouse, as well as to green tumor sizes in the control group. (F) Number of metastases observed. Each red/green pair of cell lines (separated by dotted lines) was co-injected. **, $P \leq 0.01$; ****, $P \leq 0.0001$; one-way ANOVA with Dunnett's (C) or Šidák's (F) multiple comparisons test.

To test whether IQGAP1 knockdown has any effect on metastatic ability *in vivo*, 50/50 mixes of red fluorescent control cells with green fluorescent cells expressing either control or IQGAP1-targeting shRNA were then injected into the tail veins of immunocompromised mice to observe differences in lung metastasis (Fig. 1D). Although individual metastases from IQGAP1 knockdown cells were not significantly different in size compared to control metastases (Fig. 1E), IQGAP1 knockdown did reduce overall incidence of metastasis formation (Fig. 1F). Collectively, these results suggest that IQGAP1 expression is important in invasion and metastasis of tumor cells from circulation.

IQGAP1 knockout reduces metastasis but not primary tumor growth

To create a clean genetic background, we next generated complete IQGAP1 knockouts in MA2 cells using CRISPR-Cas9. Four clonal lines were established using two different sgRNAs against IQGAP1, and expression of wild-type IQGAP1 was then re-established in each knockout line as a rescue control (Fig. 2A).

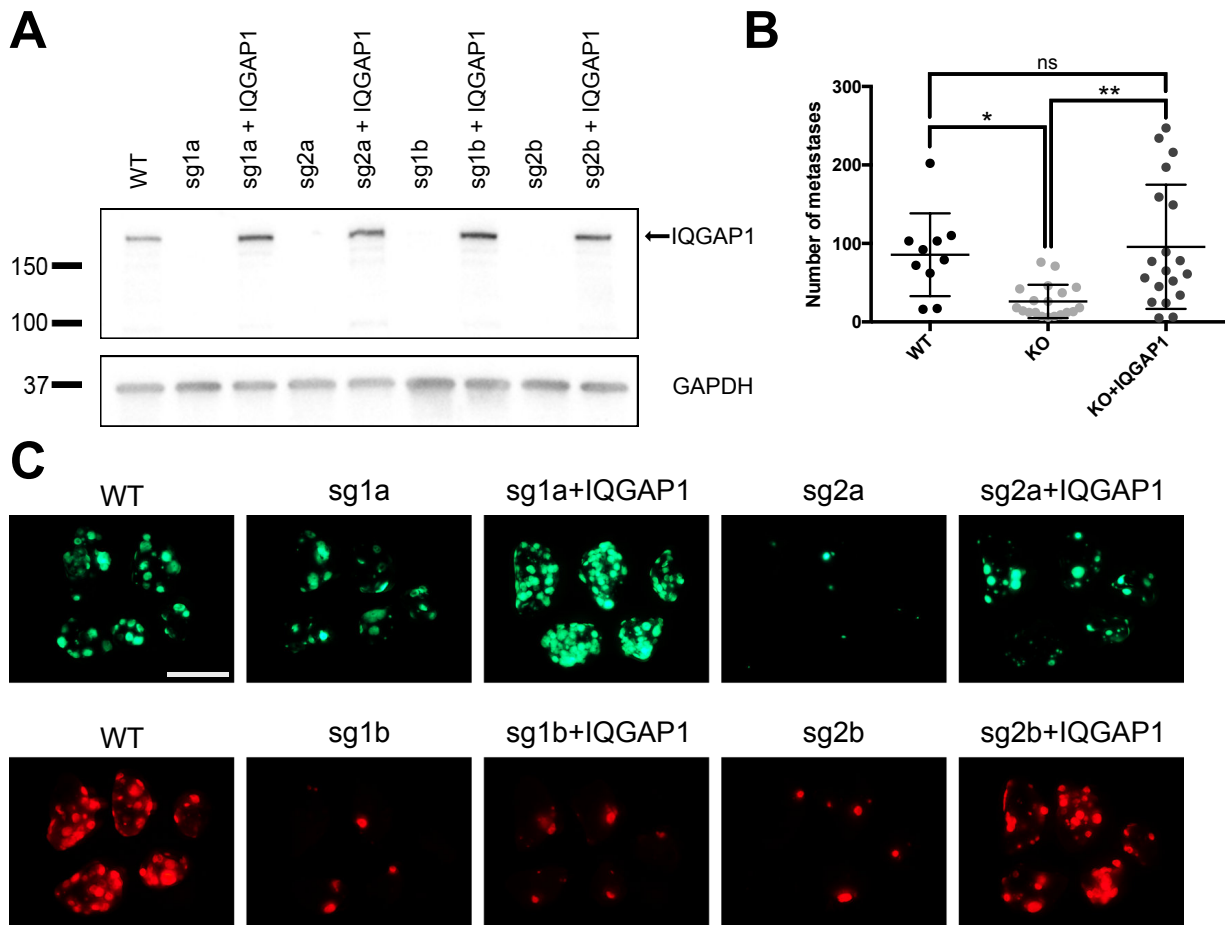

Figure 2. IQGAP1 knockout in MA2 cells reduces experimental metastasis *in vivo*.
(A) Western blot of IQGAP1 and GAPDH in parental (WT), clonal IQGAP1 knockout (sg) and rescue (+IQGAP1) MA2 lines. Molecular weight markers in kDa are indicated. Full-length IQGAP1 is shown with an arrow. Blot is cropped for clarity, with full-length blot presented in Supplementary Fig. S7B. (B and C) Tail-vein injection of clonal IQGAP1 knockout and rescue lines, each injected individually. n=10-19 mice per group. (B) Number of metastases observed. All clonal knockout and rescue lines are shown pooled. Data separated by clonal line are displayed in Supplementary Figure S3. (C) Representative images of lungs 6 weeks after injection. Scale bar, 10 mm. *, $P \leq 0.05$; **, $P \leq 0.01$; one-way ANOVA with Tukey's multiple comparisons test.

Each IQGAP1 knockout and rescue line was then assayed *in vivo* by tail-vein injection. Collectively, IQGAP1 knockout significantly reduced metastasis, while re-expressing wild-type IQGAP1 in the knockout lines restored metastatic ability. (Fig. 2B, C), with individual results varying among the clonal knockout lines (Supplementary Fig. S3), consistent with the known variability observed to result from single-cell cloning in other cell lines (Ben-David et al., 2018). These data broadly indicate that IQGAP1 knockout, like IQGAP1 knockdown, is critical in metastasis of MA2 melanoma cells from circulation.

To examine the relevance of IQGAP1 in metastasis in the context of a different cancer type, we also produced two clonal knockouts in LM2 breast cancer cells (an *in-vivo*-selected, highly metastatic derivative of MDA-MB-231) (Minn et al., 2005), using the same two sgRNAs as above (Fig. 3A). These cells were then injected orthotopically into the mammary fat pads of immunocompromised mice to allow formation of primary tumors and ensuing metastasis. IQGAP1 knockout was total and was observed throughout the primary tumors *in vivo*, in contrast with wild-type tumors, which had extensive IQGAP1 expression (Fig. 3B and Supplementary Fig. S4).

However, despite the complete lack of IQGAP1, there was no reduction in primary tumor growth; in fact, one of the clonal knockout lines had significantly increased primary tumor mass (Fig. 3C). We compared metastatic burden in the lungs and liver between the wild-type and IQGAP1 knockout cell lines (Fig. 3D) and observed an overall reduction in metastasis to both organs following the loss of IQGAP1 (Fig. 3E, F), implying that IQGAP1 has an effect on metastasis independent of primary tumor growth. IQGAP1 knockout thus reduced metastasis *in vivo* in both melanoma and breast cancer cell lines, in accordance with a more generally conserved role for IQGAP1 in the metastatic cascade.

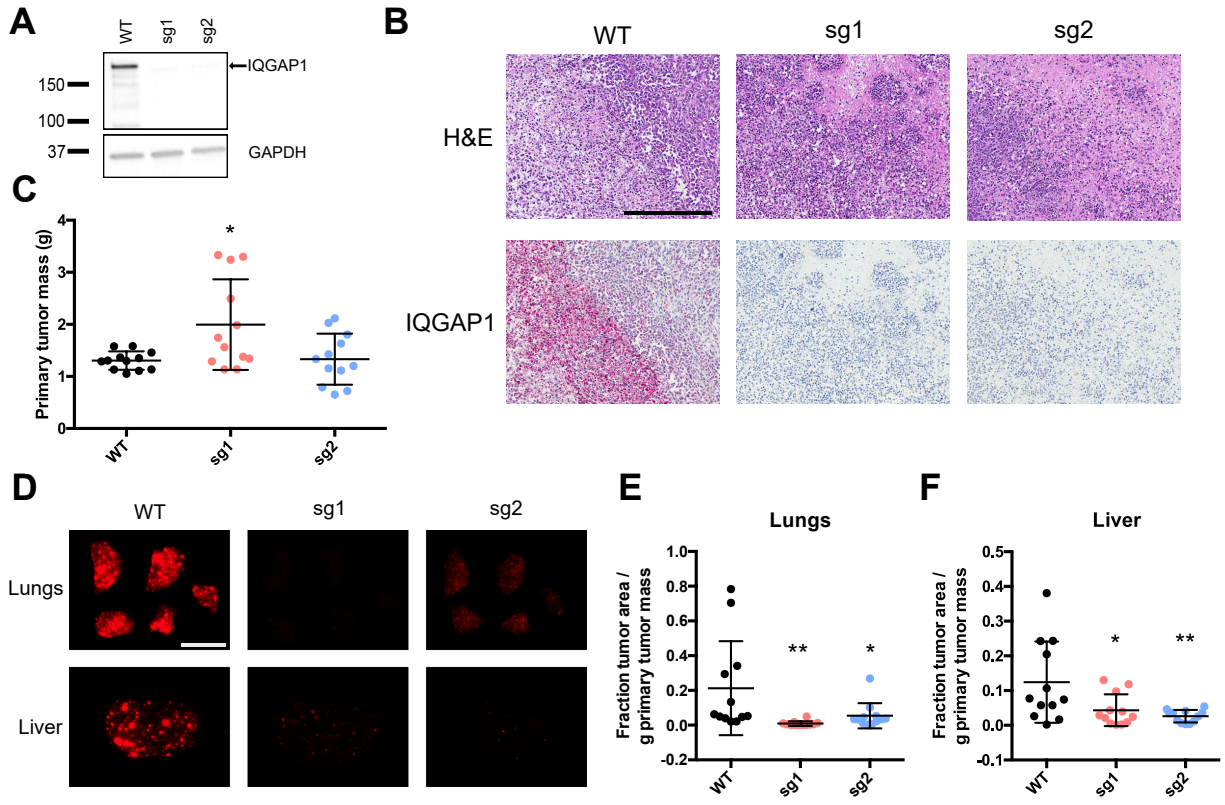

Figure 3. IQGAP1 knockout in LM2 breast cancer cells reduces spontaneous metastasis but not primary tumor growth.
(A) Western blot of IQGAP1 and GAPDH in parental (WT) and clonal IQGAP1 knockout (sg) LM2 lines. Molecular weight markers in kDa are indicated. Full-length IQGAP1 is shown with an arrow. Blot is cropped for clarity, with full-length blot presented in Supplementary Fig. S7C. (B-F) Orthotopic mammary transplant of LM2 lines, with samples collected 8 weeks after injection. n=12 mice per group. (B) Representative histology images of primary tumors showing H&E (top panels) or IQGAP1 (bottom panels) staining. Scale bar, 300 µm. (C) Distribution of primary tumor masses (g). (D) Representative images of lungs (top panels) and liver left lobes (bottom panels). Each pair of samples was taken from the same mouse. Scale bar, 10 mm. (E and F) Fraction of lung (E) or liver left lobe (F) surface area occupied by tumors, normalized to primary tumor mass (g) for each mouse. *, $P \leq 0.05$; **, $P \leq 0.01$; one-way ANOVA with Dunnett's multiple comparisons test (all pairwise comparisons to WT).

IQGAP1 knockout reduces extravasation

Metastasis from circulation, despite consisting of only the latter half of the metastatic cascade, still requires a number of distinct steps to be completed before circulating tumor cells can grow into overt metastases, including arrest, extravasation, early survival and eventual outgrowth (Lambert et al., 2017). Of these steps, the importance of IQGAP1 in invadopodia activity (Fig. 1C) is of particular relevance to extravasation, since extravasation of cells from circulation has been shown to require invadopodia (Leong et al., 2014). We therefore hypothesized that IQGAP1 may be exerting its pro-metastatic effects during extravasation.

Thus, to evaluate more directly at which stage of the metastatic cascade IQGAP1 expression may be crucial, we performed an *in vivo* extravasation assay by injecting MA2 cells into mouse tail-veins, then collecting lungs after 20 hours and examining what fraction of tumor cells had extravasated by that time (Fig. 4A). For this and future experiments, we selected one clonal knockout line (sg2a) whose knockout and rescue phenotypes most closely matched that of IQGAP1 knockdown and wild-type cells, respectively, for further study. Compared with wild-type cells, the extravasation rate of IQGAP1 knockout cells was halved, while re-expression of wild-type IQGAP1 in the same knockout background completely restored extravasation ability (Fig. 4B). These results suggest that IQGAP1 expression is crucial for extravasation of MA2 cells, and that IQGAP1's effects on extravasation may account for the bulk of its pro-metastatic ability in this system.

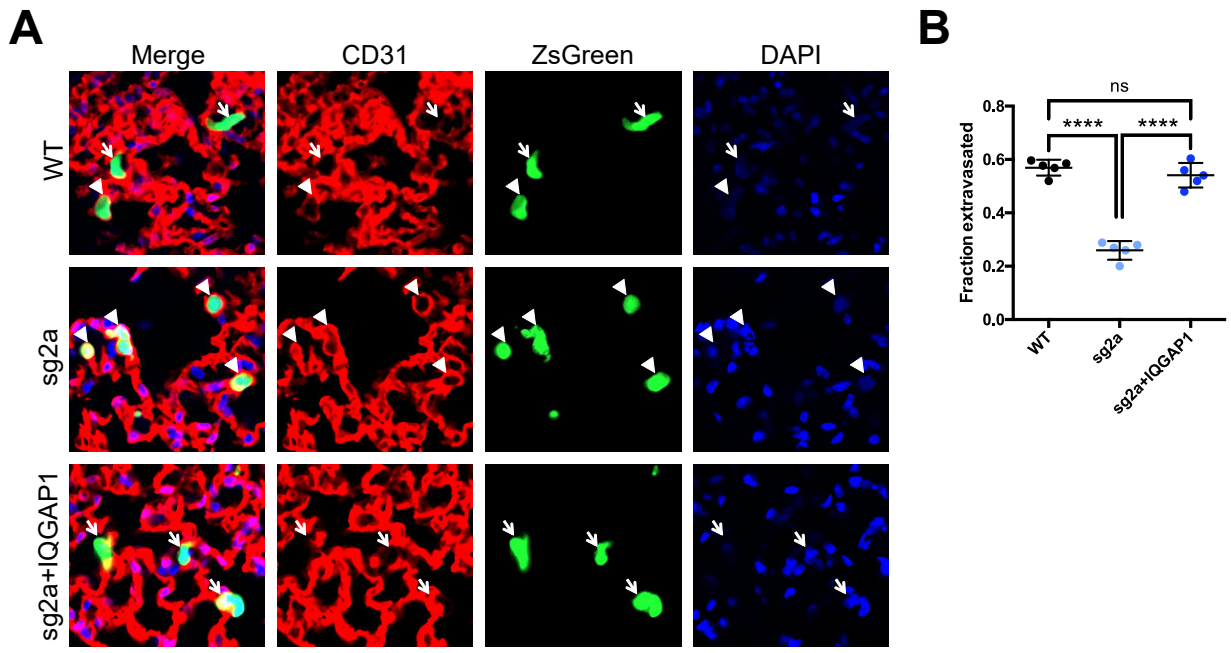

Figure 4. IQGAP1 knockout reduces extravasation of MA2 cells *in vivo*.
(A) Representative images of parental, IQGAP1 knockout or rescued cells (ZsGreen), vasculature (CD31), and nuclei (DAPI) 20 hours after tail-vein injection. Extravasated cells (arrows) and cells still in vasculature (arrowheads) are indicated. Scale bar, 10 μm. (B) Fraction of observed cells that had extravasated. n=5 mice per group. ns, $P > 0.05$; ****, $P \leq 0.0001$; one-way ANOVA with Tukey's multiple comparisons test.

IQGAP1's effects on metastasis require multiple domains

Finally, we sought to explore which domains and functions of IQGAP1 may be necessary for its effects on metastasis. In addition to its eponymous IQ motifs and RasGAP-related domain (GRD), IQGAP1 contains calponin homology (CH), coiled-coil (CC), WW and RasGAP C-terminal (RGCT) domains (Fig. 5A) (Brown and Sacks, 2006). Of particular note, the IQ domain of IQGAP1 binds to the MAPK proteins B/C-Raf and Mek1/2. (Brown and Sacks, 2006), as well as the metastasis promoter YAP (Sayedyahossein et al., 2016); the GRD binds to the Rho GTPases Rac1 and Cdc42 (Brown and Sacks, 2006); and the RGCT binds to the exocyst complex proteins Sec3/8 (Sakurai-Yageta et al., 2008). Any of these domains and binding interactions could plausibly be required for IQGAP1 to promote metastasis.

Consequently, we made MA2 cell lines expressing various mutant forms of IQGAP1 in the background of one of our clonal knockouts (sg2a): one mutant lacking all four IQ motifs (IQGAP1ΔIQ), another unable to bind Rac1 and Cdc42 (IQGAP1-T) (Fukata et al., 2002), a mutant lacking two major phosphorylation sites (IQGAP1-AA) and a final mutant missing the entire RasGAP C-terminal domain (IQGAPΔCT) (Fig. 5A and Supplementary Fig. S5). When we observed these cells in culture, we noted that IQGAP1-T and IQGAP1-AA were able to revert knockout cells from a more spread, rounded morphology back to the elongated, wild-type MA2 cell shape, while IQGAP1ΔIQ and IQGAPΔCT had no effect on apparent cell morphology (Supplementary Fig. S6).

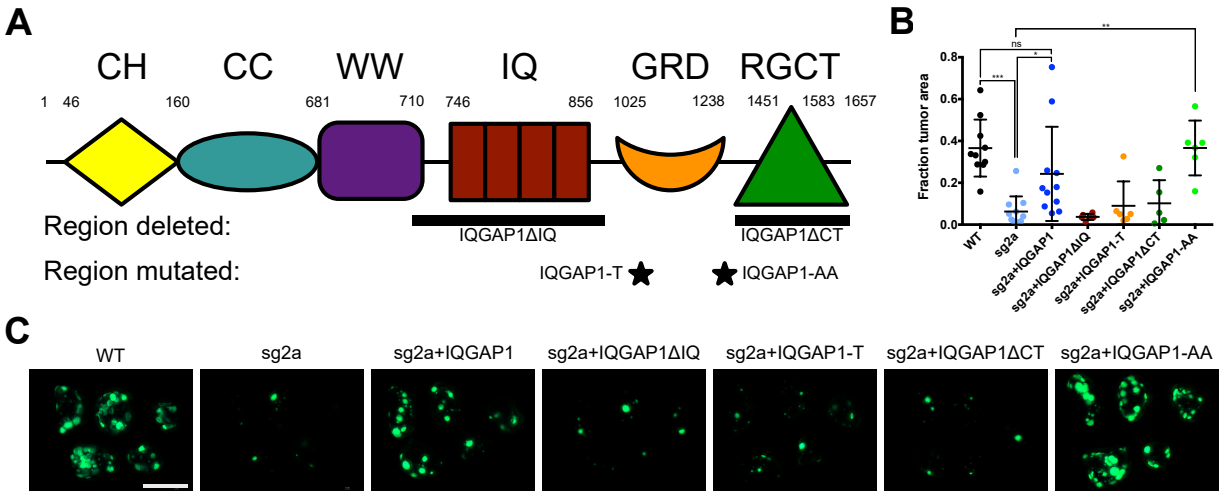

Figure 5. Effects of mutant forms of IQGAP1 on experimental metastasis in MA2 cells. (A) Domain structure of human IQGAP1, including calponin homology (CH), coiled coil (CC), WW, IQ, GAP-related domain (GRD) and RasGAP C-terminal (RGCT) domains, adapted from Brown and Sacks.(Brown and Sacks, 2006) Shown below are regions of IQGAP1 deleted or mutated in the IQGAP1 mutant constructs used in this study: IQGAP1ΔIQ, IQGAP1-T1050AX2 (IQGAP1-T), IQGAP1-S1441A/S1443A (IQGAP1-AA) and IQGAPΔCT. (B and C) Tail-vein injection of parental (WT) or clonal IQGAP1 knockout line sg2a, rescued with either WT or mutant IQGAP1. n=5-11 mice per group. (B) Fraction of lung surface area occupied by tumors. (C) Representative images of lungs 6 weeks after injection. Scale bar, 10 mm. ns, *, $P \leq 0.05$; **, $P \leq 0.01$; ***, $P \leq 0.001$; one-way ANOVA with Šidák's multiple comparisons test.

Cell lines expressing these IQGAP1 mutants were injected into mouse tail veins to assay for differences in lung metastasis (Fig. 5B, C). Consistent with our earlier results, we observed that IQGAP1 knockout reduced metastasis compared to wild-type cells, while re-expression of wild-type IQGAP1 rescued metastasis formation. However, expression of most of the IQGAP1 mutants (IQGAP1ΔIQ, IQGAP1-T and IQGAPΔCT) was unable to rescue metastatic ability. Only cells expressing IQGAP1-AA had metastasis formation restored to the level of wild-type cells. These results suggest that multiple domains of IQGAP1 are required for metastasis.

Discussion

IQGAP1 is involved in a myriad of pathways commonly associated with cancer and metastasis, including proliferation, migration and invasion. However, despite this accumulation of circumstantial evidence, direct proof of IQGAP1's importance in metastasis *in vivo* has been lacking. Furthermore, the diversity of roles performed by IQGAP1 could conceivably implicate it in any or all of the steps of the metastatic cascade: invasion from the primary tumor, intravasation, survival in circulation, extravasation, and outgrowth of the metastatic tumor. Lastly, given its enormous number of binding partners (well over a hundred) and functions (Hedman et al., 2015), it is unclear exactly which of them, either individually or in combination, would be necessary for mediating any pro-metastatic effects. These broad uncertainties represent a diverse array of challenges in understanding the behavior and potential significance of IQGAP1 in metastasis.

In this study, we sought to begin the process of unraveling the complicated web of IQGAP1's interrelated functions as they relate to metastasis through the use of direct, *in vivo* experiments. Reduction in IQGAP1 expression, through both knockdown and knockout,

dramatically reduced experimental metastasis of MA2 melanoma cells from circulation by two- to three-fold (Fig. 1F, 2B). Furthermore, IQGAP1 knockout reduced spontaneous metastasis of LM2 breast cancer cells from primary tumors to both the lungs and liver by a similar or even greater degree (Fig. 3E, F), even when normalizing for any changes in primary tumor mass (Fig. 3C). These results clearly show that IQGAP1 expression is important for metastasis in these systems, and the constancy of this effect in both melanoma and breast cancer models implies that IQGAP1 may be broadly relevant in metastasis across multiple cancers.

If IQGAP1 is, indeed, regulating metastasis, then at which stage or stages of the metastatic cascade is it having an effect? Given that IQGAP1 knockdown and knockout decrease experimental metastasis from circulation, IQGAP1 must at least be relevant in the later stages of the metastatic cascade, including arrest, extravasation, early survival and proliferation into a full metastatic tumor. Individual IQGAP1 knockdown metastases had a similar average size compared to wild-type metastases (Fig. 1E), suggesting that IQGAP1 is not having a marked effect on metastatic proliferation, or else we would expect that IQGAP1 knockdown metastases would be significantly smaller. Instead, there is simply a greatly diminished number of metastases forming. However, given IQGAP1's observed effects on invadopodia activity, and the reported importance of invadopodia in extravasation (Leong et al., 2014), we hypothesized that IQGAP1 might be involved in metastasis at the extravasation step. We observed a two- to three-fold decline in extravasation *in vivo* of IQGAP1 knockout cells compared to either wild-type or IQGAP1 rescue cells (Fig. 4B). The magnitude of this change is comparable to that of the overall decrease in metastasis due to IQGAP1 knockout (Fig. 2B), suggesting that much, if not most, of the observed difference in metastasis is likely due to differential extravasation ability. These data do not rule out the possibility that IQGAP1 may also have a lesser but still substantial

effect on arrest in circulation and early survival, particularly given its known regulation of cell-cell adhesion and MAPK signaling (Li et al., 1999; Ren et al., 2007; Roy et al., 2004, 2005). Furthermore, the fact that IQGAP1 knockout reduces spontaneous metastasis from primary tumors (Fig. 3E, F) at least as much, if not more, than it reduces metastasis from circulation (Fig. 2B) may mean that IQGAP1 has some additional influence in the early stages of the metastatic cascade. Given IQGAP1's effects on invadopodia (Fig. 1C) and extravasation (Fig. 4), this influence is most likely to apply during invasion of cancer cells from a primary tumor and subsequent intravasation into circulation. This is further supported by previous research demonstrating that IQGAP1 is overexpressed at the invasive front of human colorectal carcinomas (Nabeshima et al., 2002), and that breast cancer cells overexpressing IQGAP1 form more invasive tumors in mice (Jadeski et al., 2008). Additional, detailed studies will be required to isolate more specifically all the individual steps of the metastatic cascade in which IQGAP1 expression is relevant.

IQGAP1 may also promote tumor progression. In this study, we primarily reduced IQGAP1 expression in cell lines that were already highly proliferative and metastatic, and we did not see any reduction in primary tumor growth from LM2 breast cancer cells (Fig. 3C). However, previous results in the MCF-7 breast cancer cell line showed that altering IQGAP1 expression could affect primary tumor growth (Jadeski et al., 2008). These results could be due to differences in the cell lines used: the LM2 line is much more aggressive than MCF-7, and knocking out IQGAP1 may not have a large enough effect to cause an observable difference in growth. Additionally, the process of single-cell cloning that we used to generate our knockout cell lines may naturally select for cells that are more proliferative. IQGAP1 knockdown also shifted cell morphology from a more stretched to a more spread and rounded appearance

(Supplementary Fig. S1), along with some cytoskeletal reorganization (Supplementary Fig. S2). These changes are consistent with morphological shifts observed in previous studies that demonstrated that changes in IQGAP1 expression can induce or reverse some forms of epithelial-mesenchymal transition (EMT) (Dong et al., 2016; Su et al., 2017; Wang et al., 2014). Moreover, IQGAP1 has been shown to bind to a number of known metastasis promoters, such as RhoC and YAP (Casteel et al., 2012; Sayedyahossein et al., 2016), which already have potent effects of their own. Thus, in addition to the marked role for IQGAP1 in extravasation that we have identified, this versatile scaffold protein may have further roles in directing tumor growth, regulating EMT and coordinating other known metastasis promoters.

Finally, given IQGAP1's enormous diversity of functions and binding partners, we attempted to identify which domains of IQGAP1 mediate its effects on metastasis by expressing several mutant forms of the protein in one of our clonal knockout MA2 lines (Fig. 5A, Supplementary Fig. S5). Only IQGAP1-AA, a mutant lacking two major phosphorylation sites (Li et al., 2005), was able to rescue metastasis to the level of wild-type cells, even slightly better than rescuing with wild-type IQGAP1 (Fig. 5B, C), indicating that phosphorylation at S1441 and S1443 is at least unnecessary for IQGAP1's effects on metastasis and may even act in opposition. Interestingly, IQGAP1-AA was shown to be deficient in promoting neurite outgrowth in neuroblastoma cells compared to wild-type IQGAP1 (Li et al., 2005). This suggests that the function of these phosphorylation sites is particular to specific functions of IQGAP1, rather than globally controlling binding, as with the Ca^{2+}-dependent association of Calmodulin with IQGAP1, which negatively regulates IQGAP1's other binding interactions (Ho et al., 1999; Joyal et al., 1997; Li et al., 1999). Meanwhile, the remaining IQGAP1 mutants, those lacking all the IQ motifs (IQGAP1ΔIQ), unable to bind Rac1 and Cdc42 (IQGAP1-T), or missing the

RasGAP C-terminal domain (IQGAPΔCT), were all unable to rescue metastasis in IQGAP1 knockout cells at all. The IQ motifs are responsible for binding the MAPK B/C-Raf and Mek1/2 (Ren et al., 2007; Roy et al., 2005), as well as EGFR and YAP (McNulty et al., 2011; Sayedyahossein et al., 2016), involving this domain alone in cell survival, proliferation and migration. Indeed, the WW domain, which similarly binds the Erk1/2 MAPK, has previously been shown to be a valid therapeutic target: treatment with a peptide containing the IQGAP1 WW domain inhibited tumorigenesis and invasion of Ras-driven tumors in mice (Jameson et al., 2013). Moreover, YAP itself is a potent metastasis promoter (Lamar et al., 2012), so the interaction between IQGAP1 and YAP especially merits further investigation in the context of metastatic cancer. The inability of IQGAP1-T to regulate Rac1 and Cdc42 has very direct implications for cell migration and invasion, and cells expressing IQGAP1-T have been shown to be prone to form multiple leading edges (Fukata et al., 2002). It is therefore likely that the metastatic deficiency of cells expressing IQGAP1-T is due to their severely inhibited ability to extravasate out of blood vessels and invade into other tissues. The RGCT domain, much like the IQ domain, binds to a diverse array of proteins, including beta-catenin, E-cadherin, CLIP-170, APC and Sec3/8 (White et al., 2012). Thus, this domain is also critical in regulating proliferation, cell-cell adhesion, migration and invasion. This last function may be the most relevant in our study. The association between the exocyst complex proteins Sec3/8 and IQGAP1's RGCT domain is known to be crucial for the formation of mature invadopodia (Sakurai-Yageta et al., 2008), which are involved in both intravasation and extravasation (Gligorijevic et al., 2012; Leong et al., 2014). Consequently, it is probable that the RGCT is directly involved in mediating IQGAP1's effects on extravasation (Fig. 4). Together, the failure of the individual IQGAP1ΔIQ, IQGAP1-T and IQGAPΔCT mutants to rescue metastasis to any degree implies that IQGAP1's

effects in metastasis require several of its domains and functions, or at least a combination of binding partners that associate with different regions of the protein. More targeted studies, such as by blocking binding of specific proteins to IQGAP1, would be useful in isolating the particular binding partners important for metastasis.

In this study, we therefore present decisive evidence that IQGAP1 is critical for metastasis *in vivo*, both in melanoma and breast cancer models. This need for IQGAP1 is due largely to effects on extravasation, though other steps of the metastatic cascade may also be influenced by IQGAP1. These effects on metastasis require multiple domains of IQGAP1, involving at least several of the numerous binding partners of this versatile scaffold protein. The exact roles of IQGAP1 in metastasis merit further study, and IQGAP1 may represent a therapeutic target for metastatic cancer.

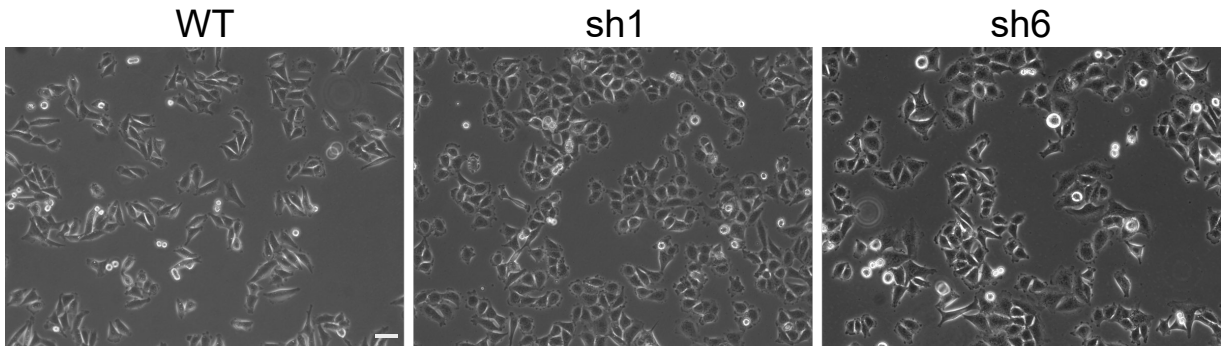

Supplementary Figure 1. Observed morphology of MA2 cells in culture.
Phase-contrast images of parental (WT) and IQGAP1 knockdown (sh1 and sh6) cells. Scale bar, 100 μm.

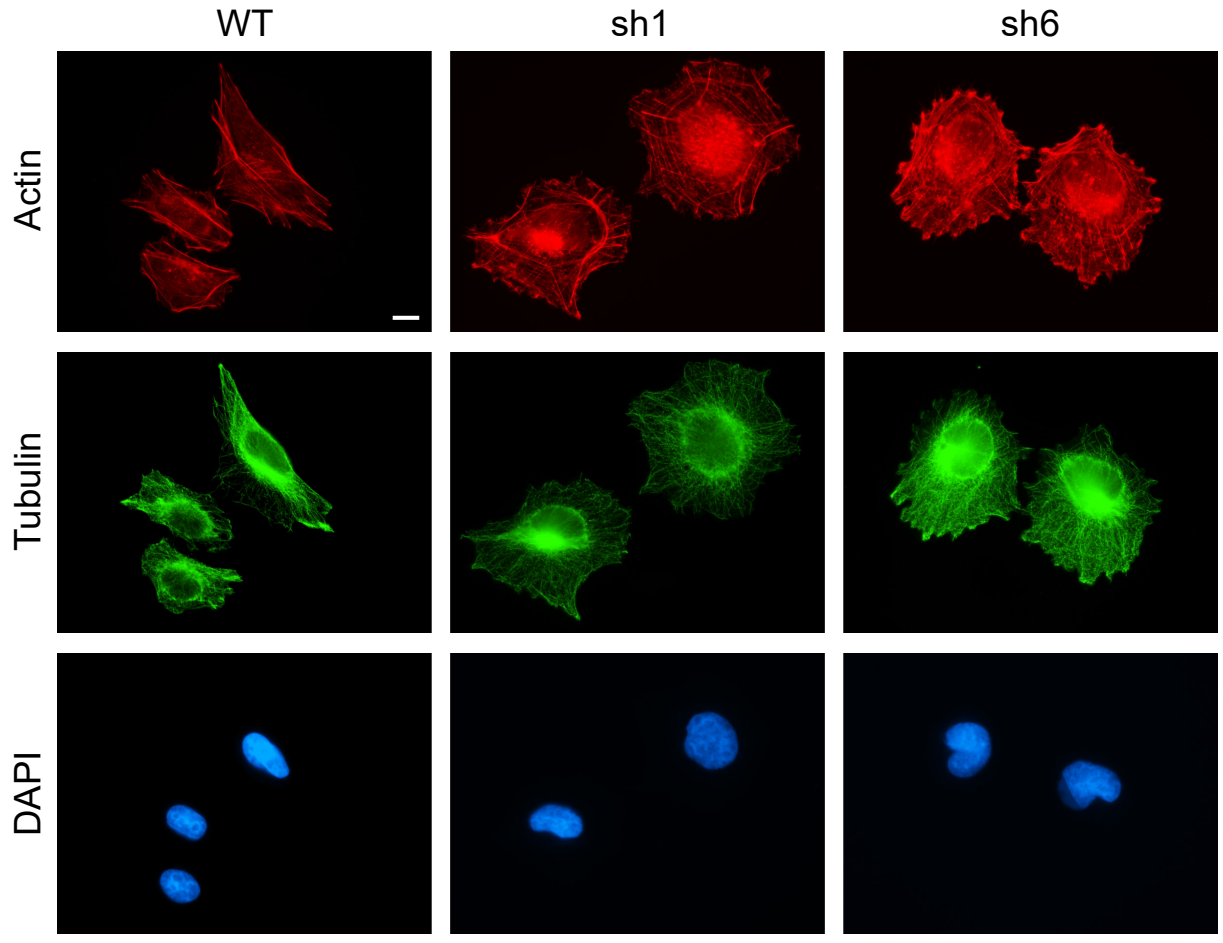

Supplementary Figure 2. Cytoskeletal staining of parental and IQGAP1 knockdown MA2 cells.
Immunofluorescence staining of actin (top panels), α-tubulin (middle panels) and DAPI (bottom panels) in parental (WT) and IQGAP1 knockdown (sh1 and sh6) cells. Scale bar, 10 μm.

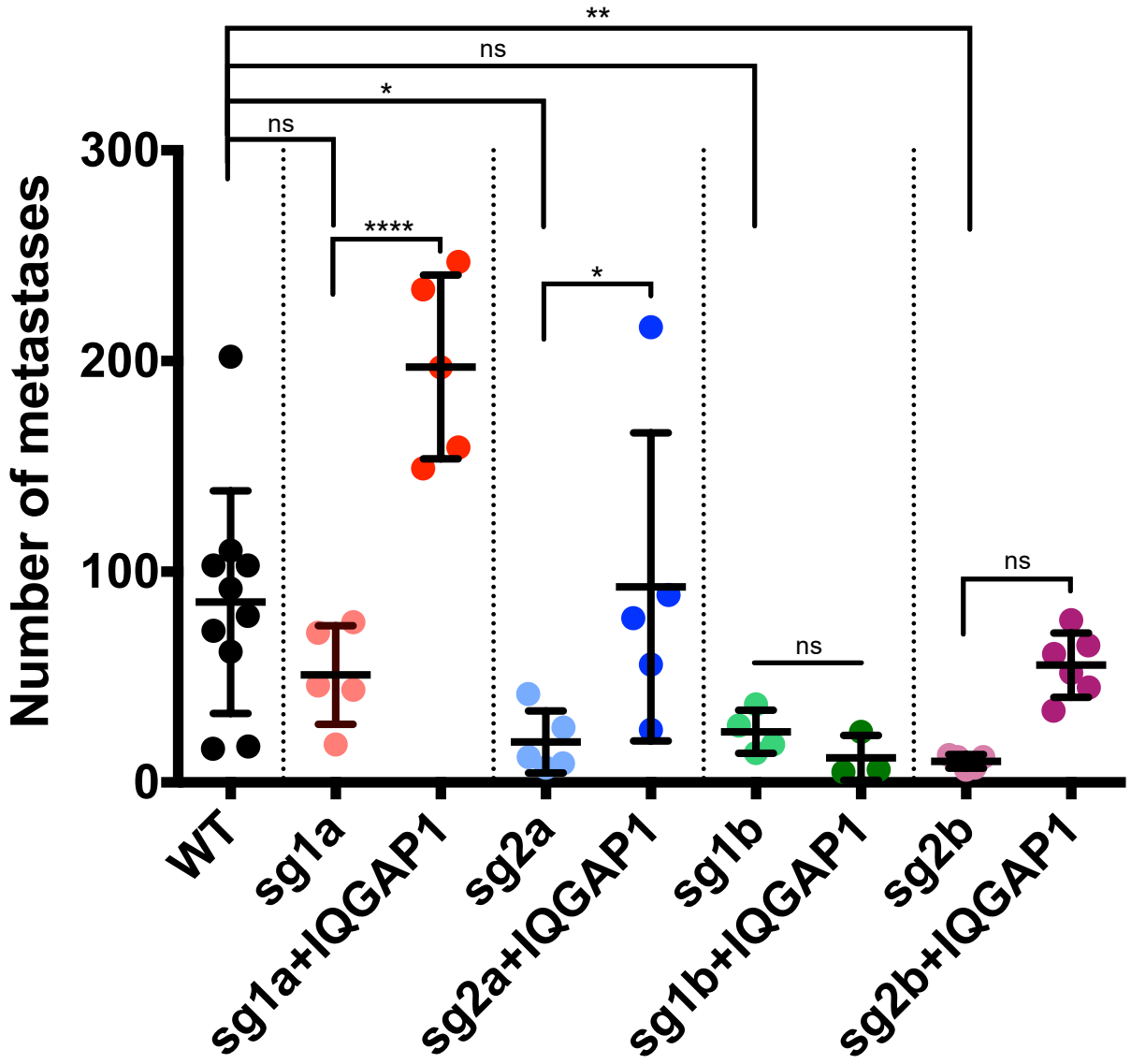

Supplementary Figure 3. Experimental metastasis of IQGAP1 clonal knockout and rescue cell lines.

Tail-vein injection of clonal IQGAP1 knockout (sg) and rescue (+IQGAP1) lines, each injected individually, with observed number of metastases shown. Data from Figure 2B are separated by clonal cell line; pairs of each clonal knockout and rescue line are shown grouped (dotted lines). n=3-10 mice per group. *, P≤ 0.05; **, P ≤ 0.01; ****, P ≤ 0.0001; one-way ANOVA with Šidák's multiple comparisons test.

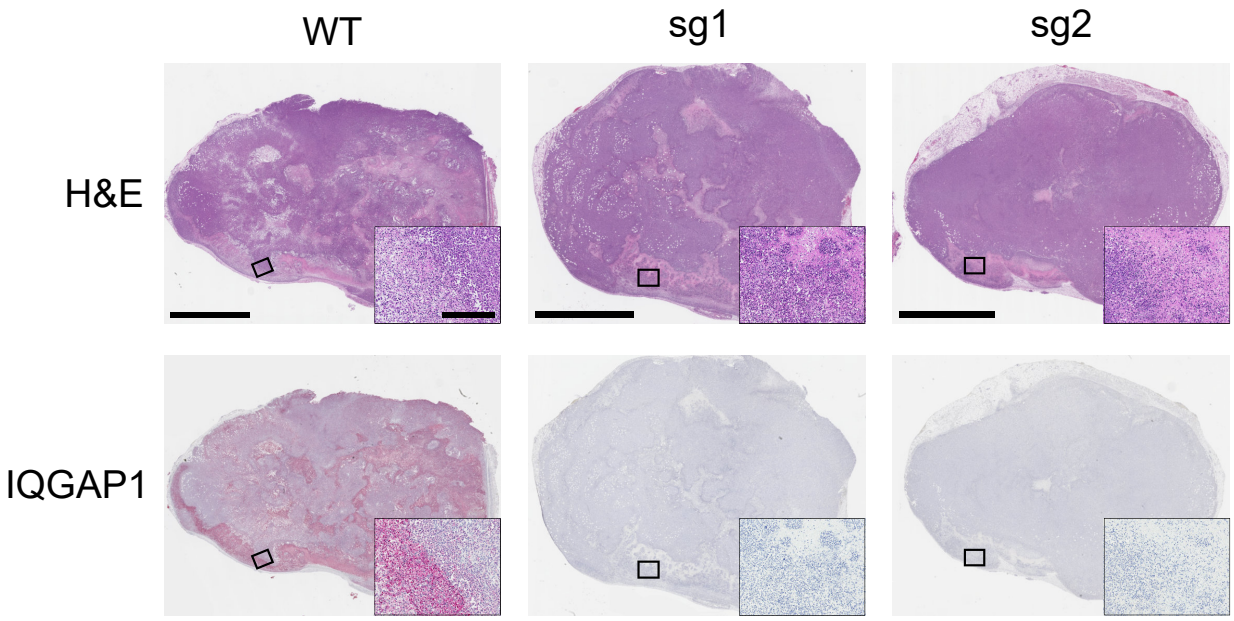

Supplementary Figure 4. Histological staining of LM2 primary tumors.
Representative histology images of full primary tumors from parental (WT) or clonal IQGAP1 knockout (sg) lines, showing H&E (top panels) or IQGAP1 (bottom panels) staining. Insets shown are the same as in Figure 3B. Boxes indicate areas from which insets were taken. Scale bars, 4 mm (full tumors) or 300 µm (insets).

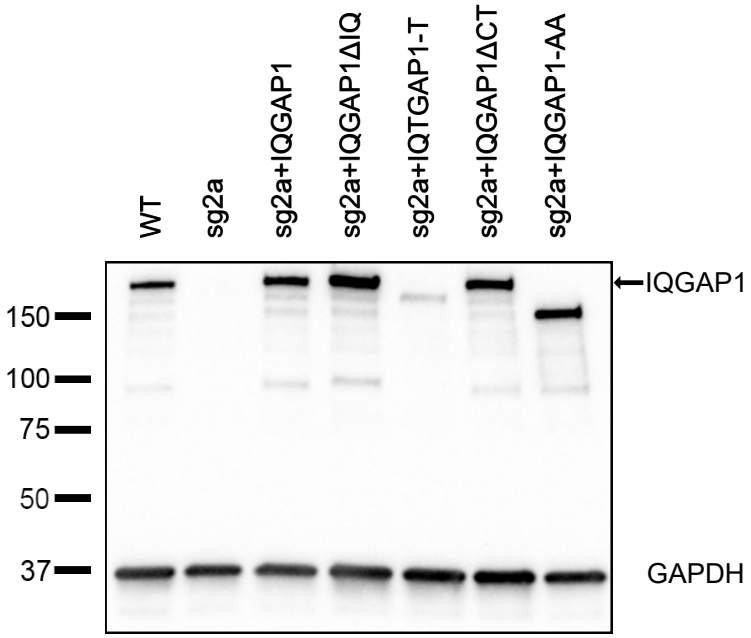

Supplementary Figure 5. Expression of IQGAP1 mutants.
Western blot of IQGAP1 and GAPDH in clonal IQGAP1 knockout line sg2a, rescued with either WT or mutant IQGAP1. Molecular weight markers in kDa are indicated. Full-length IQGAP1 is shown with an arrow.

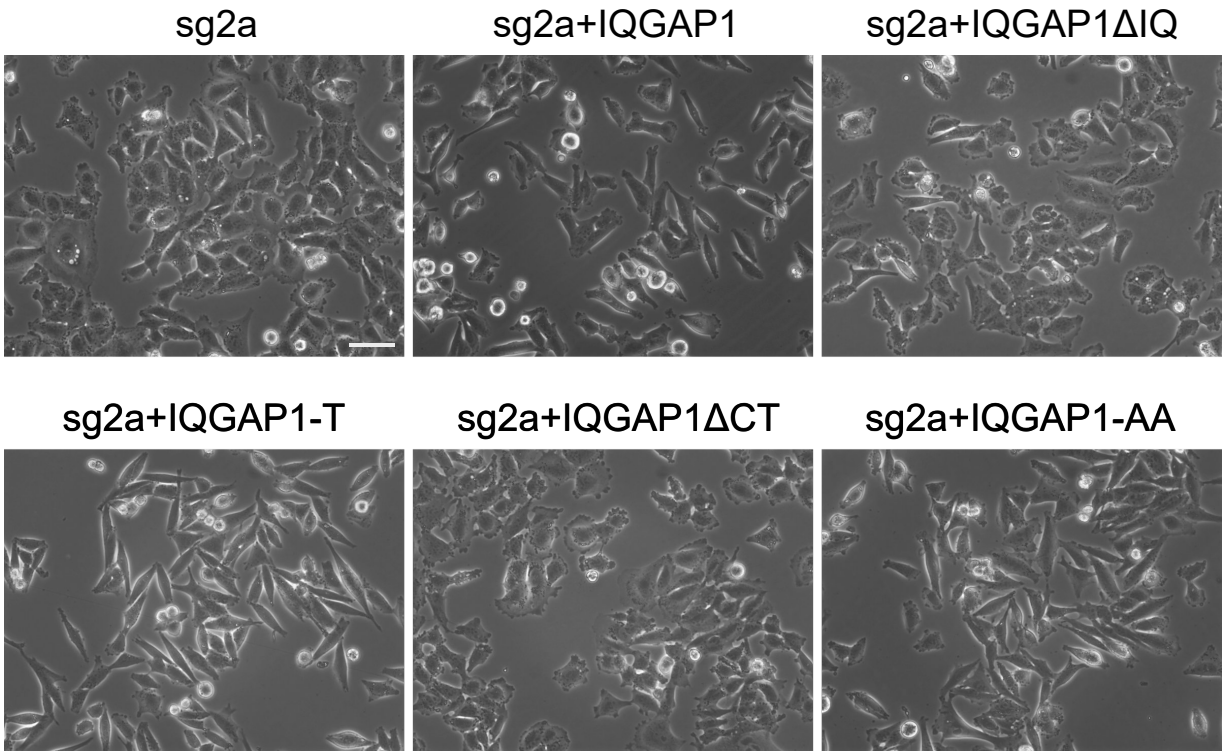

Supplementary Figure 6. Observed morphology of IQGAP1 knockout and rescue cells in culture.
Phase-contrast images of MA2 IQGAP1 clonal knockout line sg2a, and the same line rescued with WT ("+IQGAP1") or mutant IQGAP1. Scale bar, 100 μm.

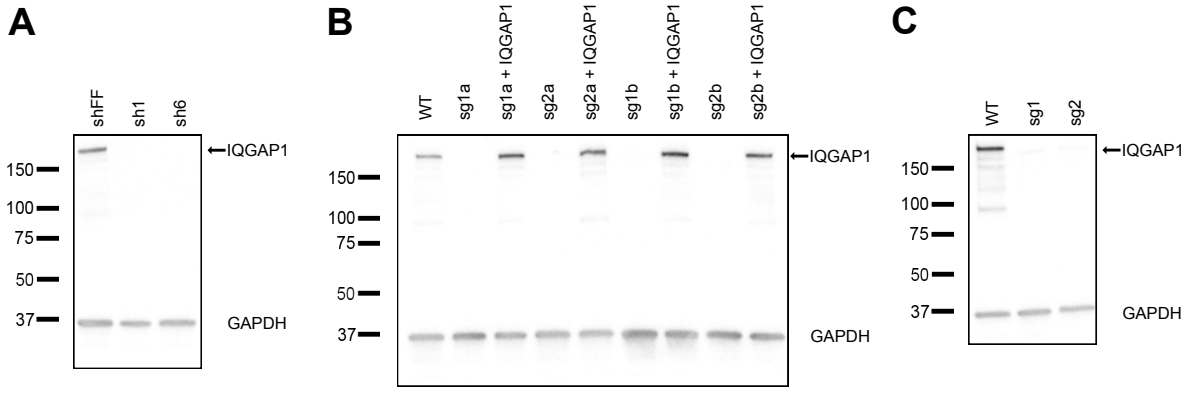

Supplementary Figure 7. Full-length western blots.
(A) Western blot of IQGAP1 and GAPDH in MA2 melanoma cells expressing shRNA against firefly luciferase (shFF) or IQGAP1 (sh1 and sh6). Full-length blot of Fig. 1A. (B) Western blot of IQGAP1 and GAPDH in parental (WT), clonal IQGAP1 knockout (sg) and rescue (+IQGAP1) MA2 lines. Full-length blot of Fig. 2A. (C) Western blot of IQGAP1 and GAPDH in parental (WT) and clonal IQGAP1 knockout (sg) LM2 lines. Full-length blot of Fig. 3A. For all blots, molecular weight markers in kDa are indicated, and full-length IQGAP1 is shown with an arrow.

Methods

Cell lines

The human melanoma MA2 cell line (Xu et al., 2008) and the human mammary carcinoma LM2-mCherry cell line (originally developed in the lab of Joan Massagué (Minn et al., 2005), a kind gift from Daniel Haber) were both cultured in HyClone high-glucose DMEM (ThermoFisher) supplemented with 2 mM glutamine and 10% fetal bovine serum (FBS, Invitrogen) in a 37°C incubator with 5% CO_2. Phase-contrast images of cells in culture were taken with a Zeiss Axiovert 200 microscope using a 10x or 5x objective.

Expression vectors

All IQGAP1 constructs were cloned into the pHAGE-IRES-puro vector (a kind gift from David Benjamin; the original pHAGE vector backbone itself was a kind gift from Tyler Jacks). pHAGE-IQGAP1-IRES-Puro (wild-type IQGAP1) was cloned from IQGAP1 cDNA (GE Healthcare, accession BC139731). The pcDNA3-myc-IQGAP1-ΔIQ (Sokol et al., 2001) and pcDNA3-myc-IQGAP1-S1441A/S1443A (Li et al., 2005) vectors (referred to as IQGAP1ΔIQ and IQGAP1-AA in this study) were kind gifts from David Sacks. The pEGFP-IQGAP1-T1050AX2 (referred to in this study as IQGAP1-T, originally developed in the lab of Kozo Kaibuchi (Fukata et al., 2002)) and pEGFP-IQGAP1-T1050AX2-ΔCC+RGC (Sakurai-Yageta et al., 2008) vectors were kind gifts from Philippe Chavrier. The T1050AX2 mutation was removed from IQGAP1-T1050AX2-ΔCC+RGC by cloning in the same region from wild-type IQGAP1, and the resulting construct is referred to as IQGAP1ΔCT in this study. MA2 cells were made

green or red fluorescent through expression of pHAGE-ZsGreen-IRES-Hygro or pHAGE-TdTomato-IRES-Hygro, respectively (kind gifts from David Benjamin). Vectors for IQGAP1 knockdown and knockout are described in the section below. Retroviral and lentiviral production and transduction of cells was performed as previously described (Stern et al., 2008).

Gene knockdown and knockout

miR30-based shRNAs targeting IQGAP1 for knockdown were designed using a tool developed by the lab of Michael Hemann (shrna.mit.edu) and cloned into MSCV-Puro-miR30, as previously described (Lamar et al., 2012; Stern et al., 2008). An shRNA against Firefly luciferase (shFF) was used as a control. sgRNAs for IQGAP1 knockout were designed using a tool developed by the lab of Michael Boutros (e-crisp.org) and cloned into lentiCRISPRv2 (Sanjana et al., 2014; Shalem et al., 2014). MA2 and LM2 cells were transiently transfected with lentiCRISPRv2 containing one of two sgRNAs against IQGAP1 (sg1 or sg2), then selected with puromycin. Cell populations were then sub-cloned to single cells. Following expansion, clonal cell lines were tested for IQGAP1 expression by western blotting (see next section). In this study, two clonal MA2 lines (a and b) were generated with each sgRNA (sg1 and sg2), resulting in four different clonal knockout lines (sg1a, sg1b, sg2a and sg2b). Each sgRNA was also used to generate a clonal LM2 line, resulting in two clonal knockout lines (sg1 and sg2).

Immunoblotting, immunohistochemistry and quantitative PCR

For immunoblotting, cells were lysed in Cell Lysis Buffer (Cell Signaling Technology) containing a complete mini-protease inhibitor cocktail (Roche) and a phosphatase-inhibitor cocktail (PhosSTOP, Roche), then 10 µg of protein lysate were separated by SDS-PAGE using

4–20% gradient gels (Bio-Rad), transferred to nitrocellulose membranes, and assayed by immunoblotting. Primary antibodies were used at the following dilutions: rabbit anti-IQGAP1, 1:1000 (ab133490, Abcam); and mouse anti-GAPDH, 1:5000 (MAB374, Millipore). Immunohistochemical staining of IQGAP1, as well as hematoxylin and eosin staining, were performed as previously described, with rabbit anti-IQGAP1 used at a 1:500 dilution (sc-10792, Santa Cruz) (Rickelt and Hynes, 2018).

For quantitative PCR (qPCR), cells were lysed in TRIzol (Invitrogen), RNA was isolated according to the manufacturer's instructions, and cDNA was synthesized by reverse transcription using the First-Strand cDNA Synthesis Kit (Promega). qPCR reactions were performed using SYBR Green Supermix (Bio-Rad) according to the manufacturer's instructions, and data analysis was performed using Bio-Rad CFX Manager Software. PCR conditions were 95°C for 10 min, followed by 40 cycles of 95°C for 20 s, 60°C for 30 s, and 72°C for 30 s. The following primers were used: IQGAP1-forward, TTCTATGCAGCTTTCTCGGG; IQGAP1-reverse, CTGTCGAACTAAGTATCCACGG; GAPDH-forward, ACATCGCTCAGACACCATG; GAPDH-reverse, TGTAGTTGAGGTCAATGAAGGG.

Immunofluorescence and gelatin degradation assay

Immunofluorescence staining was performed as described elsewhere (Krawczyk et al., 2010), except that normal goat serum was used to block for goat secondary antibodies. TRITC-phalloidin (1:1000, Sigma) was used to detect actin, along with rabbit anti-α-tubulin (1:500, ab18251, Abcam). To label cover slips with fluorescent gelatin, 18 mm circular No. 2 cover glass (VWR) was washed with a 2:1 mixture of nitric to hydrochloric acid for 2 hr, rinsed with

70% ethanol, then coated with 50 µg/ml poly-D-lysine for 20 min and fixed with 0.5% glutaraldehyde for 15 min. After washing with PBS, cover slips were then coated with FITC-gelatin (Molecular Probes) mixed with 2% sucrose. Cover slips were then coated with 20 µg/ml fibronectin (Advanced BioMatrix) and quenched with 5 mg/ml sodium borohydride (Sigma). 30,000 cells were added to each gelatin-coated cover slip. Cells were fixed 5 hours after plating with 4% paraformaldehyde and stained with .5 µg/ml DAPI (ThermoFisher). All images were taken with a Zeiss Axiovert 200 microscope using a 63x objective. Quantification of gelatin degradation area was conducted with ImageJ, and at least 50 cells were counted per line.

Tumor growth and metastasis assays

For tail-vein end-stage metastasis assays (excluding the extravasation assay detailed below), $1x10^6$ MA2 cells were injected into the lateral tail veins of 6-10-week-old male NOD-SCID mice (Jackson Laboratory) in 100 µL of Hanks' Balanced Salt Solution (HBSS, Gibco). For mixing experiments (Figure 1C-E), the cells injected were a 50/50 mix of TdTomato-labeled shFF control cells and ZsGreen-labeled experimental cells (either shFF or IQGAP1-targeting sh1 or sh6). 6 weeks after injection, lung lobes were dissected and then imaged with a Leica M165 FC dissecting microscope. ZsGreen- or TdTomato-labeled metastases were counted visually, and tumor burden was quantified by dividing tumor area by total tissue area using ImageJ. For orthotopic mammary transplant assays, $1x10^5$ LM2 cells were injected into the #4 mammary fat pads of 6- to 10-week old female NOD/SCID/IL2Rγ-null mice (Jackson Laboratory) in 25 µL of HBSS. 8 weeks after injection, primary tumors were dissected, weighed and fixed in 3.8% formaldehyde for subsequent paraffin embedding and sectioning. Lungs and liver left lobes were

also collected and imaged as described above for tail-vein metastasis assays. All procedures were performed according to the animal protocol approved by MIT's Committee on Animal Care.

In vivo extravasation assay

One hundred microliters of cell suspension in PBS ($1x10^6$ cells) were injected via lateral tail vein of NOD/SCID/gamma mice. Mice were euthanized, and lungs were collected after inflation with 4% formaldehyde and 0.3% Triton X-100 at 20 hours post injection. Fixed lungs were then cut to thin slices (0.5 mm thick) by scalpel and stained with anti-CD31 (5533070, BD Biosciences, 1:100) and Alexa 594-conjugated goat anti-rat IgG (Molecular probes). Images were taken with a Nikon A1R laser scanning confocal microscope using a 40x objective.

Statistical analysis

All data were expressed as mean ± standard deviation. Statistical analysis was conducted with GraphPad Prism 6 (GraphPad Software). All comparisons were made using one-way ANOVA, with Dunnett's, Tukey's or Šidák's multiple comparisons test as appropriate, with $P \leq 0.05$ considered significant. Significance levels were indicated as follows: ns, $P > 0.05$; *, $P \leq 0.05$; **, $P \leq 0.01$; ***, $P \leq 0.001$; ****, $P \leq 0.0001$.

References

Bashour, A.-M., Fullerton, A.T., Hart, M.J., and Bloom, G.S. (1997). IQGAP1, a Rac-and Cdc42-binding protein, directly binds and cross-links microfilaments. J. Cell Biol. *137*, 1555–1566.

Beaty, B.T., and Condeelis, J. (2014). Digging a little deeper: The stages of invadopodium formation and maturation. Eur. J. Cell Biol.

Ben-David, U., Siranosian, B., Ha, G., Tang, H., Oren, Y., Hinohara, K., Strathdee, C.A., Dempster, J., Lyons, N.J., Burns, R., et al. (2018). Genetic and transcriptional evolution alters cancer cell line drug response. Nature *560*, 325.

Brown, M.D., and Sacks, D.B. (2006). IQGAP1 in cellular signaling: bridging the GAP. Trends Cell Biol. *16*, 242–249.

Casteel, D.E., Turner, S., Schwappacher, R., Rangaswami, H., Su-Yuo, J., Zhuang, S., Boss, G.R., and Pilz, R.B. (2012). Rho Isoform-specific Interaction with IQGAP1 Promotes Breast Cancer Cell Proliferation and Migration. J. Biol. Chem. *287*, 38367–38378.

Clark, E.A., Golub, T.R., Lander, E.S., and Hynes, R.O. (2000). Genomic analysis of metastasis reveals an essential role for RhoC. Nature *406*, 532–535.

Diao, B., Liu, Y., Zhang, Y., Yu, J., Xie, J., and Xu, G.-Z. (2017). IQGAP1-siRNA inhibits proliferation and metastasis of U251 and U373 glioma cell lines. Mol. Med. Rep. *15*, 2074–2082.

Dong, P., Ihira, K., Xiong, Y., Watari, H., Hanley, S.J.B., Yamada, T., Hosaka, M., Kudo, M., Yue, J., and Sakuragi, N. (2016). Reactivation of epigenetically silenced miR-124 reverses the epithelial-to-mesenchymal transition and inhibits invasion in endometrial cancer cells via the direct repression of IQGAP1 expression. Oncotarget.

Fukata, M., Watanabe, T., Noritake, J., Nakagawa, M., Yamaga, M., Kuroda, S., Matsuura, Y., Iwamatsu, A., Perez, F., and Kaibuchi, K. (2002). Rac1 and Cdc42 capture microtubules through IQGAP1 and CLIP-170. Cell *109*, 873–885.

Gligorijevic, B., Wyckoff, J., Yamaguchi, H., Wang, Y., Roussos, E.T., and Condeelis, J. (2012). N-WASP-mediated invadopodium formation is involved in intravasation and lung metastasis of mammary tumors. J. Cell Sci. *125*, 724–734.

Gupta, G.P., and Massagué, J. (2006). Cancer Metastasis: Building a Framework. Cell *127*, 679–695.

Hart, M.J., Callow, M.G., Souza, B., and Polakis, P. (1996). IQGAP1, a calmodulin-binding protein with a rasGAP-related domain, is a potential effector for cdc42Hs. EMBO J. *15*, 2997.

Hedman, A.C., Smith, J.M., and Sacks, D.B. (2015). The biology of IQGAP proteins: beyond the cytoskeleton. EMBO Rep.

Ho, Y.-D., Joyal, J.L., Li, Z., and Sacks, D.B. (1999). IQGAP1 Integrates Ca2+/Calmodulin and Cdc42 Signaling. J. Biol. Chem. *274*, 464–470.

Jadeski, L., Mataraza, J.M., Jeong, H.-W., Li, Z., and Sacks, D.B. (2008). IQGAP1 Stimulates Proliferation and Enhances Tumorigenesis of Human Breast Epithelial Cells. J. Biol. Chem. *283*, 1008–1017.

Jameson, K.L., Mazur, P.K., Zehnder, A.M., Zhang, J., Zarnegar, B., Sage, J., and Khavari, P.A. (2013). IQGAP1 scaffold-kinase interaction blockade selectively targets RAS-MAP kinase–driven tumors. Nat. Med. *19*, 626–630.

Jin, X., Liu, Y., Liu, J., Lu, W., Liang, Z., Zhang, D., Liu, G., Zhu, H., Xu, N., and Liang, S. (2015). The Overexpression of IQGAP1 and β-Catenin Is Associated with Tumor Progression in Hepatocellular Carcinoma In Vitro and In Vivo. PloS One *10*, e0133770.

Joyal, J.L., Annan, R.S., Ho, Y.-D., Huddleston, M.E., Carr, S.A., Hart, M.J., and Sacks, D.B. (1997). Calmodulin Modulates the Interaction between IQGAP1 and Cdc42 IDENTIFICATION OF IQGAP1 BY NANOELECTROSPRAY TANDEM MASS SPECTROMETRY. J. Biol. Chem. *272*, 15419–15425.

Krawczyk, E., Suprynowicz, F.A., Sudarshan, S.R., and Schlegel, R. (2010). Membrane Orientation of the Human Papillomavirus Type 16 E5 Oncoprotein. J. Virol. *84*, 1696–1703.

Kuroda, S. (1998). Role of IQGAP1, a Target of the Small GTPases Cdc42 and Rac1, in Regulation of E-Cadherin- Mediated Cell-Cell Adhesion. Science *281*, 832–835.

Lamar, J.M., Stern, P., Liu, H., Schindler, J.W., Jiang, Z.-G., and Hynes, R.O. (2012). The Hippo pathway target, YAP, promotes metastasis through its TEAD-interaction domain. Proc. Natl. Acad. Sci. *109*, E2441–E2450.

Lambert, A.W., Pattabiraman, D.R., and Weinberg, R.A. (2017). Emerging Biological Principles of Metastasis. Cell *168*, 670–691.

Le Clainche, C., Schlaepfer, D., Ferrari, A., Klingauf, M., Grohmanova, K., Veligodskiy, A., Didry, D., Le, D., Egile, C., Carlier, M.-F., et al. (2007). IQGAP1 Stimulates Actin Assembly through the N-Wasp-Arp2/3 Pathway. J. Biol. Chem. *282*, 426–435.

Leong, H.S., Robertson, A.E., Stoletov, K., Leith, S.J., Chin, C.A., Chien, A.E., Hague, M.N., Ablack, A., Carmine-Simmen, K., McPherson, V.A., et al. (2014). Invadopodia Are Required for Cancer Cell Extravasation and Are a Therapeutic Target for Metastasis. Cell Rep. *8*, 1558–1570.

Li, Z., Kim, S.H., Higgins, J.M.G., Brenner, M.B., and Sacks, D.B. (1999). IQGAP1 and Calmodulin Modulate E-cadherin Function. J. Biol. Chem. *274*, 37885–37892.

Li, Z., McNulty, D.E., Marler, K.J.M., Lim, L., Hall, C., Annan, R.S., and Sacks, D.B. (2005). IQGAP1 Promotes Neurite Outgrowth in a Phosphorylation-dependent Manner. J. Biol. Chem. *280*, 13871–13878.

McNulty, D.E., Li, Z., White, C.D., Sacks, D.B., and Annan, R.S. (2011). MAPK Scaffold IQGAP1 Binds the EGF Receptor and Modulates Its Activation. J. Biol. Chem. *286*, 15010–15021.

Minn, A.J., Gupta, G.P., Siegel, P.M., Bos, P.D., Shu, W., Giri, D.D., Viale, A., Olshen, A.B., Gerald, W.L., and Massagué, J. (2005). Genes that mediate breast cancer metastasis to lung. Nature *436*, 518–524.

Nabeshima, K., Shimao, Y., Inoue, T., and Koono, M. (2002). Immunohistochemical analysis of IQGAP1 expression in human colorectal carcinomas: its overexpression in carcinomas and association with invasion fronts. Cancer Lett. *176*, 101–109.

Ren, J.-G., Li, Z., and Sacks, D.B. (2007). IQGAP1 modulates activation of B-Raf. Proc. Natl. Acad. Sci. *104*, 10465–10469.

Rickelt, S., and Hynes, R.O. (2018). Antibodies and methods for immunohistochemistry of extracellular matrix proteins. Matrix Biol.

Roy, M., Li, Z., and Sacks, D.B. (2004). IQGAP1 Binds ERK2 and Modulates Its Activity. J. Biol. Chem. *279*, 17329–17337.

Roy, M., Li, Z., and Sacks, D.B. (2005). IQGAP1 Is a Scaffold for Mitogen-Activated Protein Kinase Signaling. Mol. Cell. Biol. *25*, 7940–7952.

Sakurai-Yageta, M., Recchi, C., Le Dez, G., Sibarita, J.-B., Daviet, L., Camonis, J., D'Souza-Schorey, C., and Chavrier, P. (2008). The interaction of IQGAP1 with the exocyst complex is required for tumor cell invasion downstream of Cdc42 and RhoA. J. Cell Biol. *181*, 985–998.

Sanjana, N.E., Shalem, O., and Zhang, F. (2014). Improved vectors and genome-wide libraries for CRISPR screening. Nat. Methods *11*, 783–784.

Sayedyahossein, S., Li, Z., Hedman, A.C., Morgan, C.J., and Sacks, D.B. (2016). IQGAP1 Binds To YAP and Modulates Its Transcriptional Activity. J. Biol. Chem. jbc.M116.732529.

Shalem, O., Sanjana, N.E., Hartenian, E., Shi, X., Scott, D.A., Mikkelsen, T.S., Heckl, D., Ebert, B.L., Root, D.E., Doench, J.G., et al. (2014). Genome-Scale CRISPR-Cas9 Knockout Screening in Human Cells. Science *343*, 84–87.

Siegel, R.L., Miller, K.D., and Jemal, A. (2018). Cancer statistics, 2018. CA. Cancer J. Clin. *68*, 7–30.

Sokol, S.Y., Li, Z., and Sacks, D.B. (2001). The Effect of IQGAP1 on Xenopus Embryonic Ectoderm Requires Cdc42. J. Biol. Chem. *276*, 48425–48430.

Steeg, P.S. (2016). Targeting metastasis. Nat. Rev. Cancer *16*, 201–218.

Stern, P., Astrof, S., Erkeland, S.J., Schustak, J., Sharp, P.A., and Hynes, R.O. (2008). A system for Cre-regulated RNA interference in vivo. Proc. Natl. Acad. Sci. *105*, 13895–13900.

Su, D., Liu, Y., and Song, T. (2017). Knockdown of IQGAP1 inhibits proliferation and epithelial-mesenchymal transition by Wnt/β-catenin pathway in thyroid cancer. OncoTargets Ther. *10*, 1549–1559.

Wang, X.-X., Wang, K., Li, X.-Z., Zhai, L.-Q., Qu, C.-X., Zhao, Y., Liu, Z.-R., Wang, H.-Z., An, Q.-J., Jing, L.-W., et al. (2014). Targeted Knockdown of IQGAP1 Inhibits the Progression of Esophageal Squamous Cell Carcinoma In Vitro and In Vivo. PLoS ONE *9*, e96501.

White, C.D., Brown, M.D., and Sacks, D.B. (2009). IQGAPs in cancer: A family of scaffold proteins underlying tumorigenesis. FEBS Lett. *583*, 1817–1824.

White, C.D., Erdemir, H.H., and Sacks, D.B. (2012). IQGAP1 and its binding proteins control diverse biological functions. Cell. Signal. *24*, 826–834.

Xu, L., Shen, S.S., Hoshida, Y., Subramanian, A., Ross, K., Brunet, J.-P., Wagner, S.N., Ramaswamy, S., Mesirov, J.P., and Hynes, R.O. (2008). Gene Expression Changes in an Animal Melanoma Model Correlate with Aggressiveness of Human Melanoma Metastases. Mol. Cancer Res. *6*, 760–769.

Zhao, H.-Y., Han, Y., Wang, J., Yang, L.-H., Zheng, X.-Y., Du, J., Wu, G.-P., and Wang, E.-H. (2017). IQ-domain GTPase-activating protein 1 promotes the malignant phenotype of invasive ductal breast carcinoma via canonical Wnt pathway. Tumor Biol. *39*, 1010428317705769.

Chapter 3.

Distinct ECM proteins of breast cancer metastatic niches in multiple organs

This chapter was written by Jess Hebert with editing by Richard Hynes. All experiments described in this chapter were performed by Jess Hebert, except for mass spectrometry, which was performed by Sam Myers. Genevieve Abbruzzese assisted with experimental dissections. This study was designed by Jess Hebert, Alexandra Naba, Steven Carr and Richard Hynes. This chapter is adapted from a study that is being prepared for submission as:

Hebert, J.D., Myers, S.A., Naba, A., Abbruzzese, G., Carr, S.A., and Hynes, R.O. (2019). Distinct ECM proteins of breast cancer metastatic niches in multiple organs. [In Preparation].

Abstract

Metastasis remains the cause of the vast majority of cancer-related deaths, and one of the most insidious aspects of metastatic cancer is the adaptability of cells from a single primary tumor to survive in multiple, vastly different secondary sites. Nevertheless, how cells from the same primary tumor are able to adapt to all these environments is not fully understood. A critical component of every metastatic niche is the extracellular matrix (ECM), which provides structural support, migration control, and growth and survival signals. However, a comprehensive comparison of the ECM components of metastatic niches at various secondary tumor sites has not yet been conducted. In this study, we isolate metastases from the brain, lungs, liver and bone marrow, which were all derived from parental MDA-MB-231 breast cancer cells. We then enriched these tumor samples for ECM proteins and use quantitative mass spectrometry to analyze their ECM composition. Strikingly, both the tumor-cell-derived and the induced stroma-derived ECM and ECM-associated proteins differ at each site; that is, the niches created are distinct. Using these data, we compare protein abundance across all metastatic sites to determine which ECM proteins are most significantly elevated in each particular tissue relative to the others. Following this analysis, we knock down tumor cell expression of SERPINB1, a protein characteristically elevated in brain metastases, and observe reduced metastasis to the brain. This investigation offers insight into the fundamental biology of metastatic niches, as well as provides potential markers of metastatic breast cancer for imaging and therapy.

Introduction

Metastasis is responsible for the considerable majority of cancer deaths (Lambert et al., 2017), yet our understanding of its fundamental processes, as well as how to detect and treat it, remains inadequate relative to the threat it poses. This is particularly relevant in the case of triple-negative breast cancer (TNBC), a breast cancer subtype defined by the lack of expression of estrogen receptor, progesterone receptor and epidermal growth factor receptor (EGFR, also known as HER2). TNBC, which accounts for 15% of all breast carcinomas, is especially aggressive, capable of metastasizing to the brain, lungs, liver and bone marrow (Denkert et al., 2017). However, the lack of its eponymous three genes makes targeted treatment of TNBC difficult, so chemotherapy remains the standard of care (Bianchini et al., 2016). Nevertheless, even with chemotherapy treatment, the median overall survival rate for women with metastatic breast cancer is only two years (Bonotto et al., 2014). Thus, there is a clear need for additional ways to target and treat this disease.

The extracellular matrix (ECM) represents one such promising avenue of research in cancer therapy. The ECM is a critical part of the tumor microenvironment: the complete collection of tumor cells, stromal cells, vasculature and non-cellular components that make up a tumor (Place et al., 2011). ECM proteins provide structural support, migration control, and growth and survival signals to tumor cells, and tumor cells both produce ECM proteins themselves as well as induce surrounding stromal cells to alter their own ECM production presumably, at least in part, to suit the growth of the tumor (Lu et al., 2012). Moreover, the extracellular localization of the ECM makes it well-suited for use in imaging and targeting, since it is accessible to probes without the need to cross through cell membranes. Indeed, we have

successfully used ECM-targeting nanobodies for PET/CT imaging of both primary tumors and metastases in several cancer models (Jailkhani et al.).

The ECM is also essential to the construction of the metastatic niche, the microenvironment that tumor cells create when spreading to different sites, which is conducive to their survival and proliferation into overt metastases. A few specific ECM proteins have previously been identified as crucial parts of certain metastatic niches in breast cancer. Tenascin C has been shown to be produced by lung-tropic breast cancer cells in pulmonary metastases in order to enhance stem cell signaling (Oskarsson et al., 2011). Overexpression of osteopontin in breast cancer cells can also enhance lung metastasis, dependent on integrin binding by the tumor cells (Allan et al., 2006). Periostin was demonstrated to be necessary for spontaneous pulmonary metastasis of an MMTV-PyMT breast cancer model due to its role in promoting Wnt signaling (Malanchi et al., 2011). Amplified fibronectin production can promote metastasis of a wide variety of cancers (Barbazán et al., 2017; Hsu et al., 2017; Kenny et al., 2014; Malik et al., 2010). However, overall understanding of which ECM proteins are present in metastatic niches is lacking, particularly in secondary sites aside from the lung. Therefore, a more complete survey of the ECM in different metastatic sites would markedly increase our knowledge of both the role of the ECM in breast cancer metastasis, as well as how the ECM is differentially altered in various metastatic tissues.

We have previously developed methods for enriching tissue samples for their ECM protein content by taking advantage of the relative insolubility of the ECM (Naba et al., 2015), and we have used these techniques in conjunction with mass spectrometry to profile the ECM in a number of different cancers. For example, a comparison of breast cancer xenograft tumors created from either MDA-MB-231 or 231-LM2 cells identified several ECM proteins

characteristic of primary tumors more likely to metastasize, including SNED1 (Naba et al., 2014a). An assessment of patient primary colon cancers and their derived liver metastases discovered distinct ECM signatures for primary tumors and metastases, suggesting that tumor cells do not simply recapitulate the same ECM niche from one location to the other (Naba et al., 2014b). Profiling genetically engineered mouse lung adenocarcinomas and lymph node metastases revealed that Tenascin C, S100A10 and S100A11 are involved in lung cancer progression and are predictive of poor patient prognosis (Gocheva et al., 2017). Nevertheless, we have yet to examine metastases in more than one tissue derived from the same cancer.

This study seeks to conduct a comprehensive comparison of ECM components of the metastatic niche among various secondary tumor sites common in breast cancer. For this purpose, we use as a model the parental, heterogeneous MDA-MB-231 human TNBC cell line, originally derived from a patient pleural effusion (Cailleau et al., 1978), which is capable of metastasizing to the brain, lungs, liver and bone marrow in mouse xenografts. We identify which ECM proteins are commonly over-expressed at multiple different metastatic sites, and which are preferentially overexpressed in particular sites. We investigate how these specific ECM proteins, as well as the tumor matrix overall, are differentially produced by the tumor and stromal cells. Finally, as an example of the utility of this system for finding novel ECM mediators of metastasis, we show that knockdown of SERPINB1 in tumor cells can significantly reduce their brain-tropic metastasis. This survey of the ECM in metastases thus presents insight into the fundamental biology of metastatic niche formation, as well as potential metastatic markers.

Results

Quantitative measurement of the ECM in metastases highlights differences among tissues

To evaluate the composition of the metastatic niches that tumors create when growing in different tissues, we used as a model the metastatic MDA-MB-231 human triple-negative mammary carcinoma cell line (Cailleau et al., 1978). These cells were introduced into circulation via intracardiac injection in order to generate brain, liver and bone-marrow metastases, or via tail-vein injection to generate lung metastases. Brain, lung and bone metastases were harvested from NOD-SCID mice. However, as these cells did not form liver tumors in any NOD-SCID mice injected, we also injected cells into NOD-SCID-gamma mice to collect liver metastases. Bone tumors from both mouse strains were collected for purposes of comparison.

Following collection of metastatic and normal tissue samples from all four tissues, the samples were enriched for their ECM protein content as previously described (Naba et al., 2015). After performing western blots to track the quality of this ECM enrichment (Supplementary Fig. S1), the samples were digested and labeled with tandem mass tags (TMT) for quantitative mass spectrometry (Fig. 1A). Samples were named according to their tissue of origin, mouse strain, and normal or metastatic sample type (Fig. 1B, Supplementary Table S1). Even based on preliminary, label-free analysis, the different tissues had clearly different ECM protein profiles (Fig. 1C). The brain has a considerably lower quantity of ECM proteins compared to the other, relatively more matrix-rich tissues. A quantitative mass spectrometry approach was therefore needed to perform a proper comparison among these vastly different tissues.

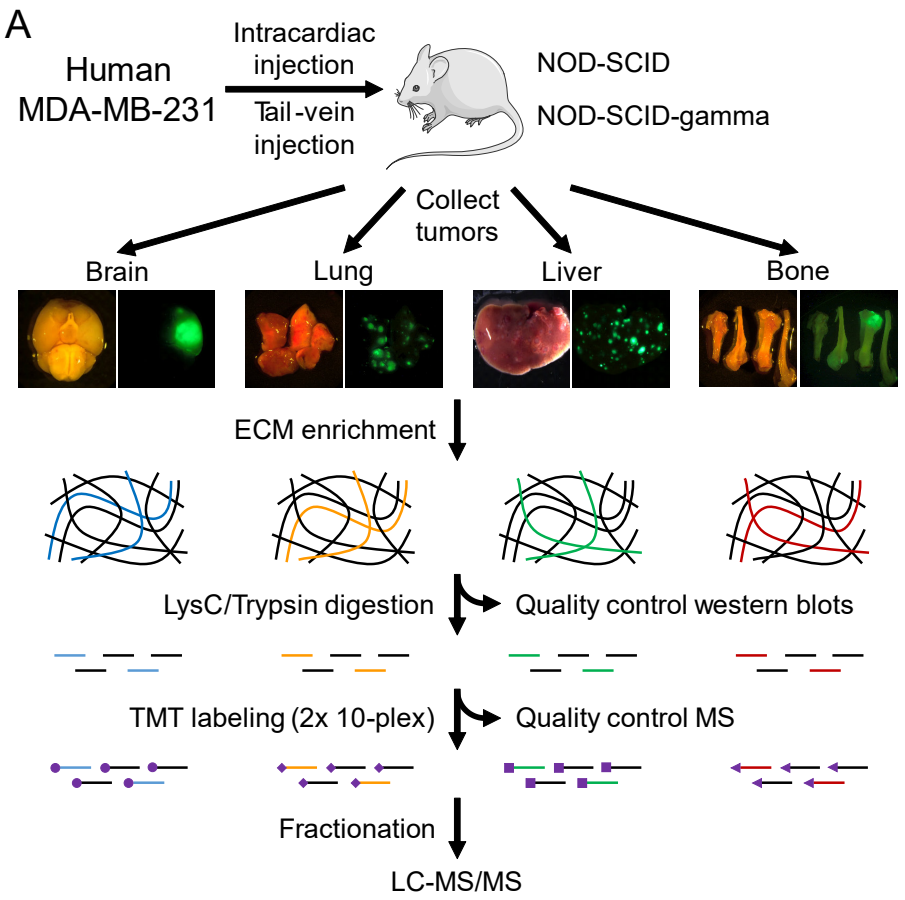

B

BrSM1

Tissue	Strain	Type
Brain	NOD **S**cid	**N**ormal
Lung	NOD Scid **G**amma	**M**etastasis
Liver		
Bone		

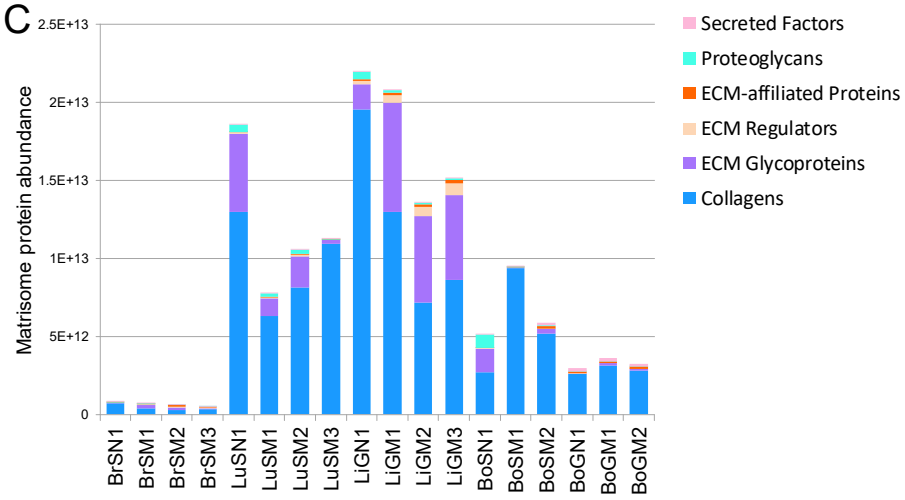

Figure 1. Overview of sample collection, preparation and mass spectrometry.
(A) Experimental workflow. MDA-MB-231 cells expressing luciferase and ZsGreen were injected into the tail-vein or heart of NOD/SCID or NOD/SCID/IL2Rγ-null mice. Tumor growth was monitored by IVIS bioluminescence imaging, and tumors were collected 4-12 weeks following injection. Normal control tissues were also collected from uninjected mice. Following ECM enrichment, quality control western blots (see Supplementary Fig. S1) and proteolytic digestion, samples were divided into two 10-plex TMT series (see Supplementary Table S1), with equal parts of all samples combined and used as a common reference control between the two series. Following stage-tip fractionation, samples were run on a Q Exactive Plus mass spectrometer. (B) Sample nomenclature. (C) Quality control pre-fractionation mass spectrometry showing total intensity of matrisome proteins observed in each sample, broken down by matrisome category.

The matrisome can be divided into core matrisome proteins (collagens, ECM glycoproteins and proteoglycans) and matrisome-associated proteins ([1] ECM regulators such as proteases and crosslinking enzymes, [2] ECM-affiliated proteins that are often found in association with the core matrisome proteins, and [3] secreted factors like growth factors) (Naba et al., 2016). Among all samples, we quantified 307 matrisome proteins (Fig. 2A), a nearly two-fold increase compared to our previous characterizations of primary breast tumors (Naba et al., 2014a), and a more than two-fold increase compared to previous analyses of other metastatic tumors (in colon and lung cancers) (Gocheva et al., 2017; Naba et al., 2014b). Due to the large number of samples analyzed, two 10-plex TMT series were used to fit all of them (Supplementary Table S1). Nevertheless, we observed 80-90% overlap between the two TMT series (Fig. 2B), with the majority of non-overlapping proteins coming from Series A, which contained all of the normal tissue samples. Accordingly, 30/42 of the non-overlapping proteins from Series A came from the stroma (mouse proteins), compared to only 8/18 non-overlapping proteins in Series B, suggesting that many of these A-only stromal proteins are likely present only in normal tissue (Supplementary Fig. S2). Moreover, despite matrisome proteins being only around 5% of the total number of proteins quantified in our data (Fig. 2C), they represented a

third of the total protein abundance due to our ECM enrichment (Fig. 2D), despite the extremely low matrix content of tissues like the brain (Fig. 1C). Finally, calculation of the Spearman correlation between each pair of samples revealed that metastatic samples tended to cluster by tissue, but that individual tissues, particularly the brain, were markedly different from one another (Fig. 2E). Some metastases were so different compared to their corresponding normal tissue that they did not form a tissue-specific clade, such as the liver. Thus, even on a global level, metastases growing in different tissues present a diversity of different metastatic ECM niches.

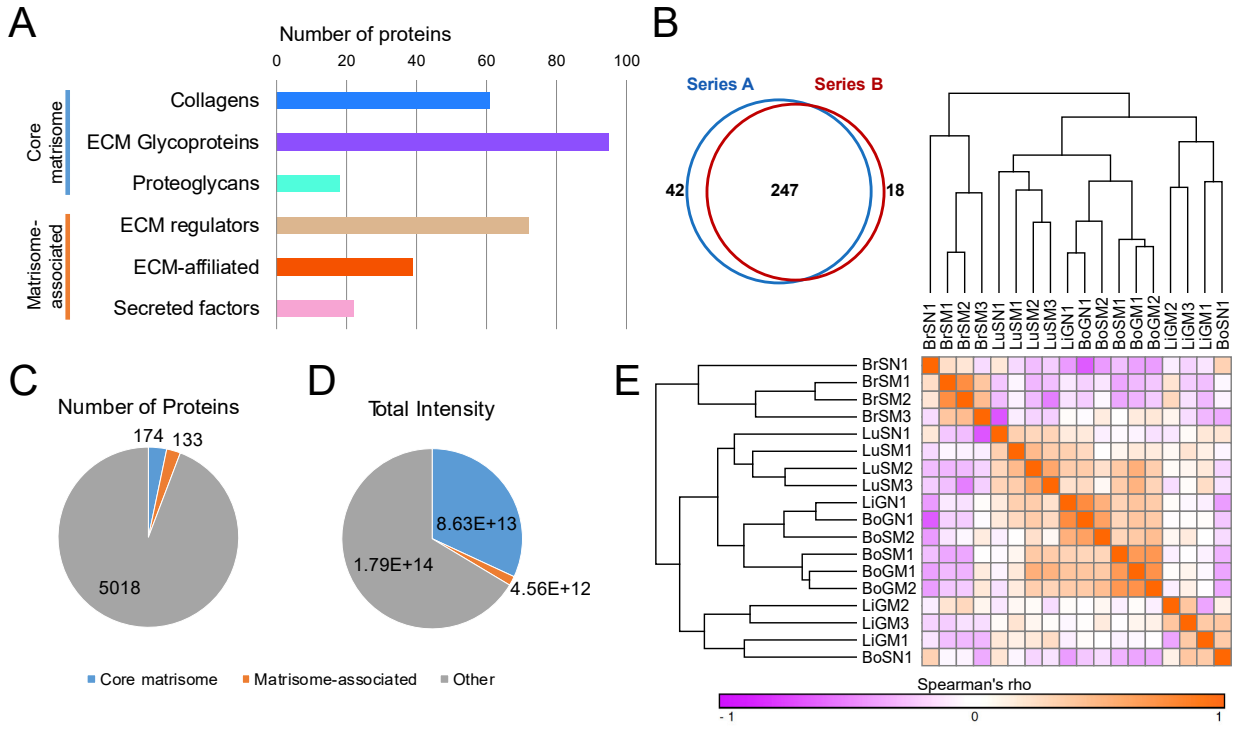

Figure 2. Overview of quantitative mass spectrometry data.
(A) Numbers of proteins quantified among all samples belonging to each matrisome category. (B) Numbers of proteins quantified in each 10-plex TMT series. (C) Numbers of matrisome and non-matrisome proteins quantified among all samples. (D) Total intensity of matrisome and non-matrisome proteins quantified among all samples. (E) Spearman's rank correlation coefficient (rho) matrix of samples, calculated using all proteins quantified.

Tumor and stromal cells produce different components of the metastatic niche

The use of a xenograft model system, in which human tumor cells grow embedded in mouse stromal tissue, allows us to distinguish whether a given protein came from the tumor or stroma based on peptide sequence differences between human and mouse versions of the same protein (Naba et al., 2012). This distinction is particularly useful in the context of metastatic niches across multiple tissues, where tumor cells are growing in notably dissimilar stromal environments. The vast bulk of the matrisome protein content of metastases was produced by the stroma (Fig. 3A). Moreover, the tumor and stroma made remarkably different types of matrisome proteins, with the tumor largely producing matrisome-associated proteins (Fig. 3B) and the stroma mostly creating core matrisome proteins (Fig. 3C).

The tumor and stromal production of matrisome proteins can be further broken down by examining whether a given protein was made only by the tumor cells, only by the stromal cells, or by both the tumor and stromal compartments (Fig. 3D). The largest component of the proteins being made exclusively by the tumor cells was secreted factors, followed by ECM regulators (Fig. 3E), suggesting that tumor cells take the lead in modulating the matrix in the tumor microenvironment. Indeed, a closer look at the 42 quantified human proteins that were produced only by the tumor cells reveals a mix of mostly matrisome-associated proteins, notably several members of the S100 family, LOX family, and serine protease inhibitor SERPINB1 (Fig. 3I). Meanwhile, the uniquely stroma-derived proteins consist largely of ECM glycoproteins (Fig. 3F), and both the tumor and stroma are responsible for producing collagens (Fig. 3G), which are mostly fibrillar (Fig. 3H). The tumor and stroma clearly take distinct roles in creating the matrix of the metastatic tumor microenvironment.

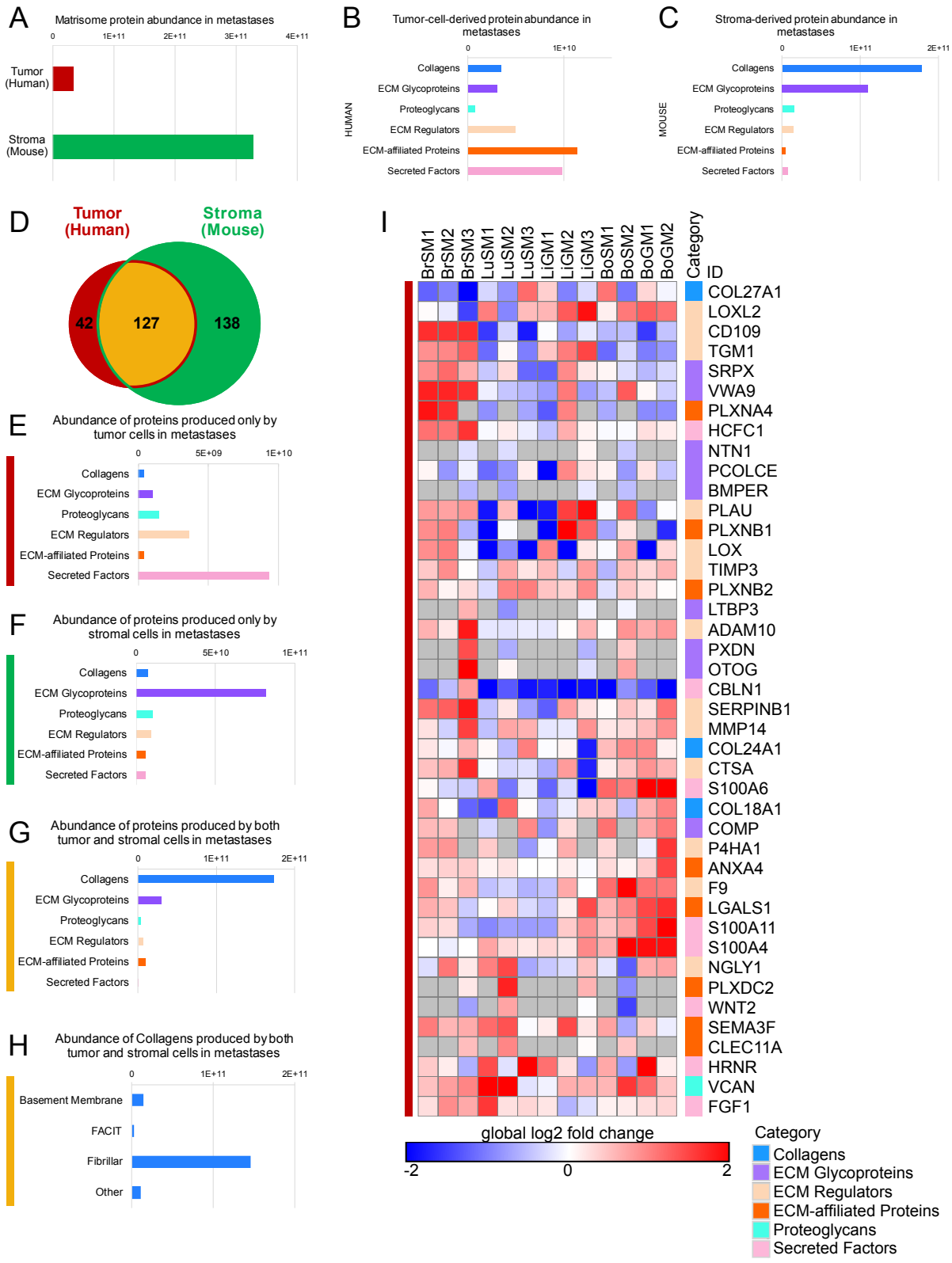
A
Matrisome protein abundance in metastases
0
1E+11
2E+11
3E+11
4E+11
Tumor (Human)
Stroma (Mouse)
B
Tumor-cell-derived protein abundance in metastases
0
1E+10
HUMAN
Collagens
ECM Glycoproteins
Proteoglycans
ECM Regulators
ECM-affiliated Proteins
Secreted Factors
C
Stroma-derived protein abundance in metastases
0
1E+11
2E+11
MOUSE
Collagens
ECM Glycoproteins
Proteoglycans
ECM Regulators
ECM-affiliated Proteins
Secreted Factors
D
Tumor (Human)
Stroma (Mouse)
42
127
138
E
Abundance of proteins produced only by tumor cells in metastases
0
5E+09
1E+10
Collagens
ECM Glycoproteins
Proteoglycans
ECM Regulators
ECM-affiliated Proteins
Secreted Factors
F
Abundance of proteins produced only by stromal cells in metastases
0
5E+10
1E+11
Collagens
ECM Glycoproteins
Proteoglycans
ECM Regulators
ECM-affiliated Proteins
Secreted Factors
G
Abundance of proteins produced by both tumor and stromal cells in metastases
0
1E+11
2E+11
Collagens
ECM Glycoproteins
Proteoglycans
ECM Regulators
ECM-affiliated Proteins
Secreted Factors
H
Abundance of Collagens produced by both tumor and stromal cells in metastases
0
1E+11
2E+11
Basement Membrane
FACIT
Fibrillar
Other
I
BrSM1
BrSM2
BrSM3
LuSM1
LuSM2
LuSM3
LiGM1
LiGM2
LiGM3
BoSM1
BoSM2
BoGM1
BoGM2
Category
ID
COL27A1
LOXL2
CD109
TGM1
SRPX
VWA9
PLXNA4
HCFC1
NTN1
PCOLCE
BMPER
PLAU
PLXNB1
LOX
TIMP3
PLXNB2
LTBP3
ADAM10
PXDN
OTOG
CBLN1
SERPINB1
MMP14
COL24A1
CTSA
S100A6
COL18A1
COMP
P4HA1
ANXA4
F9
LGALS1
S100A11
S100A4
NGLY1
PLXDC2
WNT2
SEMA3F
CLEC11A
HRNR
VCAN
FGF1
global log2 fold change
-2
0
2
Category
Collagens
ECM Glycoproteins
ECM Regulators
ECM-affiliated Proteins
Proteoglycans
Secreted Factors

Figure 3. Tumor-cell- and stroma-derived production of matrisome proteins.
All proteins shown in this figure refer to TMT Series B unless otherwise noted, as Series B contains only metastatic samples (see Supplementary Table S1). (A) Total intensity of tumor-cell-derived (human) and stroma-derived (mouse) matrisome proteins quantified. (B-C) Total intensity of (human) tumor-cell-derived (B) and (mouse) stroma-derived (C) matrisome proteins in metastases, broken down by matrisome category. (D) Number of proteins quantified in metastases that were produced only by tumor cells (human, red, left), only by stromal cells (mouse, green, right) or by both cell compartments (center, yellow). (E-G) Total intensity of matrisome proteins produced by the indicated cells in metastases, broken down by matrisome category. (E) Produced only by tumor cells (F) Produced only by stromal cells (G) Produced by both tumor and stromal cells. (H) Total intensity of collagen types produced by both tumor and stromal cells in metastases: basement membrane, fibril-associated collagens with interrupted triple helices (FACIT), and other. (I) Heatmap of global log2 fold change values for the 42 proteins quantified that were produced only by tumor cells, including both TMT Series A and B. Gray boxes indicate proteins not detected in a given sample.

The tumor and stroma create distinct metastatic niches in each tissue

In addition to broad differences in the types of matrix proteins made by the tumor and stroma, quantitative mass spectrometry also allows the identification of particular proteins that characterize the metastatic niche of each tissue. We performed a marker selection analysis, comparing the metastatic samples from each particular tissue to all other metastatic samples, looking for proteins that are significantly elevated only in that tissue (see Methods and Ref. (Myers et al., 2019)). These comparisons did not simply identify the most elevated proteins in each tissue, but rather the proteins most significantly elevated in one tissue relative to all others. Separate analyses were conducted for tumor-cell-derived (human) and stroma-derived (mouse) proteins. Beginning with tumor-cell-derived proteins (Fig. 4A), the brain had a particularly large set of characteristic proteins of a variety of matrisome categories, including several that were produced only by the tumor: CD109, SERPINB1, HCFC1 and Cerebellin-1 (CBLN1) (Fig. 3F). The lung metastases were characterized by several basement membrane proteins, including collagen COL4A4 and Laminin-121 (α1β2γ1, formerly known as Laminin-3). The liver was not particularly set apart by its tumor-cell-derived protein production, aside from COL6A5, but the

bone marrow metastatic niche had significantly increased levels of both S100A6 and S100A11, both of which were produced only by the tumor cells (Fig. 3F). We also compared the total set of metastatic samples to all normal tissues to identify proteins that were broadly over-represented in metastases of MDA-MB-231 cells to all tissues (Fig. 4B). The most broadly abundant protein overall was S100A4. Also notable were a couple of Annexin family members (ANXA1 and ANXA2), the proteoglycan Perlecan (HSPG2, found both in basement membranes and in other matrices), and the protease Cathepsin D (CTSD). MDA-MB-231 tumor cells thus have both a common set of matrisome proteins they secrete in different tissue environments, as well as unique adaptations to each site, both in terms of specific proteins and types of proteins.

Figure 4. Tumor-cell-derived proteins specifically elevated at metastatic sites.
(A) Marker selection of tumor-cell-derived proteins among different metastatic sites (see Methods). Shown are all proteins significantly elevated in each particular metastatic tissue (identified on the left) relative to all other metastatic tissues. (B) Marker selection of tumor-cell-derived proteins significantly elevated across all metastatic samples relative to all normal samples. All proteins shown in both heatmaps are significantly elevated in metastases of the indicated tissue compared to all other metastases (signal to noise ratio, $P < 0.05$ and FDR < 0.1).

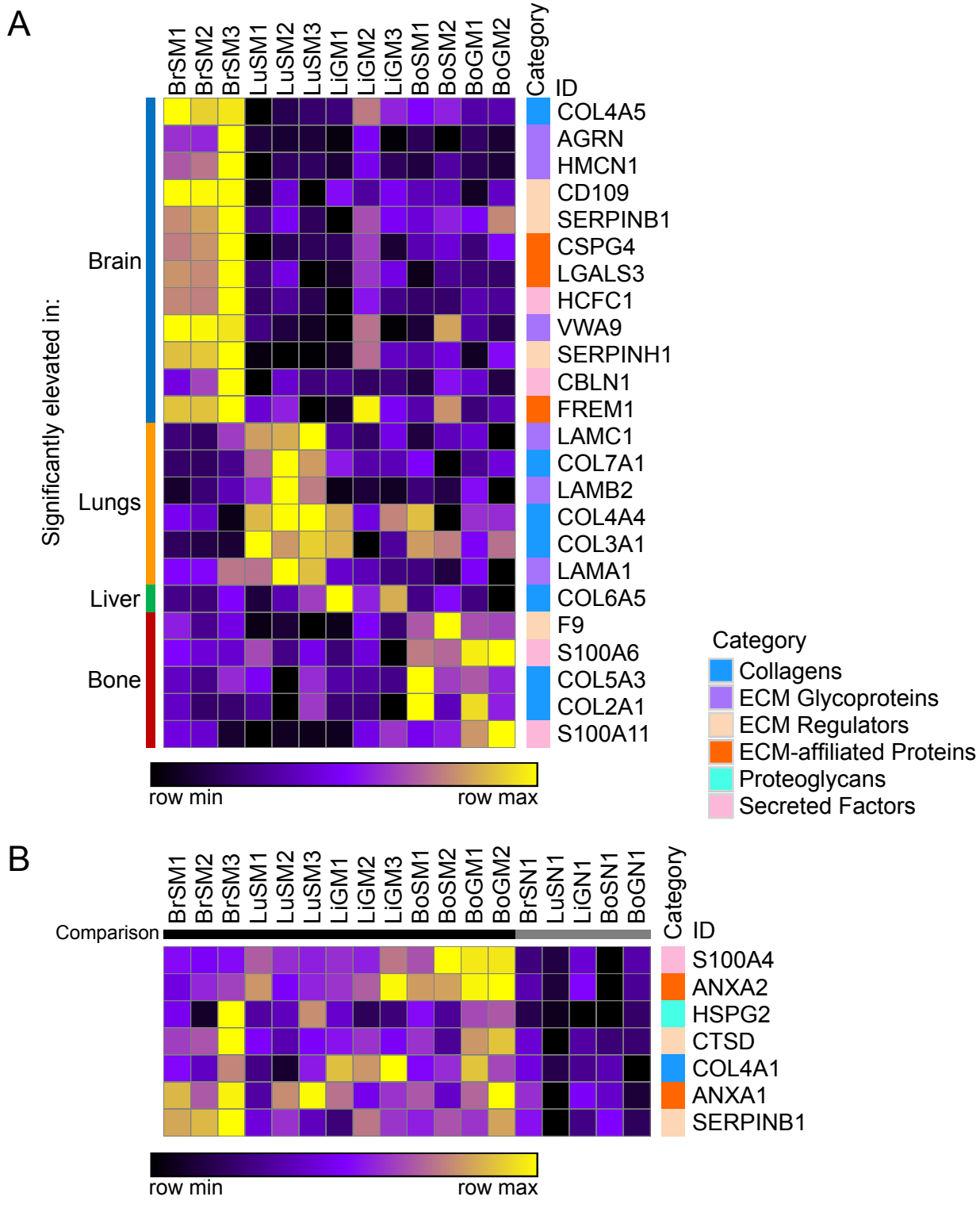
A
BrSM1
BrSM2
BrSM3
LuSM1
LuSM2
LuSM3
LiGM1
LiGM2
LiGM3
BoSM1
BoSM2
BoGM1
BoGM2
Category
ID
COL4A5
AGRN
HMCN1
CD109
SERPINB1
CSPG4
LGALS3
HCFC1
VWA9
SERPINH1
CBLN1
FREM1
LAMC1
COL7A1
LAMB2
COL4A4
COL3A1
LAMA1
COL6A5
F9
S100A6
COL5A3
COL2A1
S100A11
Significantly elevated in:
Brain
Lungs
Liver
Bone
row min
row max
Category
Collagens
ECM Glycoproteins
ECM Regulators
ECM-affiliated Proteins
Proteoglycans
Secreted Factors
B
BrSM1
BrSM2
BrSM3
LuSM1
LuSM2
LuSM3
LiGM1
LiGM2
LiGM3
BoSM1
BoSM2
BoGM1
BoGM2
BrSN1
LuSN1
LiGN1
BoSN1
BoGN1
Category
ID
Comparison
S100A4
ANXA2
HSPG2
CTSD
COL4A1
ANXA1
SERPINB1
row min
row max

A parallel marker selection analysis uncovered stroma-derived proteins particular to each metastatic niche (Fig. 5A). The brain, once again, displayed a wide variety of niche proteins, many of which are known to be expressed specifically in the brain, such as the secreted neuronal glycoprotein Lgi1 and its receptor Adam22 (Fukata et al., 2006), as well as Brevican (Bcan). The lung stroma, much like the tumor-cell-derived lung matrix, was distinguished by a great many basement membrane proteins, including six different Laminin chains and five type IV Collagens, though it also contained lung-specific proteins like pulmonary surfactant-associated protein A1 (Sftpa1). The liver stroma contained the known metastasis promoters Tenascin-C and Fibronectin, as well as a number of proteins typically associated with the coagulation response (Fibrinogens, Thrombin and Von Willebrand factor). Additionally, the bone niche had significantly elevated levels of Thrombospondin-1, yet another S100 protein (S100a13), the protease Cathespin-G (Ctsg), and the protease inhibitors Cystatin C and Stefin-2 (Cst3 and Stfa2). Given that these stromal proteins were simply the most specifically abundant in each metastatic tissue, a number of them may simply represent variation among normal tissue ECM. Accordingly, a similar marker selection can be performed by subtracting the normal abundance of each protein from the value in each metastatic sample (Supplementary Fig. S3). This method identified fewer stromal proteins significantly elevated in each tissue, but many of the top proteins found by each analysis were similar. Finally, we performed a marker selection for stroma-derived proteins broadly elevated in normal tissue compared to metastases (Fig. 5B), which could, in principle, represent potential suppressors of metastasis. Indeed, among this list was Tubulointerstitial nephritis antigen-like 1 (Tinagl1), which was recently shown to inhibit the progression and metastasis of TNBC (Shen et al., 2019). Metastatic niches demonstrate an

enormous amount of diversity from tissue to tissue in their matrisome composition, both in tumor and stromal production.

Figure 5. Stroma-derived proteins specifically elevated and lowered in metastases.
(A) Marker selection of stroma-derived proteins among different metastatic sites (see Methods). Shown are all proteins significantly elevated in each particular metastatic tissue (identified on the left) relative to all other metastatic tissues. (B) Marker selection of stroma-derived proteins significantly decreased across all metastatic samples relative to all normal samples. All proteins shown in both heatmaps are significantly elevated in metastases of the indicated tissue compared to all other metastases (signal to noise ratio, $P < 0.05$ and FDR < 0.1).

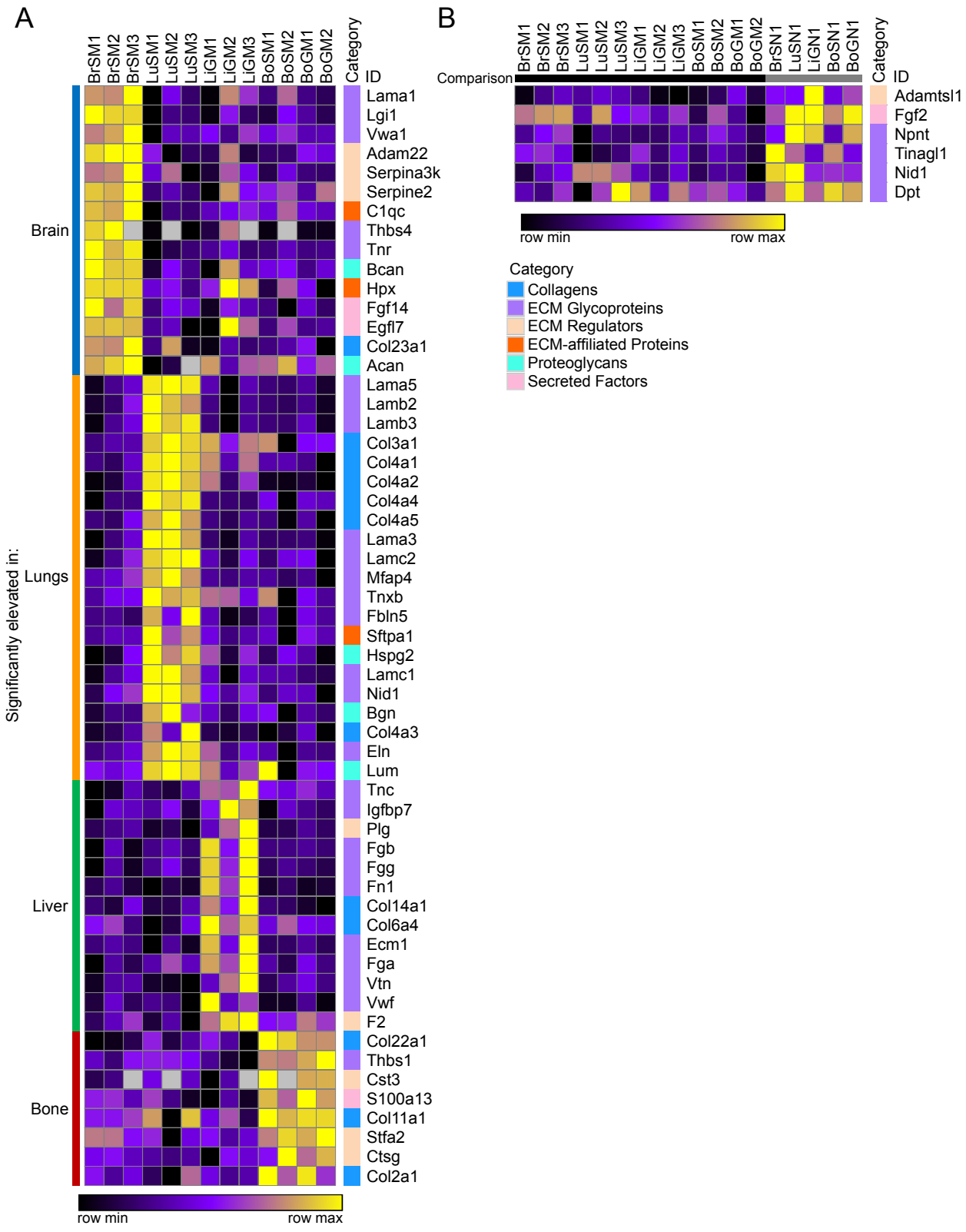
A
BrSM1
BrSM2
BrSM3
LuSM1
LuSM2
LuSM3
LiGM1
LiGM2
LiGM3
BoSM1
BoSM2
BoGM1
BoGM2
Category
ID
Lama1
Lgi1
Vwa1
Adam22
Serpina3k
Serpine2
C1qc
Thbs4
Tnr
Bcan
Hpx
Fgf14
Egfl7
Col23a1
Acan
Lama5
Lamb2
Lamb3
Col3a1
Col4a1
Col4a2
Col4a4
Col4a5
Lama3
Lamc2
Mfap4
Tnxb
Fbln5
Sftpa1
Hspg2
Lamc1
Nid1
Bgn
Col4a3
Eln
Lum
Tnc
Igfbp7
Plg
Fgb
Fgg
Fn1
Col14a1
Col6a4
Ecm1
Fga
Vtn
Vwf
F2
Col22a1
Thbs1
Cst3
S100a13
Col11a1
Stfa2
Ctsg
Col2a1
Significantly elevated in:
Brain
Lungs
Liver
Bone
row min
row max
B
Comparison
BrSM1
BrSM2
BrSM3
LuSM1
LuSM2
LuSM3
LiGM1
LiGM2
LiGM3
BoSM1
BoSM2
BoGM1
BoGM2
BrSN1
LuSN1
LiGN1
BoSN1
BoGN1
Category
ID
Adamtsl1
Fgf2
Npnt
Tinagl1
Nid1
Dpt
row min
row max
Category
Collagens
ECM Glycoproteins
ECM Regulators
ECM-affiliated Proteins
Proteoglycans
Secreted Factors

SERPINB1 knockdown demonstrates tissue-specific dependency

Given the proteins identified above that are characteristic of various metastatic niches, we finally tested whether any could be deterministic of metastatic tropism. That is, could knocking down a protein produced only by brain metastases specifically inhibit metastasis to the brain? This is most readily achieved for tumor-cell-derived proteins. We focused on the brain due to its relative abundance of unique markers and the less well studied nature of the brain niche itself. SERPINB1 is elevated in both brain and lung metastases compared to normal tissue, though its overall level is highest in the brain (Fig. 6A). We knocked down SERPINB1 expression in MDA-MB-231 cells using CRISPRi (Fig. 6B) and introduced those cells into circulation in NOD-SCID mice via intracardiac injection. SERPINB1 knockdown significantly reduced brain metastasis by more than two-fold, slightly (but not significantly) reduced lung metastasis, and did not change the average amount of bone metastasis (Fig. 6C, D). These *in vivo* results are consistent with the observed protein levels in different metastatic tissues from our mass spectrometric analysis. We tested knockdown of a number of additional brain metastasis and overall metastasis markers, but, while a few showed some effect on metastatic tropism, none was statistically significant given the sample sizes studied (Supplementary Fig. S4). This may imply that these matrisome proteins are insufficiently consequential to tropism on their own, while altering several of them simultaneously might have a greater effect. Regardless, our results demonstrate that our data on metastatic niches can be used to find matrisome proteins with tissue-specific effects on metastasis.

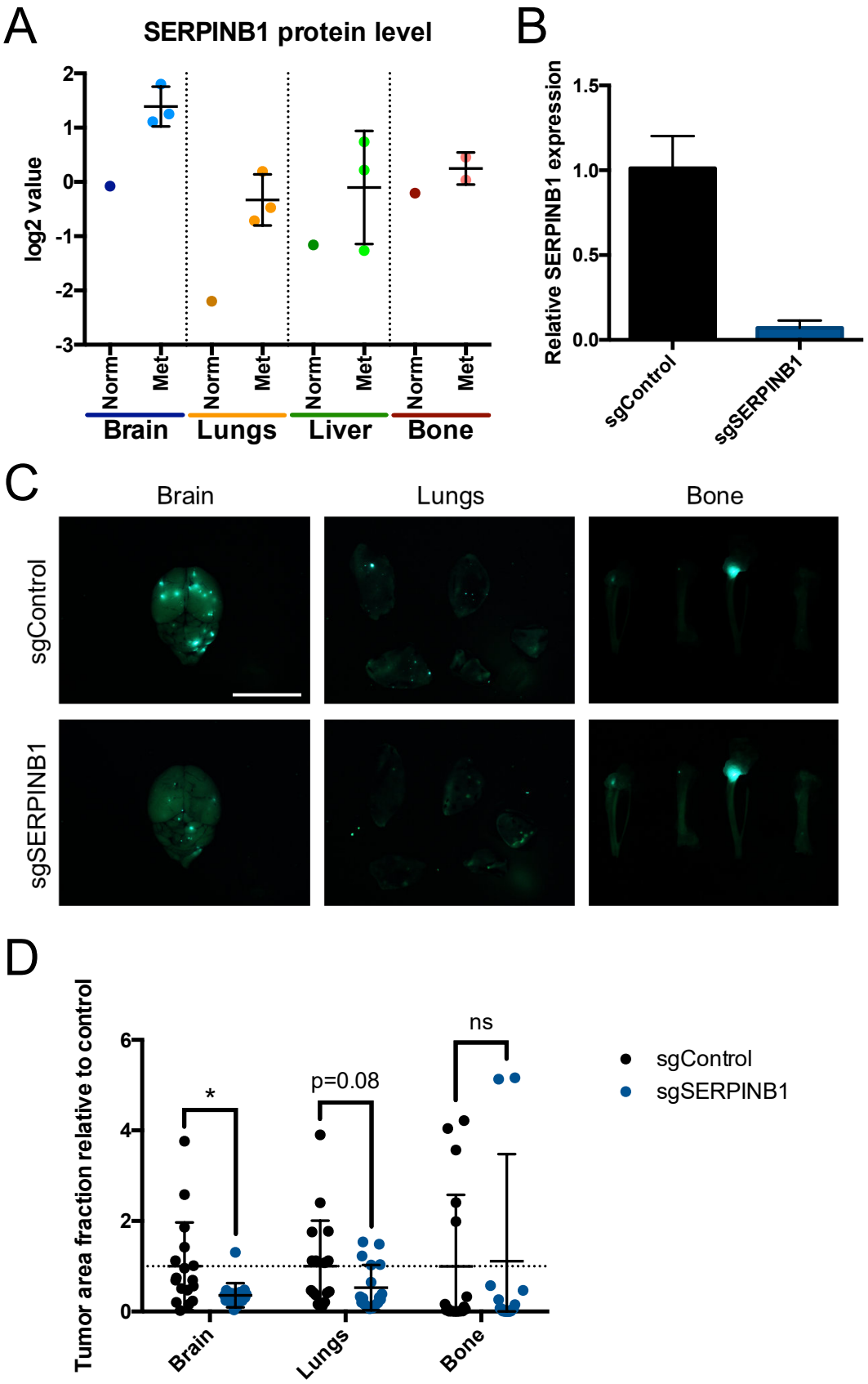
A
SERPINB1 protein level
log2 value
2
1
0
-1
-2
-3
Norm
Met
Brain
Lungs
Liver
Bone
B
Relative SERPINB1 expression
1.5
1.0
0.5
0.0
sgControl
sgSERPINB1
C
Brain
Lungs
Bone
sgControl
sgSERPINB1
D
Tumor area fraction relative to control
6
4
2
0
*
p=0.08
ns
Brain
Lungs
Bone
sgControl
sgSERPINB1

Figure 6. Effects of SERPINB1 knockdown on metastatic tropism and growth.
(A) Quantitative mass spectrometry of SERPINB1 protein levels (log2 fold change values relative to pooled control sample) in each normal (Norm) and metastatic (Met) tissue. All bone samples shown are from NOD-SCID mice. (B) qPCR of SERPINB1 expression in MDA-MB-231 cells expressing sgRNA against mouse Timp1 (sgControl) or SERPINB1. (C) Representative images of brains, lungs, and bones 3 weeks after intracardiac injection of sgControl or sgSERPINB1 cells. Scale bar, 10 mm. (D) Fraction of tissue surface area occupied by tumors. n=18 mice per group. ns, not significant; *, $P \leq 0.05$; two-tailed Student's t-test.

Discussion

In this study, we performed an unbiased, quantitative mass spectrometric survey of ECM proteins present in MDA-MB-231 xenograft metastases to the brain, lungs, liver and bone marrow. This analysis quantified 307 total matrisome proteins produced by either or both the human tumor cells and mouse stromal cells, and it identified both tumor- and stroma-derived proteins characteristic of particular metastatic niches and overall metastasis. Finally, as one example of an ECM protein affecting metastatic tropism, we showed that knockdown of SERPINB1 in tumor cells significantly reduced their metastasis to the brain.

We used MDA-MB-231 cells as the model for this study because of their broad metastatic capability, wide experimental use, and extensive prior research into their tropism (Bos et al., 2009; Minn et al., 2005; Naba et al., 2014a; Sevenich et al., 2014). However, prior studies have largely relied on several rounds of *in vivo* selection of these cells to enhance their metastatic tropism to particular organs, followed by microarray analysis to compare gene expression differences among the different *in vivo*-selected variants. Our work, in contrast, uses the more heterogeneous parental cell line, which permits a wider variety of responses to the challenge of growing in different tissues, as well as allowing a more direct comparison among the various metastases, since they were all grown from the exact same cell line. Furthermore, in addition to focusing on the matrisome, itself an understudied part of the tumor microenvironment, our

analysis made use of quantitative proteomics to provide a more accurate picture of the actual protein composition of these metastases relative to RNA-based methods, given the known differences between mRNA and protein levels (Edfors et al., 2016; Mertins et al., 2016; Payne, 2015; Vogel and Marcotte, 2012). We present this study as a useful experimental model to explore how one particular cancer can metastasize to multiple tissues, rather than a complete representation of the wide spectrum of breast cancers and their behavior in humans. Indeed, MDA-MB-231 cells are unusual among triple negative cell lines in that they have mutated KRAS (Chavez et al., 2010; Lehmann et al., 2011), so the proteins identified in this study may be context-dependent.

The use of a xenograft system with human tumor cells and mouse stromal cells allowed us to distinguish whether a protein was produced by the tumor or stromal cells due to amino acid differences in the peptides observed through mass spectrometry. This ability to discern the origin of each protein provided valuable insight into how both cell types contribute to the construction of each metastatic niche. For instance, the vast bulk of the ECM in metastases was produced by the stroma (Fig. 3A). This might indicate that the tumor cells primarily co-opt and direct the more specialized ECM-producing stromal cells (such as fibroblasts) in the construction of the ECM niche, which also correlates with the observation that tumor cells primarily produced matrisome-associated proteins (Fig. 3B), especially secreted factors (Fig. 3E). It may also be affected by the relatively small size (1-4 mm) and young age (4-12 weeks) of these metastases. Indeed, if even younger metastases could be analyzed, they might have relatively different ECM production from the tumor and stromal cells. Tenascin C, for example, has been shown to be produced by tumor cells in early metastases, while production is shifted to the stroma as those

metastases grow in size (Insua-Rodríguez and Oskarsson). It would be interesting to compare the overall ECM composition of metastases over time to study such changes.

In order to identify ECM proteins characteristic of each metastatic niche, we used a marker selection process, whereby we compared metastases from one tissue at a time to all other metastases. As there would be no human proteins present in these mouse tissues without the introduction of the human MDA-MB-231 cells, all of the tumor-cell-derived proteins characteristic of each metastatic niche (Fig. 4A) represent particular adaptations of the tumor cells to each tissue. Some of these tumor-cell-derived proteins were also produced by the stroma, but it is meaningful that the tumor cells would secrete this ECM in addition to any stromal protein content. These analyses identified a large number of tumor-cell-derived proteins in the brain, which may reflect a comparably great difference between the ECM of the brain relative to the other tissues, as well as a much lower background of normal ECM relative to other tissues (Fig. 1C). We found a much greater set of stroma-derived ECM proteins characteristic of each niche (Fig. 5A). Some of these stroma-derived proteins could represent normal tissue-to-tissue variation: regardless of the presence of tumors, these tissues have varied ECM compositions even in a healthy context. However, many of these same site-specific stroma-derived proteins remained characteristically different even when we conducted the marker selection analysis by normalizing to normal tissue protein levels (Supplementary Fig. S4), indicating that such proteins are actually elevated in metastases in these tissues. Nevertheless, it remains possible that the stromal cells are responding to the presence of tumor cells by upregulating some of the normal ECM components, in which case the tumor cells may be adapting more to the ECM they encounter in each tissue, or non-specifically promoting ECM production, rather than radically altering the ECM. The production of so many ECM-affiliated proteins and secreted factors by

the tumor cells (Fig. 3B) certainly suggests that the tumor cells are, at least, modifying the ECM environment in metastatic tissues, even if they aren't reshaping its entire content. We have not yet tested the importance of the site-specific stroma-derived proteins, as they are considerably more difficult to perturb compared to tumor-cell-derived proteins. Nevertheless, these stroma-derived proteins are equally interesting potential targets, and the continued development of CRISPR-Cas9-based methods of genome modification may make the creation of such mouse models more practical in the near future.

Finally, we wanted to know if it were possible to alter the metastatic tropism of the parental MDA-MB-231 cells by inhibiting their ability to produce an ECM protein that was characteristic of a certain niche. We found that knockdown of SERPINB1, a protein made only by the tumor cells (Fig. 3I) and elevated in brain metastases compared to other tissues (Fig. 4A), significantly reduced brain metastasis and somewhat reduced lung metastasis (Fig. 6D), consistent with a similar but lesser protein elevation in lung metastases (Fig. 6A). As its name implies, SERPINB1 is a serine protease suicide inhibitor, which has been known mostly to protect neutrophils from their own proteases, as SERPINB1 inhibits neutrophil elastase, cathepsin G, proteinase 3, chymotrypsin, and granzyme H. The few studies of its functions in cancer have mainly shown that its overexpression suppresses migration and invasion of tumor cells, contrary to the more traditional role of metastasis promoters in supporting those processes (Chou et al., 2012; Huasong et al., 2015). Given its elevated presence in the extracellular space of more established metastases, it may instead have a role in promoting the survival and growth of tumor cells after they have extravasated. Further study into SERPINB1 specifically will be needed to elucidate its precise role in promoting brain metastasis.

This study makes use of the MDA-MB-231 TNBC cell line as a model to conduct a controlled comparison among metastatic niches formed by the same tumor cells when growing in different tissues. The data illustrate the different contributions of the tumor and stromal cells in establishing these niches, and identify ECM proteins that are characteristic of metastases in each tissue, as well as proteins produced by the tumor cells in all metastases. These proteins represent interesting opportunities for future study of the biology of metastasis formation, as well as potential prospects for imaging and targeting.

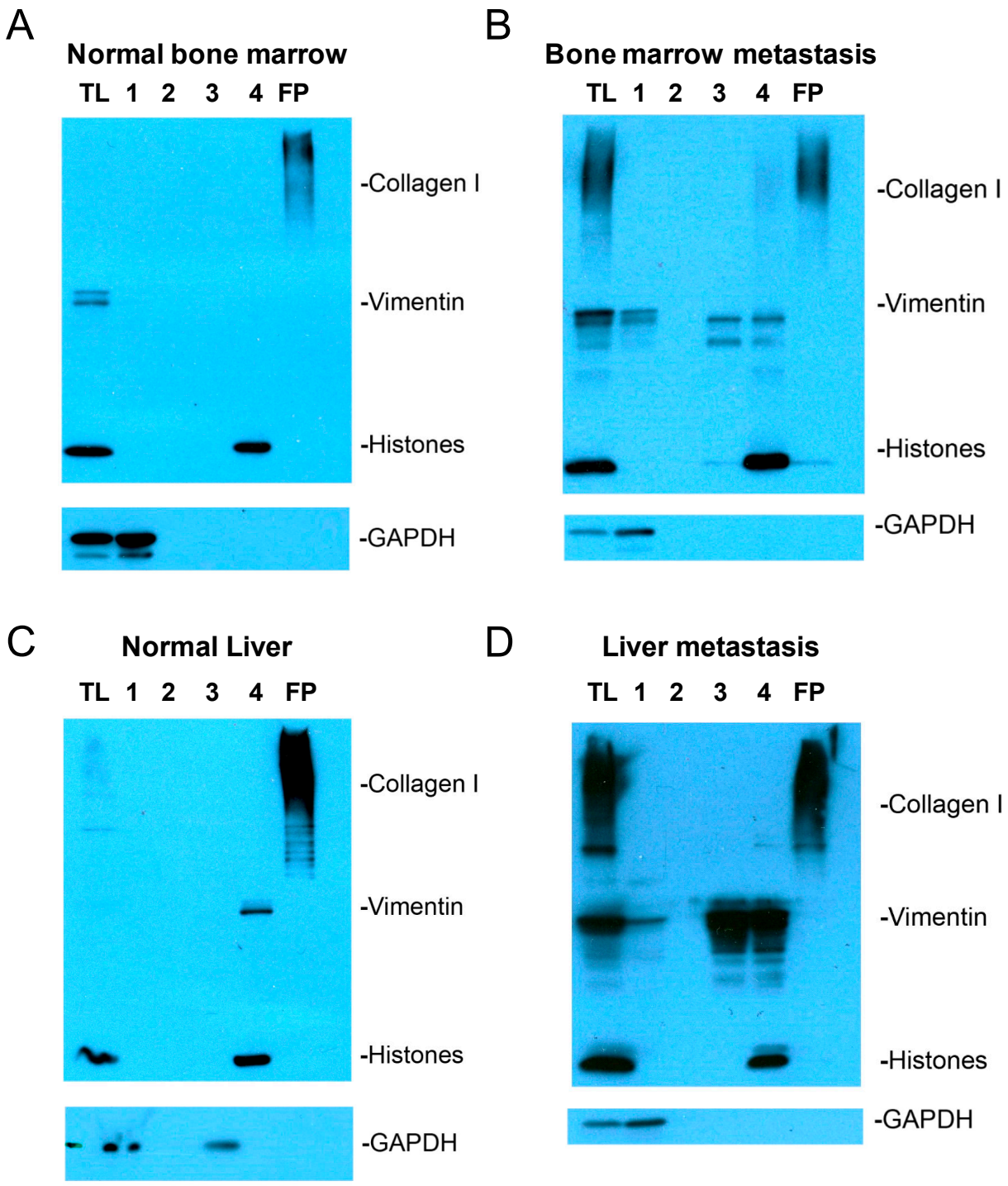

Supplementary Figure S1. Quality control western blots.
Example quality control western blots of sample fractions collected during ECM enrichment to monitor extraction of contaminant proteins, including total lysate (TL), intermediate fractions (1 to 4) and final pellet (FP). Shown are samples of normal mouse bone marrow (A), bone marrow metastasis (B), normal mouse liver (C) and liver metastasis (D).

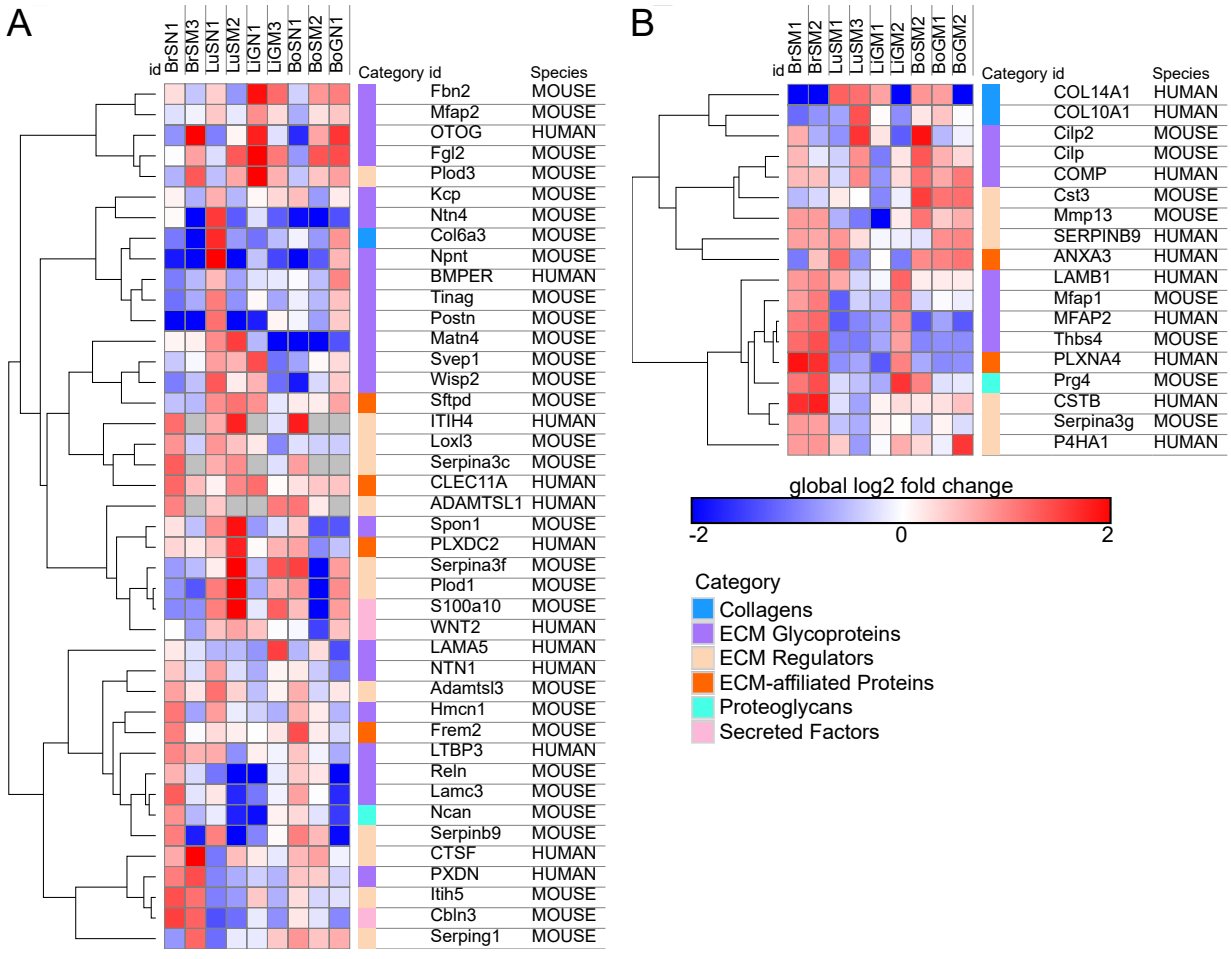

Supplementary Figure S2. Proteins identified in only one TMT series.
Heatmaps of global log2 fold change values for the 60 proteins quantified that were observed in only TMT Series A (A) or TMT Series B (B). Gray boxes indicate proteins not detected in a given sample.

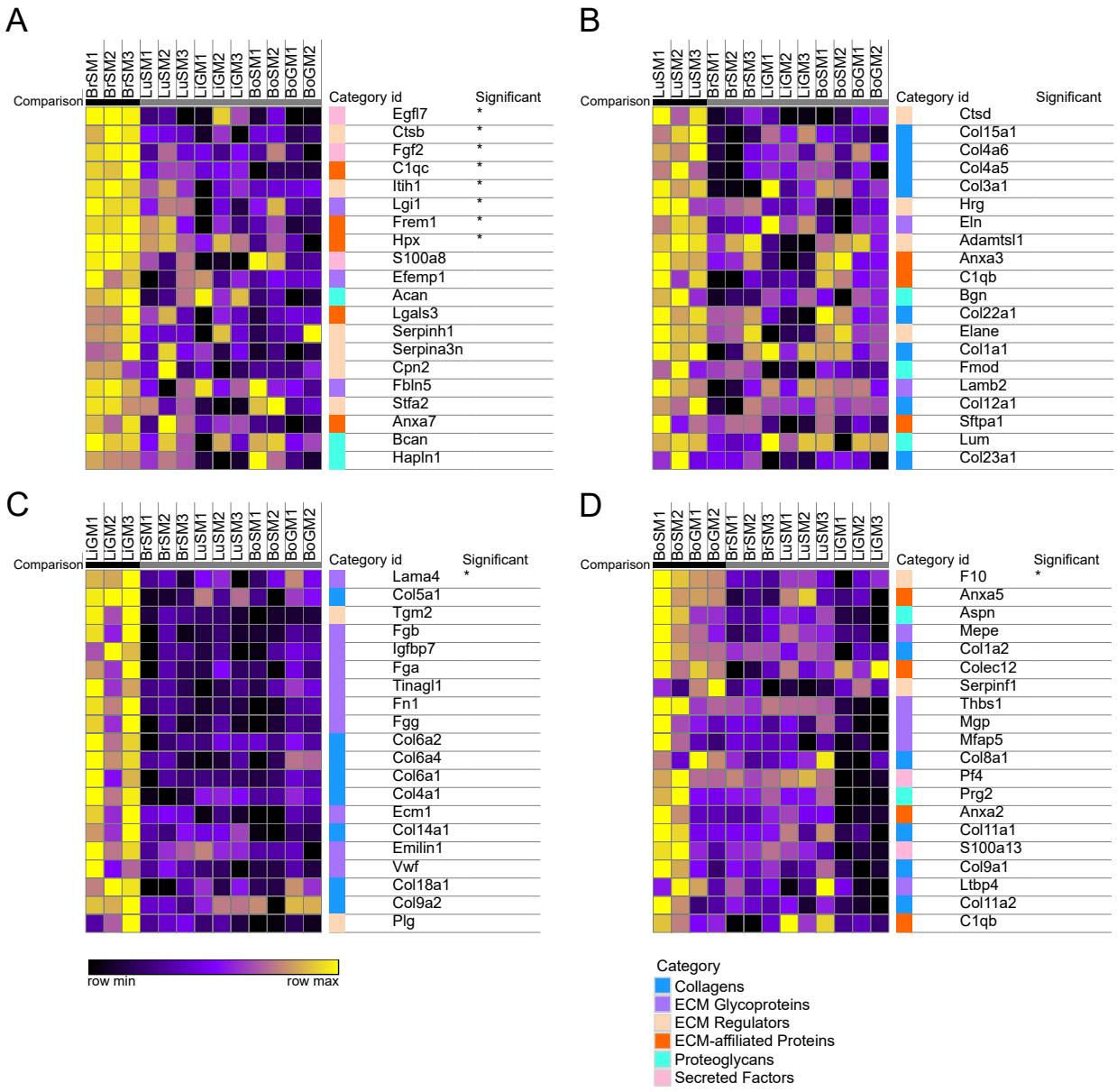

Supplementary Figure S3. Stromal proteins elevated in metastases relative to normal tissue.

Marker selection of stroma-derived proteins among different metastatic sites. The value shown for each protein has been normalized by subtracting the value of the same protein from the corresponding normal tissue. All values shown thus represent changes in protein abundance in a given metastatic sample compared to normal tissue. Marker selection has then been performed to distinguish stroma-derived proteins elevated in each particular metastatic tissue (comparisons identified above) relative to all other metastatic tissues, with the top 20 proteins shown for brain (A), lung (B), liver (C) and bone (D) metastases. Proteins significantly elevated the tissue of comparison are marked with a * (signal to noise ratio, $P < .05$ and $FDR < .1$).

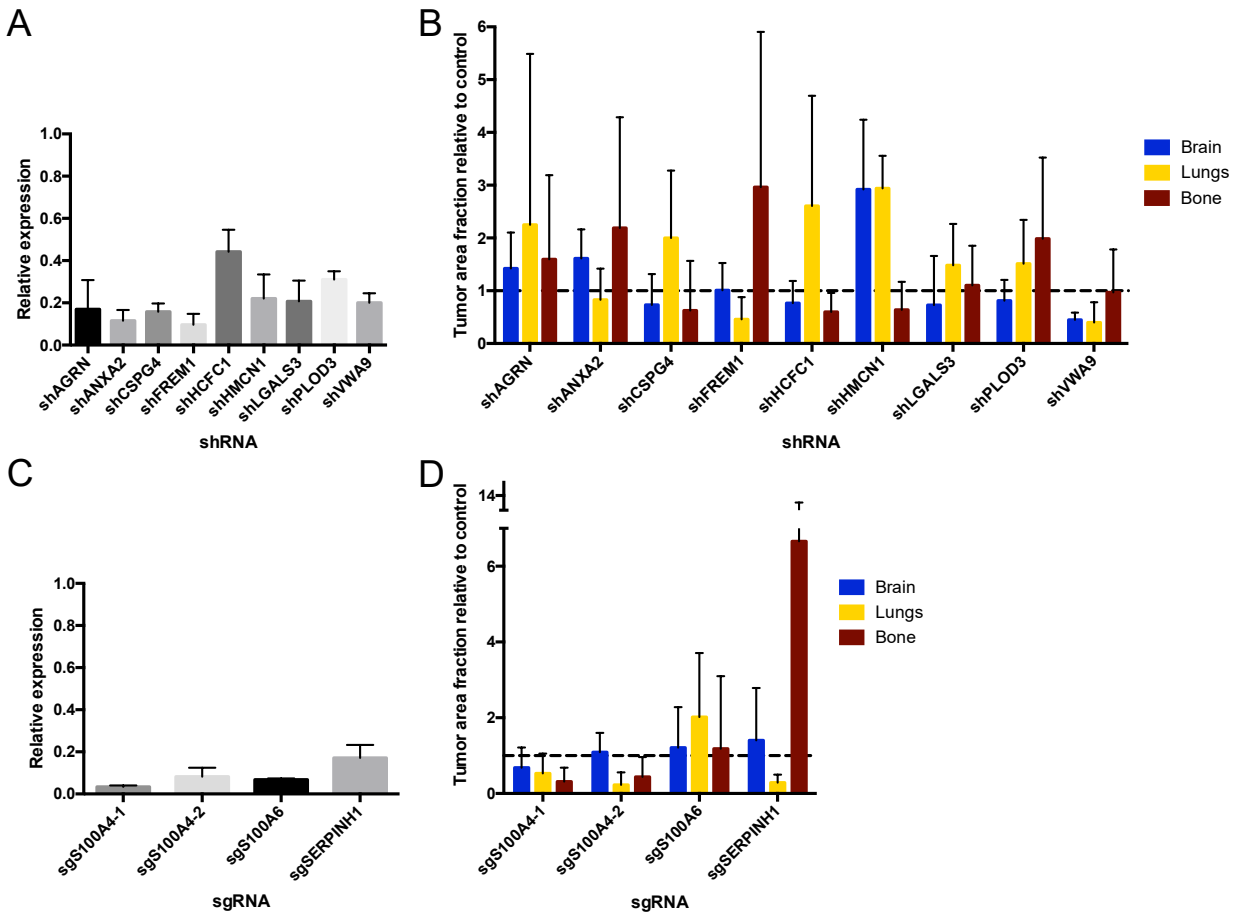

Supplementary Figure S4. Additional proteins evaluated for altered metastatic tropism. (A) qPCR of expression in MDA-MB-231 of proteins targeted for shRNA-mediated knockdown, relative to cells expressing a control shRNA (against Firefly luciferase). (B) Fraction of tissue surface area occupied by tumors in mice that received intracardiac injections of cells expressing the shRNAs shown. ANXA2 was identified as a broad marker of metastasis, while the rest were markers of brain metastasis (see Fig. 4A). All results are displayed compared to the average tumor burden in each tissue caused by cells expressing a control shRNA. n=3-7 mice per group. (C) qPCR of expression in MDA-MB-231 of proteins targeted for sgRNA-mediated knockdown, relative to cells expressing a control sgRNA (against mouse Timp1). (D) Fraction of tissue surface area occupied by tumors in mice that received intracardiac injections of cells expressing the sgRNAs shown. S100A4 was identified as marker of overall metastasis, S100A6 was identified as a marker of bone metastasis, and SERPINH1 was identified as a marker of brain metastasis (see Fig. 4A). All results are displayed compared to the average tumor burden in each tissue caused by cells expressing a control sgRNA. n=6-8 mice per group.

Methods

Cells and vectors

The human MDA-MB-231 mammary carcinoma cell line (Cailleau et al., 1978) expressing herpes simplex virus thymidine kinase 1, green fluorescent protein (GFP) and firefly luciferase (Minn et al., 2005) was a kind gift of Joan Massagué (Memorial Sloan Kettering Cancer Center, New York, NY). These cells were further retrovirally infected to express ZsGreen using MSCV-ZsGreen-2A-Puro (Lamar et al., 2012). Cells were cultured in HyClone high-glucose DMEM (ThermoFisher, San Jose, CA) supplemented with 2 mM glutamine and 10% fetal bovine serum (FBS, Invitrogen, Carlsbad, CA) in a 37°C incubator with 5% CO_2. Production of retrovirus and lentivirus, as well as transduction of cells, was performed as previously described (Stern et al., 2008).

Gene knockdown and quantitative PCR

miR30-based shRNAs (Supplementary Table S2) were designed using a tool developed by the laboratory of Michael Hemann (shrna.mit.edu) and cloned into MSCV-Blast-miR30, as previously described (Stern et al., 2008). An shRNA against Firefly luciferase (shFF) was used as a control. sgRNAs for CRISPRi (Supplementary Table S3) were designed using a tool developed by the lab of Feng Zhang (crispr.mit.edu) and cloned into U6-sgRNA-CMV-tdTomato, a kind gift of Michael Hemann (Braun et al., 2016). This vector was used in tandem with Lenti-dCas9-KRAB-Blast, a gift from Gary Hon (Addgene plasmid # 89567 ; http://n2t.net/addgene:89567 ; RRID:Addgene_89567) (Xie et al., 2017). Retroviral and

lentiviral production and transduction of cells were performed as previously described (Stern et al., 2008).

For quantitative PCR (qPCR), cells were lysed in TRIzol (Invitrogen, Carlsbad, CA), RNA was isolated according to the manufacturer's instructions, and cDNA was synthesized by reverse transcription using the First-Strand cDNA Synthesis Kit (Promega, Madison, WI). qPCR reactions were performed using SYBR Green Supermix (Bio-Rad, Hercules, CA) according to the manufacturer's instructions, and data analysis was performed using Bio-Rad CFX Manager Software. PCR conditions were 95°C for 10 min, followed by 40 cycles of 95°C for 20 s, 60°C for 30 s, and 72°C for 30 s. Primers used are listed in Supplementary Table S4.

Experimental metastasis assays

Metastatic tumor samples for this study were generated by injecting female NOD-SCID or NOD/SCID/IL2Rγ-null mice (Jackson Laboratory, Bar Harbor, ME) with 250,000 or 50,000 MDA-MB-231 cells in 100 μL of Hanks' Balanced Salt Solution (HBSS, Thermo Fisher Scientific, San Jose, CA) for 4-12 weeks, via injection into the lateral tail vein (for lung tumors) or intracardiac injection into the left ventricle (for brain, liver and bone tumors). Intracardiac injections were guided using a Vevo 770 ultrasound imaging system (VisualSonics, Toronto, Canada). Metastases were isolated through their ZsGreen fluorescence, and bone-tumor samples were collected by flushing the bone marrow from femurs and tibias with phosphate-buffered saline (PBS) after confirming the presence of ZsGreen-positive tumors. At least 25 mg of tumor tissue were used for each sample for analysis, which required pooling several tumors for each sample, except for brain tumors, which were sizeable enough (30-50 mg) to be used singly.

For assays of metastatic tropism, 500,000 or 250,000 MDA-MB-231 cells were injected intracardiac into NOD-SCID mice (as above). 3 or 4 weeks after injection, brains, lungs and bones (femurs and tibias) were dissected and imaged with a Leica M165 FC dissecting microscope (Leica, Wetzlar, Germany). Tumor burden was quantified by dividing ZsGreen-positive tumor area by total tissue area using ImageJ. Data for metastasis assays were expressed as mean ± standard deviation. Statistical analysis was conducted with GraphPad Prism 6 (GraphPad Software). All comparisons were made using two-tailed Student's t-tests, controlled for a false discovery rate (FDR) below 0.1 (according to the Benjamini-Hochberg procedure), with $P \leq 0.05$ considered significant (*). All procedures were performed according to an animal protocol approved by MIT's Committee on Animal Care.

ECM protein enrichment, immunoblotting and in-solution digestion

Tissue samples were homogenized with a Bullet Blender (Next Advance, Averill Park, NY) according to the manufacturer's instructions. Enrichment of tissue samples for their ECM protein content was performed using the CNMCS compartmental extraction kit (Millipore, Billerica, MA) as previously described (Naba et al., 2015), except that brain samples were incubated a second time in the CS buffer to remove additional non-ECM proteins. Quality control of the enrichment process was monitored by immunoblotting as previously described (Naba et al., 2012) with the following antibodies: rabbit anti-Collagen I (Millipore, Billerica, MA), rabbit anti-Vimentin produced in our laboratory (Hynes and Destree, 1978), rabbit anti-pan-histone (Millipore) and mouse anti-GAPDH (Millipore). ECM protein resuspension, alkylation, deglycosylation and digestion were performed as previously described (Naba et al., 2015).

Sample preparation

Digests were desalted using C18 (Empore, 3M, St. Paul, MN) Stage tips (Rappsilber et al., 2007), and 5% was used for label-free analysis. After vacuum centrifugation and resuspension in 0.1% formic acid, half of this sample was analyzed via LC-MS/MS to determine the amount of total peptide approximated by the total ion current (TIC) and the intensity of ECM proteins. This was performed to estimate the abundance of ECM peptides in the digest to enable more equal mixing of samples. Approximately five micrograms of peptides were labeled with TMT according to the on-column protocol (Myers et al., 2018, 2019). Roughly 0.9 ug of each sample was combined (15 ug total) and labeled with TMT-131 as the common reference sample. This was split in two, on-column labeled in parallel and re-mixed after confirmation of individual labeling efficiency. Ammonium formate (20 mM) was added to each on-column labeling prior to mixing and drying. After vacuum centrifugation, samples were step-fractionated using a Stage tip packed with four punches of SDB-RPS (Empore) extraction disks. Step fractions were eluted in 20 mM ammonium formate with increasing percentages of acetonitrile (ACN), 5, 7.5, 10, 12.5, 15, 17.5, 25, and 55%. Samples were dried by vacuum centrifugation, resuspended in 0.1% formic acid and stored at -80^{o}C until data acquisition.

Data acquisition and analysis

LC-MS/MS was performed as previously described (Mertins et al., 2016; Myers et al., 2018). Data were searched and interpreted using Spectrum Mill version 6.0 (Agilent Technologies, Santa Clara, CA) using parameters similar to those previously described (Naba et al., 2012, 2014a). MS/MS spectra were searched against a combined dataset including both human and

mouse Uniprot entries downloaded on 17 Oct 2014, containing 100,236 entries, including 150 common laboratory contaminants. Matrisome proteins were identified as described previously (Naba et al., 2012). TMT log2 fold change ratios were median- and median absolute deviation-normalized to the total set of ECM proteins quantified in each sample, such that the overall distribution of log2 fold change ratios for each sample was centered at zero and had a standardized variability.

Hierarchical clustering, correlation and marker selection analysis were performed using Morpheus (https://software.broadinstitute.org/morpheus/). Clustering was performed using one minus the Pearson correlation. Correlation analysis was conducted by calculating Spearman's rank correlation coefficient (rho) for the total protein set of each sample. Marker selection was performed as described previously (Myers et al., 2019) to identify proteins significantly different between two sample sets, with signal to noise used as the metric and 10,000 test permutations, and with significance determined as $P \leq 0.05$ and FDR<.1 (Benjamini-Hochberg procedure for multiple comparisons correction).

Supplementary Tables

Supplementary Table S1. Overview of nomenclature and tandem mass tag (TMT) assignment.
Complete list of sample IDs along with their tissues of origin, the mouse strain from which the normal tissues were derived and in which the metastases were grown, the 10-plex TMT series in which they were run, and which of the 10 TMT labels was used for each sample. The tenth TMT label (131) was used for a common reference pool, containing equal parts of all samples, run in both TMT series.

ID	Tissue	Mouse strain	Type	TMT series	TMT label
BrSN1	Brain	NOD-SCID	Normal	A	129C
BrSM1	Brain	NOD-SCID	Metastasis	B	128N
BrSM2	Brain	NOD-SCID	Metastasis	B	129C
BrSM3	Brain	NOD-SCID	Metastasis	A	128C
LuSN1	Lung	NOD-SCID	Normal	A	128N
LuSM1	Lung	NOD-SCID	Metastasis	B	128C
LuSM2	Lung	NOD-SCID	Metastasis	A	127N
LuSM3	Lung	NOD-SCID	Metastasis	B	129N
LiGN1	Liver	NOD-SCID-gamma	Normal	A	130N
LiGM1	Liver	NOD-SCID-gamma	Metastasis	B	130N
LiGM2	Liver	NOD-SCID-gamma	Metastasis	B	130C
LiGM3	Liver	NOD-SCID-gamma	Metastasis	A	126
BoSN1	Bone marrow	NOD-SCID	Normal	A	130C
BoSM1	Bone marrow	NOD-SCID	Metastasis	B	126
BoSM2	Bone marrow	NOD-SCID	Metastasis	A	127C
BoGN1	Bone marrow	NOD-SCID-gamma	Normal	A	129N
BoGM1	Bone marrow	NOD-SCID-gamma	Metastasis	B	127N
BoGM2	Bone marrow	NOD-SCID-gamma	Metastasis	B	127C

Supplementary Table S2. shRNA sequences.
List of all shRNA 97mers used for gene knockdown. Targeting nucleotides are bolded and underlined.

Target Gene	Sequence (97mer)
Firefly luciferase (Control)	TGCTGTTGACAGTGAGCG**AGCTCCCGTGAATTGGAATCC**TAGTGAAGCC ACAGATGTA**GGATTCCAATTCAGCGGGAGC**CTGCCTACTGCCTCGGA
AGRN	TGCTGTTGACAGTGAGCG**CCACCAGGATCTTCTTTGTGAA**TAGTGAAGC CACAGATGTA**TTCACAAAGAAGATCCTGGTGT**TGCCTACTGCCTCGGA
ANXA2	TGCTGTTGACAGTGAGCG**CCAGAGTCTACAAGGAAATGTA**TAGTGAAGC CACAGATGTA**TACATTTCCTTGTAGACTCTGT**TGCCTACTGCCTCGGA
FREM1	TGCTGTTGACAGTGAGCG**ACCCTTTAAATGTGAAATCTAA**TAGTGAAGC CACAGATGTA**TTAGATTTCACATTTAAAGGGC**TGCCTACTGCCTCGGA
HCFC1	TGCTGTTGACAGTGAGCG**AACCGTTCACTATTGTAGAGTA**TAGTGAAGC CACAGATGTA**TACTCTACAATAGTGAACGGTG**TGCCTACTGCCTCGGA
HMCN1	TGCTGTTGACAGTGAGCG**AACTCAGGCTGTCAAATTAAAT**TAGTGAAGC CACAGATGTA**ATTTAATTTGACAGCCTGAGTC**TGCCTACTGCCTCGGA
LGALS3	TGCTGTTGACAGTGAGCG**ACCTCGCATGCTGATAACAATT**TAGTGAAGC CACAGATGTA**AATTGTTATCAGCATGCGAGGC**TGCCTACTGCCTCGGA
PLOD3	TGCTGTTGACAGTGAGCG**ATCGGATCTTTCAGAACCTCAA**TAGTGAAGC CACAGATGTA**TTGAGGTTCTGAAAGATCCGAG**TGCCTACTGCCTCGGA
VWA9	TGCTGTTGACAGTGAGCG**CCAGATGTACAGAAGATTTTAA**TAGTGAAGC CACAGATGTA**TTAAAATCTTCTGTACATCTGT**TGCCTACTGCCTCGGA

Supplementary Table S3. sgRNA sequences.

Gene	Species	sgRNA sequence
Timp1 (Control)	Mouse	CATATTCCCCAAACTTCCTG
SERPINB1	Human	CAAATTTGGGGATCTTGCAC
SERPINH1	Human	GGAGGAAGCTCGCACTCTGA
S100A4 sg1	Human	TAGGGCTTACCCGTTACCCA
S100A4 sg2	Human	GGTGGGCACCCGTGGGTAAC
S100A6	Human	AGCCAGCGCAGCGTCAATGT

Supplementary Table S4. qPCR primers used.
List of all primer pairs used for qPCR. All primers shown are designed to recognize human sequences.

Gene	Direction	Sequence (5' to 3')
ACTIN	Forward	ACCTTCTACAATGAGCTGCG
ACTIN	Reverse	CCTGGATAGCAACGTACATGG
AGRN	Forward	CTCAACTCCAGCCTCATGC
AGRN	Reverse	GAAGCCGCACAGCATTC
ANXA2	Forward	AGAGTTTCCCGCTTGGTTGA
ANXA2	Reverse	TGTTCAAAGCATCCCGCTCA
CSPG4	Forward	GAGCCCAGGCACGAAAAATG
CSPG4	Reverse	GTATGTTTGGCCCCTCCGAA
FREM1	Forward	TGCCTTGCCTCTCTTTACCAG
FREM1	Reverse	AGGTGTATCAGGGTCGGTCA
HCFC1	Forward	CCTGGCTCCATCCAACACAT
HCFC1	Reverse	TCGATGCCATTGGCCACTTC
HMCN1	Forward	GCTGATGGTAGTCTGTATGTGG
HMCN1	Reverse	TCCTCGTTGATCTCCAAACAC
LGALS3	Forward	TGGGGAAGGGAAGAAAGACA
LGALS3	Reverse	TGAGCATCATTCACTGCAACC
PLOD3	Forward	CTGGGCCTGGGAGAGGAGTG
PLOD3	Reverse	TCACGTCGTAGCTATCCACAAACAT
S100A4	Forward	TCTTGGTTTGATCCTGACTGCT
S100A4	Reverse	TCACCCTCTTTGCCCGAGTA
S100A6	Forward	TAAACCGCGAATGTGCGTTG
S100A6	Reverse	GACTGGCCTTATAGCGGTCG
SERPINB1	Forward	ACTTAGGCGACCTCGGGA
SERPINB1	Reverse	TGCTCCATGGTGAAAACCGA

SERPINH1	Forward	TCCGGAAGCGTTTCCAACTT
SERPINH1	Reverse	CCGCGACACGATTCTACTCT
VWA9	Forward	ATGGGCACGGGCATTTCTTC
VWA9	Reverse	CAGGTCGGGTCATGGAAAGG

References

Allan, A.L., George, R., Vantyghem, S.A., Lee, M.W., Hodgson, N.C., Engel, C.J., Holliday, R.L., Girvan, D.P., Scott, L.A., Postenka, C.O., et al. (2006). Role of the Integrin-Binding Protein Osteopontin in Lymphatic Metastasis of Breast Cancer. The American Journal of Pathology *169*, 233–246.

Barbazán, J., Alonso-Alconada, L., Elkhatib, N., Geraldo, S., Gurchenkov, V., Glentis, A., Niel, G. van, Palmulli, R., Fernández, B., Viaño, P., et al. (2017). Liver Metastasis Is Facilitated by the Adherence of Circulating Tumor Cells to Vascular Fibronectin Deposits. Cancer Res *77*, 3431–3441.

Bianchini, G., Balko, J.M., Mayer, I.A., Sanders, M.E., and Gianni, L. (2016). Triple-negative breast cancer: challenges and opportunities of a heterogeneous disease. Nature Reviews Clinical Oncology *13*, 674–690.

Bonotto, M., Gerratana, L., Poletto, E., Driol, P., Giangreco, M., Russo, S., Minisini, A.M., Andreetta, C., Mansutti, M., Pisa, F.E., et al. (2014). Measures of Outcome in Metastatic Breast Cancer: Insights From a Real-World Scenario. The Oncologist *19*, 608–615.

Bos, P.D., Zhang, X.H.-F., Nadal, C., Shu, W., Gomis, R.R., Nguyen, D.X., Minn, A.J., van de Vijver, M.J., Gerald, W.L., Foekens, J.A., et al. (2009). Genes that mediate breast cancer metastasis to the brain. Nature *459*, 1005–1009.

Braun, C.J., Bruno, P.M., Horlbeck, M.A., Gilbert, L.A., Weissman, J.S., and Hemann, M.T. (2016). Versatile in vivo regulation of tumor phenotypes by dCas9-mediated transcriptional perturbation. PNAS *113*, E3892–E3900.

Cailleau, R., Olivé, M., and Cruciger, Q.V.J. (1978). Long-term human breast carcinoma cell lines of metastatic origin: Preliminary characterization. In Vitro *14*, 911–915.

Chavez, K.J., Garimella, S.V., and Lipkowitz, S. (2010). Triple Negative Breast Cancer Cell Lines: One Tool in the Search for Better Treatment of Triple Negative Breast Cancer. Breast Dis *32*, 35–48.

Chou, R.-H., Wen, H.-C., Liang, W.-G., Lin, S.-C., Yuan, H.-W., Wu, C.-W., and Chang, W.-S.W. (2012). Suppression of the invasion and migration of cancer cells by SERPINB family genes and their derived peptides. Oncol. Rep. *27*, 238–245.

Denkert, C., Liedtke, C., Tutt, A., and von Minckwitz, G. (2017). Molecular alterations in triple-negative breast cancer—the road to new treatment strategies. The Lancet *389*, 2430–2442.

Edfors, F., Danielsson, F., Hallström, B.M., Käll, L., Lundberg, E., Pontén, F., Forsström, B., and Uhlén, M. (2016). Gene-specific correlation of RNA and protein levels in human cells and tissues. Molecular Systems Biology *12*, 883.

Fukata, Y., Adesnik, H., Iwanaga, T., Bredt, D.S., Nicoll, R.A., and Fukata, M. (2006). Epilepsy-related ligand/receptor complex LGI1 and ADAM22 regulate synaptic transmission. Science *313*, 1792–1795.

Gocheva, V., Naba, A., Bhutkar, A., Guardia, T., Miller, K.M., Li, C.M.-C., Dayton, T.L., Sanchez-Rivera, F.J., Kim-Kiselak, C., Jailkhani, N., et al. (2017). Quantitative proteomics identify Tenascin-C as a promoter of lung cancer progression and contributor to a signature prognostic of patient survival. Proc. Natl. Acad. Sci. U.S.A. *114*, E5625–E5634.

Hsu, J.-Y., Chang, J.-Y., Chang, K.-Y., Chang, W.-C., and Chen, B.-K. (2017). Epidermal growth factor-induced pyruvate dehydrogenase kinase 1 expression enhances head and neck squamous cell carcinoma metastasis via up-regulation of fibronectin. FASEB J. *31*, 4265–4276.

Huasong, G., Zongmei, D., Jianfeng, H., Xiaojun, Q., Jun, G., Sun, G., Donglin, W., and Jianhong, Z. (2015). Serine protease inhibitor (SERPIN) B1 suppresses cell migration and invasion in glioma cells. Brain Res. *1600*, 59–69.

Hynes, R.O., and Destree, A.T. (1978). 10 nm filaments in normal and transformed cells. Cell *13*, 151–163.

Insua-Rodríguez, J., and Oskarsson, T. The extracellular matrix in breast cancer. Advanced Drug Delivery Reviews.

Jailkhani, N., Ingram, J., Rashidian, M., Rickelt, S., Tian, C., Mak, H., Jiang, Z.-G., Ploegh, H.L., and Hynes, R.O. Non-invasive imaging of tumor progression, metastasis and fibrosis using a nanobody targeting the extracellular matrix. PNAS *In Press*.

Kenny, H.A., Chiang, C.-Y., White, E.A., Schryver, E.M., Habis, M., Romero, I.L., Ladanyi, A., Penicka, C.V., George, J., Matlin, K., et al. (2014). Mesothelial cells promote early ovarian cancer metastasis through fibronectin secretion. J. Clin. Invest. *124*, 4614–4628.

Lamar, J.M., Stern, P., Liu, H., Schindler, J.W., Jiang, Z.-G., and Hynes, R.O. (2012). The Hippo pathway target, YAP, promotes metastasis through its TEAD-interaction domain. PNAS *109*, E2441–E2450.

Lambert, A.W., Pattabiraman, D.R., and Weinberg, R.A. (2017). Emerging Biological Principles of Metastasis. Cell *168*, 670–691.

Lehmann, B.D., Bauer, J.A., Chen, X., Sanders, M.E., Chakravarthy, A.B., Shyr, Y., and Pietenpol, J.A. (2011). Identification of human triple-negative breast cancer subtypes and preclinical models for selection of targeted therapies. Journal of Clinical Investigation *121*, 2750–2767.

Lu, P., Weaver, V.M., and Werb, Z. (2012). The extracellular matrix: A dynamic niche in cancer progression. J Cell Biol *196*, 395–406.

Malanchi, I., Santamaria-Martínez, A., Susanto, E., Peng, H., Lehr, H.-A., Delaloye, J.-F., and Huelsken, J. (2011). Interactions between cancer stem cells and their niche govern metastatic colonization. Nature *481*, 85–89.

Malik, G., Knowles, L.M., Dhir, R., Xu, S., Yang, S., Ruoslahti, E., and Pilch, J. (2010). Plasma Fibronectin Promotes Lung Metastasis by Contributions to Fibrin Clots and Tumor Cell Invasion. Cancer Res *70*, 4327–4334.

Mertins, P., Mani, D.R., Ruggles, K.V., Gillette, M.A., Clauser, K.R., Wang, P., Wang, X., Qiao, J.W., Cao, S., Petralia, F., et al. (2016). Proteogenomics connects somatic mutations to signalling in breast cancer. Nature *534*, 55–62.

Minn, A.J., Gupta, G.P., Siegel, P.M., Bos, P.D., Shu, W., Giri, D.D., Viale, A., Olshen, A.B., Gerald, W.L., and Massagué, J. (2005). Genes that mediate breast cancer metastasis to lung. Nature *436*, 518–524.

Myers, S.A., Wright, J., Peckner, R., Kalish, B.T., Zhang, F., and Carr, S.A. (2018). Discovery of proteins associated with a predefined genomic locus via dCas9-APEX-mediated proximity labeling. Nat. Methods *15*, 437–439.

Myers, S.A., Rhoads, A., Cocco, A.R., Peckner, R., Haber, A., Schweitzer, L.D., Krug, K., Mani, D.R., Clauser, K.R., Rozenblatt-Rosen, O., et al. (2019). Streamlined protocol for deep proteomic profiling of FAC-sorted cells and its application to freshly isolated murine immune cells. Molecular & Cellular Proteomics mcp.RA118.001259.

Naba, A., Clauser, K.R., Hoersch, S., Liu, H., Carr, S.A., and Hynes, R.O. (2012). The Matrisome: In Silico Definition and In Vivo Characterization by Proteomics of Normal and Tumor Extracellular Matrices. Molecular & Cellular Proteomics *11*, M111.014647-M111.014647.

Naba, A., Clauser, K.R., Lamar, J.M., Carr, S.A., and Hynes, R.O. (2014a). Extracellular matrix signatures of human mammary carcinoma identify novel metastasis promoters. ELife *3*, e01308.

Naba, A., Clauser, K.R., Whittaker, C.A., Carr, S.A., Tanabe, K.K., and Hynes, R.O. (2014b). Extracellular matrix signatures of human primary metastatic colon cancers and their metastases to liver. BMC Cancer *14*, 518.

Naba, A., Clauser, K.R., and Hynes, R.O. (2015). Enrichment of Extracellular Matrix Proteins from Tissues and Digestion into Peptides for Mass Spectrometry Analysis. J Vis Exp.

Naba, A., Clauser, K.R., Ding, H., Whittaker, C.A., Carr, S.A., and Hynes, R.O. (2016). The extracellular matrix: Tools and insights for the “omics” era. Matrix Biology *49*, 10–24.

Oskarsson, T., Acharyya, S., Zhang, X.H.-F., Vanharanta, S., Tavazoie, S.F., Morris, P.G., Downey, R.J., Manova-Todorova, K., Brogi, E., and Massagué, J. (2011). Breast cancer cells produce tenascin C as a metastatic niche component to colonize the lungs. Nat. Med. *17*, 867–874.

Payne, S.H. (2015). The utility of protein and mRNA correlation. Trends Biochem. Sci. *40*, 1–3.

Place, A.E., Jin Huh, S., and Polyak, K. (2011). The microenvironment in breast cancer progression: biology and implications for treatment. Breast Cancer Research *13*, 227.

Rappsilber, J., Mann, M., and Ishihama, Y. (2007). Protocol for micro-purification, enrichment, pre-fractionation and storage of peptides for proteomics using StageTips. Nat Protoc *2*, 1896–1906.

Sevenich, L., Bowman, R.L., Mason, S.D., Quail, D.F., Rapaport, F., Elie, B.T., Brogi, E., Brastianos, P.K., Hahn, W.C., Holsinger, L.J., et al. (2014). Analysis of tumour- and stroma-supplied proteolytic networks reveals a brain-metastasis-promoting role for cathepsin S. Nat Cell Biol *16*, 876–888.

Shen, M., Jiang, Y.-Z., Wei, Y., Ell, B., Sheng, X., Esposito, M., Kang, J., Hang, X., Zheng, H., Rowicki, M., et al. (2019). Tinagl1 Suppresses Triple-Negative Breast Cancer Progression and Metastasis by Simultaneously Inhibiting Integrin/FAK and EGFR Signaling. Cancer Cell *35*, 64-80.e7.

Stern, P., Astrof, S., Erkeland, S.J., Schustak, J., Sharp, P.A., and Hynes, R.O. (2008). A system for Cre-regulated RNA interference in vivo. PNAS *105*, 13895–13900.

Vogel, C., and Marcotte, E.M. (2012). Insights into the regulation of protein abundance from proteomic and transcriptomic analyses. Nat. Rev. Genet. *13*, 227–232.

Xie, S., Duan, J., Li, B., Zhou, P., and Hon, G.C. (2017). Multiplexed Engineering and Analysis of Combinatorial Enhancer Activity in Single Cells. Mol. Cell *66*, 285-299.e5.

Chapter 4.

Discussion and Future Directions

This chapter was written by Jess Hebert with editing by Richard Hynes.

Summary of Results

This thesis explored two different aspects of metastasis. First, I investigated the intracellular scaffold protein, IQGAP1, for potential roles in promoting metastasis. IQGAP1 had previously been identified as important for tumorigenesis and tumor progression, it had been demonstrated to drive proliferation, migration and invasion (White et al., 2009), and it was one of a very select set of genes upregulated in highly metastatic melanoma cells (Clark et al., 2000). However, IQGAP1 had not been shown to have actual pro-metastatic activity *in vivo*. I found that both knockdown and knockout of IQGAP1 in MA2 melanoma cells sharply inhibited their ability to form experimental metastases in the lungs from circulation, and re-expressing IQGAP1 in knockout cells could restore their metastatic ability. Moreover, knocking out IQGAP1 in LM2 breast cancer cells impaired the formation of spontaneous metastases without slowing primary tumor growth. By specifically examining the early stages of metastasis following injection of cells into circulation, we observed that IQGAP1 knockout cells had severely diminished extravasation ability. Finally, by expressing several IQGAP1 mutants in a knockout background, I determined that IQGAP1's pro-metastatic effects are likely dependent on multiple domains and functions. Collectively, these results suggest that IQGAP1 is critical for metastasis through its regulation of extravasation, though it may also be important in other steps of the metastatic cascade.

Second, this thesis undertook an inspection of metastatic niches in different organs formed by the same tumor cells. I injected MDA-MB-231 human triple-negative breast cancer cells into the circulation of immunocompromised mice and collected tumors that formed in the brain, lungs, liver and bone marrow. We then enriched these tumor samples for their ECM protein content and performed quantitative mass spectrometry to compare the ECM proteins

present in different metastases, as well as in normal tissues, using human versus mouse peptide sequence discrepancies to distinguish between tumor-cell- and stroma-derived proteins. Across all metastases, I found that the vast bulk of ECM proteins were produced by the stromal cells, which largely made core matrisome proteins, while the tumor cells mostly secreted matrisome-associated proteins such as S100, Annexin and SERPIN family members. I then compared the metastatic samples from each particular tissue to all other metastatic samples, in order to find the ECM proteins specifically elevated in each tissue. With this approach, I identified a diverse array of both tumor-cell- and stroma-derived proteins characteristic of metastases to each tissue. As an example, I knocked down in tumor cells one of these proteins that was elevated in brain metastases, SERPINB1, and injected these cells into circulation. Cells with knocked down SERPINB1 showed a significant reduction in metastasis to the brain, along with a slight reduction in metastasis to the lungs and no observable change in metastasis to the bone marrow. These results are consistent with a tissue-selective role for SERPINB1 in metastasis. Our data thus provide new insight into the creation of metastatic niches by the tumor and stromal cells, and the tissue-specific ECM proteins I identified offer potential new avenues of research into metastatic tropism.

Future directions

Our findings regarding IQGAP1 have raised a number of additional questions. First, while we demonstrated that IQGAP1 expression is critical for extravasation, we have not ruled out the possibility that IQGAP1 could also be promoting metastasis in other ways. For instance, intravasation is a similar but non-identical process to extravasation. Both steps are known to involve invadopodia, which IQGAP1 regulates, so it would be logical to hypothesize that

IQGAP1 may also promote intravasation (Gligorijevic et al., 2012; Leong et al., 2014; Sakurai-Yageta et al., 2008). Intravital imaging of primary tumors could be helpful in determining whether IQGAP1 expression regulates invasion from the primary tumor and extravasation. Furthermore, IQGAP1 has been shown to stimulate proliferation in a number of cancers (Diao et al., 2017; Jadeski et al., 2008; Wang et al., 2014; Zhao et al., 2017). This ability could translate to promotion of metastatic outgrowth, or possibly escape from dormancy. Staining of proliferation markers in early metastases with modulated IQGAP1 expression could reveal whether its expression is relevant at these stages. Such detailed follow-up studies, isolating individual steps of the metastatic cascade, will be necessary to ascertain the full extent of IQGAP1's effects on metastasis.

I also tested several mutants of IQGAP1 to see if they would have impaired effects on metastasis. Indeed, deletion of IQGAP1's C-terminal domain or IQ motifs completely abrogated its promotion of metastasis, while removing two major phosphorylation sites did not. However, these deletions represented fairly major changes to the overall protein, with the C-terminal domain and IQ motifs each known to bind several other proteins (Brown and Sacks, 2006). Additionally, conformational changes in IQGAP1 have been shown to regulate some of its binding interactions, so it remains possible that these deletion mutants were simply unable to form the proper conformations for normal IQGAP1 function (Liu et al., 2016). In any case, more specific investigation into IQGAP1's binding interactions in the context of metastasis would be needed to narrow down by what mechanism it is promoting metastasis. This would require inhibiting particular binding interactions between IQGAP1 and individual proteins through more precise binding site mutations.

Finally, further research should be conducted into the other IQGAP family members. While the overwhelming majority of research has focused on IQGAP1, the family contains two other proteins in humans, IQGAP2 and IQGAP3 (White et al., 2009). However, expression of these other two proteins is much more limited than the ubiquitously expressed IQGAP1, and IQGAP2 appears to have tumor-suppressive effects (White et al., 2009). While research on IQGAP3 is extremely limited even in comparison to IQGAP2, its expression seems to be correlated with poor prognosis, similar to IQGAP1 (Kumar et al., 2017). Nevertheless, key protein domains are fairly well conserved among all three members of the family (Watanabe et al., 2015; White et al., 2009). These facts, together with our results regarding IQGAP1 in metastasis, raise a number of further questions regarding this protein family. Why does IQGAP2 apparently act as a tumor suppressor, despite its similarity to IQGAP1? Exactly which binding interactions are shared among all three IQGAPs, and which are particular to one protein? Are IQGAP2 and IQGAP3 somehow compensating for the lack of IQGAP1 in our experiments, such that removing one or both of them in addition would result in even more severe metastatic defects? This entire family of proteins merits further scrutiny, and their combined role in metastasis and cancer in general may be greater than previously realized.

Next, my analysis of the ECM in different metastatic niches represents only an initial survey of possibilities for further study. I identified SERPINB1 as one protein with varying levels among different metastases, and I showed that knocking down SERPINB1 in tumor cells significantly reduced brain metastasis following intracardiac injection. However, while I tested the effects of SERPINB1 knockdown on tropism as an example for this investigation into metastatic niches, I have not discovered precisely why it is so highly expressed in brain metastases, nor why its expression is critical for brain metastasis. SERPINB1 has been

previously known for its role in protecting neutrophils from their own proteases, and its overexpression in cancer cells has been reported to suppress migration and invasion *in vitro* (Chou et al., 2012; Huasong et al., 2015). On the contrary, in the context of our model, SERPINB1 expression by the tumor cells is promoting their own metastasis. The known function for SERPINB1 in neutrophils raises the possibility that it may have some immune-modulatory function in metastases. Staining sections of brain metastases for neutrophils and other immune cell populations could help evaluate whether this is a possible explanation. The presence or absence of SERPINB1 expression could potentially be affecting immune-cell recruitment or activation, or acting to protect the tumor from immune clearance. Nevertheless, the particular importance of such an effect in the brain is unclear and might require additional comparisons with metastases to the bone, which appear unaffected by SERPINB1 expression.

While I have focused here on SERPINB1, my research identified dozens of other potential metastasis promoters and markers. I began by looking at those tissue-specific ECM proteins produced by the tumor cells, as their experimental manipulation is considerably more straightforward compared with that of the stromal proteins. However, the rise of CRISPR-Cas9-based methods has made the testing of stromal factors considerably faster and more accessible than ever before, and such methods will likely continue to improve in the following years. This will open up a multitude of new avenues of research that have heretofore been omitted out of expediency and cost. We could more easily test potential stromal promoters of metastasis to different tissues, or even alter their expression at different stages of metastatic growth to test the relevance of their presence in early- or late-stage metastases. We could also assay the stroma-derived ECM proteins found commonly decreased among all metastases, which could hypothetically be suppressors of metastasis.

Next, I conducted follow-up experiments testing the effects of knocking down ECM proteins of interest with intracardiac injections, for several reasons. I was primarily interested in changes in metastatic tropism, and the intracardiac injection allowed us to assay metastasis to several tissues at once. Intracardiac injections also let us test experimental metastasis from circulation, including any effects on arrest, extravasation and micrometastatic seeding. These were the same conditions in which I first derived the tumors used for our quantitative mass spectrometry, thereby identifying our ECM proteins of interest. To test those proteins, I therefore wanted to use the same injection method. However, with intracardiac injections, I have noticed large variability from injection to injection, and experiment to experiment, even compared with other techniques like tail-vein injections. Intracardiac injections introduce a number of cells into circulation, and those cells are distributed throughout the entire mouse, meaning that the actual number of cells arriving in each organ may be inconsistent. This variability required us to use many more mice than desired to obtain enough statistical power for proper comparisons among experimental groups. It also meant that I briefly tested and moved on from several potential promoters of metastasis simply because they did not have a severe-enough phenotype in a single pilot experiment. Consequently, for future follow-up experiments, we could employ more targeted injections to ensure consistent delivery of cells to a specific tissue: intracarotid or intracranial injections for the brain, tail-vein injections for the lungs, intrasplenic injections for the liver, and intratibial injections for the bone. These directed methods could be useful when testing ECM proteins that we hypothesize to have specific effects in certain organs.

Finally, the development of new methods and improvement of current technologies may change the types of experiments that become possible. For instance, when I first prepared our tumor samples, I knew from previous studies that we required samples of at least 25 mg in order

to have sufficient material for eventual mass spectrometry following ECM enrichment, which removes much of the tumor mass. This also required us, in many cases, to pool several metastatic tumors into one sample to ensure that it would have sufficient material for analysis. This likely added noise to our data, both due to heterogeneity among the tumors pooled together and due to imperfect margins on the micro-dissected metastases that could have contributed some adjacent normal stromal tissue. The methods that we employed in our study may not be necessary for much longer, though. Mass spectrometers are becoming ever more sensitive. Even using the same enrichment methods, we continue to detect more ECM proteins year after year. This improved sensitivity may allow us to examine smaller and earlier-stage metastases, and it may eventually obviate the need for ECM enrichment at all, which would permit entirely unbiased proteomic observation of the entire tumor microenvironment. Such analyses could also be supplemented with techniques like the fluorouracil-labeled RNA sequencing recently developed by Massagué and colleagues, which makes possible high-sensitivity collection of RNA from early-stage metastases without the need for cell sorting (Basnet et al., 2019). Collectively, future improvement in techniques and instruments will allow more thorough surveys of metastases than currently possible.

One significant question left unaddressed by our study of the ECM in metastatic niches is whether the differences we observe among metastases represent varying adaptations to different environments upon arrival, or simply the pre-selection of more fit "seeds." For my experiments, I injected a heterogeneous population of parental MDA-MB-231 cells, which will naturally vary in their overall metastatic ability, as well as their tropism to certain organs. This is evidenced by the fact that these same cells have been *in vivo*-selected to metastasize to several different organs, indicating that it is possible to select for stable tropism characteristics (Bos et al., 2009; Kang et

al., 2003; Minn et al., 2005). It is therefore conceivable that our experiments selected a group of cells from the parental population that were already more suited to growth in a certain organ. Nevertheless, *in vivo* selection experiments typically require several rounds of repeated injection and isolation, and cells become more metastatic and tropic over the course of these rounds. This would seem to imply that, even if the cells that metastasized to a particular tissue were naturally more adept at doing so from the start, they also acquired additional adaptations that continued to improve their metastatic fitness. It would be interesting to compare the ECM in metastatic niches formed from parental and *in vivo*-selected cells to see if any changes observed in tumors have become more extreme following selection.

Final remarks

What could this research imply for the future of cancer therapy as it relates to metastasis? Even in the time that this thesis work was being conducted, there have been significant contributions to the literature regarding metastasis that have dramatically altered how treatment of metastatic cancer will have to be approached. Some of the most substantial of these findings deals with the timing of metastatic dissemination. It was long believed that metastasis was a late event in cancer progression, which left open the possibility of preventing metastasis in patients presenting with a primary tumor by inhibiting any number of steps in the metastatic cascade (Steeg, 2016). While there may be some circumstances where this is still the case, recent research has revealed that primary tumors can begin disseminating cells into circulation at a very early stage, meaning that, by the time a patient has come into the clinic, they likely already have tumor cells circulating and disseminating (Harper et al., 2016; Hosseini et al., 2016). Thus, while a metastasis prevention therapy may still be useful in stopping the development of additional

tumors, such as during and following surgical removal of a primary tumor, it seems unlikely to be effective in averting metastasis entirely.

Consequently, much of the hope for treating metastatic cancer now lies in systemic or targeted therapies. While this does represent a sharp reduction in available strategies compared to the suite of metastasis prevention options previously under consideration, there are still a number of promising options. First, the knowledge that metastatic cells disseminate very early, despite the fact that the growth of overt metastases is a late-stage development, means that disseminated tumor cells frequently remain dormant for an extended period. Dormancy does make them resistant to traditional chemotherapies, which act on actively dividing cells, but therapies that could wake these tumor cells from dormancy, or target them despite their dormancy, could be valuable in preventing metastatic outgrowth. Next, the recent success of immune checkpoint blockade therapies has raised the possibility that such approaches could be broadly applicable in turning the immune system against even distant metastases. Nevertheless, the significant auto-immune risks associated with using such drugs in high doses, or for extended periods, makes a more targeted method desirable (Luke et al., 2017).

It is here that our research on the ECM in metastases may be of use. As the ECM is, by definition, extracellular, it is much more accessible to probes and drugs in comparison to intracellular proteins, which require passage through the plasma membrane. We have recently shown that nanobody probes targeting the EIIIB domain of fibronectin or tenascin C are capable of detecting a variety of primary tumors and metastases *in vivo* through positron emission tomography-computed tomography (PET-CT) (Jailkhani et al. and unpublished). Moreover, we have used these same EIIIB-detecting nanobodies to create chimeric antigen receptor (CAR) T cells, which demonstrate efficacy against solid melanoma tumors (Xie et al., 2019), and these

nanobodies could in principle act as vectors to target drugs, isotopes, toxins or nanoparticles to tumors, including metastases. The ECM therefore represents a real possibility for targeting tumors, and continued surveying of different metastatic niches can provide us with a library of ECM proteins that characterize different metastases, including commonly upregulated proteins that may be broadly applicable, and rarer proteins that could represent more specific targets. I hope that the work in this thesis will inspire further investigation into the ECM in a wide variety of primary tumors and metastases, and lead to the development of more therapies for metastatic cancer.

References

Basnet, H., Tian, L., Ganesh, K., Huang, Y.-H., Macalinao, D.G., Brogi, E., Finley, L.W., and Massagué, J. (2019). Flura-seq identifies organ-specific metabolic adaptations during early metastatic colonization. Elife *8*.

Bos, P.D., Zhang, X.H.-F., Nadal, C., Shu, W., Gomis, R.R., Nguyen, D.X., Minn, A.J., van de Vijver, M.J., Gerald, W.L., Foekens, J.A., et al. (2009). Genes that mediate breast cancer metastasis to the brain. Nature *459*, 1005–1009.

Brown, M.D., and Sacks, D.B. (2006). IQGAP1 in cellular signaling: bridging the GAP. Trends in Cell Biology *16*, 242–249.

Chou, R.-H., Wen, H.-C., Liang, W.-G., Lin, S.-C., Yuan, H.-W., Wu, C.-W., and Chang, W.-S.W. (2012). Suppression of the invasion and migration of cancer cells by SERPINB family genes and their derived peptides. Oncol. Rep. *27*, 238–245.

Clark, E.A., Golub, T.R., Lander, E.S., and Hynes, R.O. (2000). Genomic analysis of metastasis reveals an essential role for RhoC. Nature *406*, 532–535.

Diao, B., Liu, Y., Zhang, Y., Yu, J., Xie, J., and Xu, G.-Z. (2017). IQGAP1-siRNA inhibits proliferation and metastasis of U251 and U373 glioma cell lines. Molecular Medicine Reports *15*, 2074–2082.

Gligorijevic, B., Wyckoff, J., Yamaguchi, H., Wang, Y., Roussos, E.T., and Condeelis, J. (2012). N-WASP-mediated invadopodium formation is involved in intravasation and lung metastasis of mammary tumors. Journal of Cell Science *125*, 724–734.

Harper, K.L., Sosa, M.S., Entenberg, D., Hosseini, H., Cheung, J.F., Nobre, R., Avivar-Valderas, A., Nagi, C., Girnius, N., Davis, R.J., et al. (2016). Mechanism of early dissemination and metastasis in Her2+ mammary cancer. Nature *540*, 588–592.

Hosseini, H., Obradović, M.M.S., Hoffmann, M., Harper, K.L., Sosa, M.S., Werner-Klein, M., Nanduri, L.K., Werno, C., Ehrl, C., Maneck, M., et al. (2016). Early dissemination seeds metastasis in breast cancer. Nature *540*, 552–558.

Huasong, G., Zongmei, D., Jianfeng, H., Xiaojun, Q., Jun, G., Sun, G., Donglin, W., and Jianhong, Z. (2015). Serine protease inhibitor (SERPIN) B1 suppresses cell migration and invasion in glioma cells. Brain Res. *1600*, 59–69.

Jadeski, L., Mataraza, J.M., Jeong, H.-W., Li, Z., and Sacks, D.B. (2008). IQGAP1 Stimulates Proliferation and Enhances Tumorigenesis of Human Breast Epithelial Cells. Journal of Biological Chemistry *283*, 1008–1017.

Jailkhani, N., Ingram, J., Rashidian, M., Rickelt, S., Tian, C., Mak, H., Jiang, Z.-G., Ploegh, H.L., and Hynes, R.O. Non-invasive imaging of tumor progression, metastasis and fibrosis using a nanobody targeting the extracellular matrix. PNAS *In Press*.

Kang, Y., Siegel, P.M., Shu, W., Drobnjak, M., Kakonen, S.M., Cordón-Cardo, C., Guise, T.A., and Massagué, J. (2003). A multigenic program mediating breast cancer metastasis to bone. Cancer Cell *3*, 537–549.

Kumar, D., Hassan, M.K., Pattnaik, N., Mohapatra, N., and Dixit, M. (2017). Reduced expression of IQGAP2 and higher expression of IQGAP3 correlates with poor prognosis in cancers. PLoS ONE *12*, e0186977.

Leong, H.S., Robertson, A.E., Stoletov, K., Leith, S.J., Chin, C.A., Chien, A.E., Hague, M.N., Ablack, A., Carmine-Simmen, K., McPherson, V.A., et al. (2014). Invadopodia Are Required for Cancer Cell Extravasation and Are a Therapeutic Target for Metastasis. Cell Reports *8*, 1558–1570.

Liu, J., Kurella, V.B., Lecour, L., Vanagunas, T., and Worthylake, D.K. (2016). The IQGAP1 N-terminus Forms Dimers and the Dimer Interface is Required for Binding F-actin and Ca2+/calmodulin. Biochemistry.

Luke, J.J., Flaherty, K.T., Ribas, A., and Long, G.V. (2017). Targeted agents and immunotherapies: optimizing outcomes in melanoma. Nat Rev Clin Oncol *14*, 463–482.

Minn, A.J., Gupta, G.P., Siegel, P.M., Bos, P.D., Shu, W., Giri, D.D., Viale, A., Olshen, A.B., Gerald, W.L., and Massagué, J. (2005). Genes that mediate breast cancer metastasis to lung. Nature *436*, 518–524.

Sakurai-Yageta, M., Recchi, C., Le Dez, G., Sibarita, J.-B., Daviet, L., Camonis, J., D'Souza-Schorey, C., and Chavrier, P. (2008). The interaction of IQGAP1 with the exocyst complex is required for tumor cell invasion downstream of Cdc42 and RhoA. The Journal of Cell Biology *181*, 985–998.

Steeg, P.S. (2016). Targeting metastasis. Nat Rev Cancer *16*, 201–218.

Wang, X.-X., Wang, K., Li, X.-Z., Zhai, L.-Q., Qu, C.-X., Zhao, Y., Liu, Z.-R., Wang, H.-Z., An, Q.-J., Jing, L.-W., et al. (2014). Targeted Knockdown of IQGAP1 Inhibits the Progression of Esophageal Squamous Cell Carcinoma In Vitro and In Vivo. PLoS ONE *9*, e96501.

Watanabe, T., Wang, S., and Kaibuchi, K. (2015). IQGAPs as key regulators of actin-cytoskeleton dynamics. Cell Struct. Funct.

White, C.D., Brown, M.D., and Sacks, D.B. (2009). IQGAPs in cancer: A family of scaffold proteins underlying tumorigenesis. FEBS Letters *583*, 1817–1824.

Xie, Y.J., Dougan, M., Jailkhani, N., Ingram, J., Fang, T., Kummer, L., Momin, N., Pishesha, N., Rickelt, S., Hynes, R.O., et al. (2019). Nanobody-based CAR T cells that target the tumor microenvironment inhibit the growth of solid tumors in immunocompetent mice. PNAS 201817147.

Zhao, H.-Y., Han, Y., Wang, J., Yang, L.-H., Zheng, X.-Y., Du, J., Wu, G.-P., and Wang, E.-H. (2017). IQ-domain GTPase-activating protein 1 promotes the malignant phenotype of invasive ductal breast carcinoma via canonical Wnt pathway. Tumour Biol. *39*, 1010428317705769.